Theoretical and experimental investigations of intra- and inter-segmental control networks and their application to locomotion of insects and crustaceans

Inaugural-Dissertation

zur

Erlangung des Doktorgrades

der Mathematisch-Naturwissenschaftlichen Fakultät

der Universität zu Köln

vorgelegt von

Martyna Grabowska

aus Toruń

Köln 2014

Berichterstatter (Gutachter): PD Dr. Silvia Gruhn

Prof. Dr. Ansgar Büschges

Prof. Dr. Axel Schneider

Tag der mündlichen Prüfung: 04.12.2014

Contents

1. Zusammenfassung 4
2. Abstract 6
3. Introduction 8
4. Published Studies 16
4.1 Quadrupedal gaits in hexapod animals- inter-leg coordination in free-walking adult stick insects 16
4.2 A Neuro-Mechanical Model Explaining the Physiological Role of Fast and Slow Muscle Fibers at Stop and Start of an Insect Leg. 29
4.3 A network model comprising 4 segmental, interconnected ganglia, and its application to simulate multi-legged locomotion in crustaceans 44
5. Unpublished Study 70
5.1 Investigation of an inter-segmental pathway arising at the metathoracic segment and modulating a pilocarpine-induced rhythm in the prothoracic protractor-retractor CPG 70
6. Discussion 14
7. Conclusion 25
8. Bibliography 26
9. Teilpublikationen 37
10.1 List of publications 37
10.2 Short communications 37
10. Supplementary Figure 38
11. Acknowledgments 39
12. Erklärung 40

1. Zusammenfassung

Beim Laufen terrestrischer Tiere müssen die Bewegungen der Laufbeine kontinuierlich koordiniert werden um eine erfolgreiche Fortbewegung zu gewährleisten. Laufen ist ein zyklischer Prozess, dabei besteht ein einzelner Schritt aus einer Stemmphase, die für den Antrieb des Körpers sorgt, und aus einer Schwingphase, die das Bein zur nächsten Stemmphasenposition führt. Sensorische Signale, die ihren Ursprung in den sich in den Beinen befindenden sensorischen Organen haben, modulieren die rhythmische Aktivität der Motoneurone und damit die rhythmische Aktivität der antagonistischen Muskelpaare im Bein. Die Koordination der einzelnen Gelenke und der Aktivität der entsprechenden Muskelpaare eines Beins wird als intrasegmentale Koordination bezeichnet. Für das Laufen ist nicht nur die Koordination eines Beines essentiell, sondern auch die Koordination der gegenüberliegenden, und ipsilateralen Beine. Letzteres wird als intersegmentale Koordination bezeichnet und ist ebenfalls stark von sensorischen Einflüssen abhängig.

In dieser Arbeit stelle ich drei Publikationen (Grabowska et al., 2012; Tóth et al., 2013; Grabowska et al., in rev.) und die Ergebnisse einer experimentellen Arbeit vor, die sich mit verschiedenen Aspekten der intra- und intersegmentalen Koordination befassen. Ein sehr gut untersuchter Modellorganismus für Fortbewegung ist die Stabheuschrecke *Carausius morosus.* An der Stabheuschrecke habe ich die intersegementale Koordination der Beine beim Laufen einerseits durch Videoanalyse des Laufverhaltens und andererseits durch elektrophysiologische Experimente zu intersegmentalen Verbindungen untersucht. Des Weiteren wurden experimentellen Ergebnisse zu inter- und intrasegmentalen Verbindungen in der Stabheuschrecke in mathematischen Modellen zusammengefasst, um das Laufverhalten zu beschreiben und um Hypothesen für bislang unbekannte neuronale Kontrollprozessen aufzustellen.

Als erstes wird eine Studie vorgestellt, die sich mit dem Laufverhalten der Stabheuschrecke befasst (Grabowska et al., 2012). Hierfür wurden Laufsequenzen von adulten Stabheuschrecken gefilmt, die auf Untergründen mit unterschiedlichen Steigungen geradeaus gelaufen sind. Abhängig von der Steigung, benutzen die Tiere unterschiedliche Koordinationsmuster der Laufbeinbewegung . Schließlich wurden Koordinationsmuster von Stabheuschrecken untersucht, denen wir Vorder-, Mittel- oder Hinterbeine amputiert hatten. In Abhängigkeit vom amputierten Beinpaar erlaubten die Koordinationsmuster der verbliebenen Beine funktionelles Laufen oder nicht. Daraus konnten wir schließen, dass afferente Informationen von Sinnesorganen der von laufenden Vorder-, Mittel- und Hinterbeine unterschiedlich zur Bildung von koordiniertem Laufen beitragen.

Der zweite Teil beschäftigt sich mit einem neuromechanischen Modell, das das Anhalten und Starten eines Beines der Stabheuschrecke während des Laufens beschreibt (Tóth et al., 2013). Ein bereits bestehendes Modell für ein intrasegmentales neuronales Netzwerk des einzelnen Beins der Stabheuschrecke wurde um ein Model des Skelettmuskelsystems der Stabheuschrecke erweitert. Der Fokus lag auf der Ansteuerung der Aktivität von schnellen und langsamen Muskelfasern verschiedener Muskelpaare eines Stabheuschreckenbeins beim Starten und Anhalten während des Laufens. Für die Kopplung der einzelnen Beingelenke und der zugehörigen Muskulatur in diesem Modell wurden experimentell gewonnen Einflüsse sensorischer Signale verwendet, die Position und Winkelgeschwindigkeit der einzelnen Beingelenke kodieren. Die aus diesen Simulationen gewonnenen Ergebnisse,

wie die zeitliche Komponente aktivierter Muskeln beim Anhalten und Starten von Stabheuschrecken, sowie der Zeitpunkt wann ein Schritt innerhalb eines Schrittzyklus beendet oder begonnen werden kann, zeigten große Ähnlichkeit mit den experimentellen Daten aus der Stabheuschrecke. Daher kann dieses Modell als physiologisch relevant angesehen werden und führt zu fundierten Hypothesen über die neuronalen Ansteuerungsprozesse der Beinmuskeln beim Starten und Stoppen von laufenden Stabheuschrecken.

Im dritten Teil dieser Arbeit wurde das zuvor genannte 3-CPG-MN Modell für die laufende Stabheuschrecke erweitert, um zu testen, ob es als fundamentaler Baustein für die Simulation von Fortbewegung von Tieren mit acht Laufbeinen, wie zum Beispiel bei Krebstieren, dienen kann (Grabowska et al., in rev.). Dazu wurde das 3-CPG-MN Netzwerk um ein weiteres segmentales Modul erweitert und es wurden zwei unterschiedliche Netzwerkarchitekturen des erweiterten Modelles getestet. Der allgemeine Aufbau der einzelnen Module des 3-CPG-MN Modells wurde dabei nicht verändert. Die Simulation bestimmten Laufverhaltens (Koordinationsmuster, Schrittfrequenz, Übergänge) von Krebstieren ist abhängig von dem Zeitpunkt eintreffender intersegmentaler erregender sensorischer Signale innerhalb einer Zyklusperiode des Protraktor/Retraktor-System des beeinflussten Segments. Mit Rücksicht auf eine Netzwerkarchitektur des 3-CPG-MN Modells, bei der eine kaudal-rostrale intersegmentale Verbindung jedes zweite Segment verbindet, konnte das 4-CPG-MN Modell alle Arten des Laufverhaltens von vorwärtslaufenden Krabben und Flusskrebsen reproduzieren. Dieses Modell unterstreicht die wichtige Rolle der zeitlichen Komponente der erregenden, sensorischen intersegmentalen Verbindungen in Tieren, die sich mit acht Beinen fortbewegen und schlägt mögliche neuronale intersegmentale Verbindungen vor.

Zum Schluss werden experimentelle Daten vorgestellt, die zeigen, dass der zentrale Mustergenerator des Protraktor/Retraktor Systems (Thorax-Coxa Gelenk) im Prothorakalganglion im Rhythmus des laufenden ipsilateralen Hinterbeins beeinflusst wird. Diese ipsilaterale Verbindung wurde für das 3-CPG-MN-Modell von Daun-Gruhn und Tóth (2011) für die laufende Stabheuschrecke angenommen. Die Experimente haben gezeigt, dass ein durch Pilocarpin erzeugter Rhythmus der Protraktor- und Retraktor-Motoneurone im Prothorakalganglion an den Rhythmus eines vorwärts- und rückwärst laufenden, ipsilaterlalen Hinterbeins gekoppelt werden konnte. Mit diesen Experimenten ergeben sich für die Stabheuschrecke zum ersten Mal Hinweise für eine weit reichende intersegmentale Verbindung, die modulierende Signale von einem laufenden Hinterbein zu prothorakalen CPGs überträgt.

2. Abstract

Movements of the walking legs in terrestrial animals have to be coordinated continuously in order to produce successful locomotion. Walking is a cyclic process: A single step consists of a stance phase and a swing phase. In the stance phase, the leg muscles provide propulsion of the animal's body. During the swing phase, the leg is positioned to the starting position of the next stance phase. Sensory input, arising from sensory organs in the legs, modulates the rhythmic motoneuronal activity and therefore the rhythmic activity of the antagonistic muscles pairs in a leg. The coordination of leg joints, and thus of the respective muscle pairs, is called intra-segmental coordination. For coordinated walking not only the proper coordination of one leg is important, but also the coordination of contralateral and ipsilateral legs. The latter is called inter-segmental coordination and also strongly depends on sensory feedback.

In this thesis I present three publications (Grabowska et al., 2012; Toth et al., 2013; Grabowska et al., in rev.) and results of an experimental study focusing on different aspects of intra- and inter-segmental coordination. Starting with experimental data on the stick insect *Carausius morosus*, a well studied model organism for locomotion, I analyzed inter-segmental coordination of legs during walking behavior of stick insects by video analysis. I also performed electrophysiological experiments that provide insight into the inter-segmental connections of different thoracic segments. Furthermore, experimental results were summarized in mathematical models in order to reproduce stick insect locomotion and to provide new hypotheses about so far unknown neuronal controlling processes.

First, a study of the walking behavior of the stick insect is introduced (Grabowska et al., 2012). For this purpose, walking sequences of adult animals, walking straight on surfaces with increasing and decreasing slopes, were recorded. Depending on the slope, the animals used different coordination patterns. Subsequent, walking patterns of animals with amputated front, hind or middle legs were analyzed. It became evident that the resulting coordination patterns were regular or maladapted, depending on the amputated leg pairs. We therefore assumed that afferent information from walking front, middle, and hind legs contribute differently to coordination.

The second part presents a neuromechanical model that describes starting and stopping of a stick insect leg during walking (Tóth et al., 2013). An existing model of the intra-segmental neuronal network of the stick insect leg was extended by a model of its musculo-skeletal system. The focus of the model was on the neuronal control of slow and fast muscle fiber activity of the three proximal leg muscle groups at start and stop of a leg within a stepping cycle. Using the effects of sensory signals that encode position and velocity of the leg joints like the temporal components of activated muscles during start and stop, observed in experiments, as well as the timing of starting and stopping processes within a step cycle, the simulation results were in good agreement with the observed data of the stick insect. Therefore, this model can be regarded as physiologically relevant and leads to hypotheses about the neuronal control of the musculo-skeletal system that can reveal details of stop and starting in the walking animals.

In the third part of this thesis the above mentioned 3-CPG-MN network model, which has been developed based on stick insect data, was extended to serve as a basic module for eight-legged locomotion in walking crustaceans

(Grabowska et al., in rev.). For this purpose, the existing 3-CPG-MN network model was extended by an additional segmental module. The basic properties of the 3-CPG-MN network modules remained unchanged. By testing two different network topologies of the new 4-CPG-MN network model, specific walking behavior (coordination patterns, stepping frequency, and transitions) of crustaceans could be replicated by only changing the timing of the inter-segmental excitatory sensory input on the influenced segment. Considering the topology of the 3-CPG-MN network model, namely a caudal-rostral inter-segmental connection connecting every second CPG, the 4-CPG-MN network model was able to reproduce all kinds of walking behavior of forward walking crabs and crayfish. This network stresses the importance of the timing of excitatory signals that are provided by inter-segmental pathways in animals with eight walking legs and four thoracic segments, and proposes possible inter-segmental sensory pathways.

Finally, results of experimental data are introduced showing that the rhythm of protractor/retractor central pattern generating networks (thorax-coxa joint) in the prothoracic ganglion can be influenced by a stepping ipsilateral hind leg of the stick insect. This inter-segmental pathway was hypothesized in the 3-CPG-MN network model of Daun-Gruhn and Tóth (2011) for stick insect walking. The experiments showed that a pilocarpine-induced rhythm in the prothoracic protractor and retractor motoneurons could be entrained by an intact forward or backward walking hind leg. In stick insects, this is the evidence for a long range ipsilateral inter-segmental connection that mediates sensory information from a stepping hind leg to the prothoracic CPGs.

3. Introduction

All animals have to use some form of locomotion in order to navigate through the environment. Depending on the animal, and the environment the animal lives in, this can be swimming, flying, crawling or walking. All these forms of locomotion have in common that they emerge from interactions of activities of the nervous system, the sense organs, and the corresponding muscles (Orlowsky et al., 1999). In particular, rhythm generating networks are responsible for rhythmic behaviors of motoneurons (MNs), which induce rhythmic muscular activity. Sensory organs in the locomotor organs detect changes in position, load, and velocity and encode this information into sensory signals. These sensory signals can be inhibitory or excitatory and modulate the motor network, which consists of rhythm generating networks and motoneurons, in time and magnitude. An example of locomotion is walking in legged animals. In walking, a step has a stance (retraction) and a swing (protraction) phase, and this is valid for all types of walking. During stance phase proper propulsion of the animal's body takes place, during swing phase the leg is moved to a position where stance phase can start. This stepping behavior of a single leg is possible due to the activities of antagonistic muscle pairs, and, in turn, the activities of the corresponding *motoneurons* innervating these muscles (Orlowsky et al., 1999). The rhythmic activity of the motoneuron pools is controlled by *central pattern generators* (CPGs) (crickets: Grillner, 2003; lamprey: Wallen and Williams, 1984; crayfish swimmerets: Skinner and Mulloney, 1998; Manduca crawling: Johnston and Levine, 2002; turtle: Stein, 2008; stick insect: Büschges, 2005). CPGs are neural networks situated in the central nervous systems of vertebrates and invertebrates. They are capable of generating rhythmic motoneuron activity, and therefore rhythmic muscle activity, in the absence of phasic sensory feedback (Büschges, 2005; Grillner, 2003; Pearson, 2000; Calabrese, 1995; Grillner, 2006; Harris-Warrick, 1993; Marder and Calabrese, 1996; Marder and Bucher, 2001; Marder et al., 2007; Orlowsky et al., 1999; Selverston and Moulins, 1985). Nevertheless, sensory feedback crucially affects the function of CPG networks, since sensory input to a CPG can modify the timing and magnitude of the CPG's output (Büschges, 2005; Grillner 2003; Pearson, 2004). Therefore, sensory feedback contributes to the interaction of different muscle groups during a proper step of a single leg, thus shaping the intra-segmental coordination (Büschges et. al, 2008; Akay et al., 2001; Bässler and Büschges, 1998; Akay et al., 2004). It also plays a role in the inter-segmental coordination, i.e. the coordination between different legs (Cruse, 1990; Büschges et al., 1995; Dürr et al., 2004; Ludwar et al., 2005; Borgmann et al., 2007, 2009).

Walking animals typically use a high variety of gaits and coordination patterns and are able to use different ones within one walking sequence. In vertebrates, a switch between the different gaits happens

due to an increase or decrease in walking speed. Thus, different gaits (walk, trot, or gallop, for instance) correlate with different speeds within one species (Alexander, 1989). Invertebrates, such as insects, spiders, and crustaceans, can also navigate through different environments using different coordination patterns and different speeds. Although, the different coordination patterns can also be associated with different walking speeds, the transitions between those are, in contrast to vertebrates (Hoyt and Taylor, 1981), continuous (Cruse et al., 2009; Wendler, 1964; Wendler, 1966). Concerning the stick insect and also other insects (Burns, 1973; Graham, 1972; Hughes, 1952; Wendler, 1964, 1966; Delcomyn, 1971; Graham, 1985), three regular coordination patterns are known. Slow walking insects prefer a metachronal or wave coordination pattern for locomotion, where one leg of the animal is in protraction phase after another in a metachronal order. For fast locomotion, the animals use a tripod coordination pattern, where three legs are in swing phase at the same time (Bender et al., 2011; Cruse et al., 2009; Graham, 1985). Within this range of walking speeds, there is also an intermediate coordination pattern (Hughes, 1952; Wilson, 1966; Graham, 1985; Delcomyn, 1981; Ritzmann and Büschges, 2007). This is the so-called tetrapod coordination pattern, where only one leg swings together with a leg diagonally on the other side, so that at least four legs at any given time are in their retraction phase (Cruse et al., 2009; Graham, 1985). Previous studies mostly analysed walking on a plane surface (Graham, 1972). In nature, however, locomotion of insects strongly depends on the environmental conditions, such as the surface structure, slope and also the orientation of the body, especially during climbing (Spirito and Mushrush, 1979; Delcomyn, 1981; Graham, 1985; Duch and Pflüger, 1995; Dürr, 2005; Gruhn et al., 2009; Bender et al., 2011). Moreover, previous studies showed a dependency of the developmental stages of the animals on the generation of coordination patterns. For example, it was shown that juvenile stick insects preferred walking in a strictly regular tripod coordination pattern when walking at higher speeds and in a tetrapod coordination pattern when walking more slowly. Adult stick insects, in contrast, exclusively walked in a tetrapod coordination pattern (Graham, 1972). In this study only regular coordination patterns were taken into account, although the author mentioned incidental occurrences of errors in the normal metachronal sequences. These errors were described as additional protractions of the front legs during normal locomotion. It is known that stick insects use their front legs to explore the environment and they are therefore considered for being mainly used as sensors (Cruse, 1976). Nevertheless, they also seem to contribute to regular locomotion.

In addition to the behavioral studies, insects are often used as model organisms for the analysis of walking behavior on the neuronal level because of their easily accessible nervous systems and their easily observable walking behavior. The neuronal control of walking in insects was studied extensively over the last decades, investigating both the intra- and inter-segmental coordination. In spite of this, there are still a lot of unanswered questions related to the generation of walking patterns, and especially to the role of inter-segmental coordination in this process. Among other insects (cockroach, cricket), the Indian stick insect *Carausius morosus* is a very suitable model organism to investigate locomotion. The stick insect uses its six segmented legs for walking and climbing. The leg movements of a single leg are

controlled by antagonistic muscle pairs. The *protractor coxae* and *retractor coxae* muscles of the thorax-coxa (ThC) joint are responsible for forward and backward movements. The *levator trochanteris* and *depressor trochanteris* muscles of the coxa-trochanter (CTr) joint carry out the upward and downward movements of the femur of the leg. Finally, the *flexor tibiae* and *extensor tibiae* muscles of the femur-tibia (FTi) joint are responsible for flexion and extension of the leg (Graham and Epstein, 1985). During a single step cycle, consisting of swing and stance phase, the activities of these muscle pairs are in well-defined phase relations to each other (Epstein and Graham, 1983; Graham and Epstein, 1985; Büschges and Gruhn, 2008). From experimental studies, it is known that these specific phase relations are due to sensory information, arising at sensory organs, situated in the stick insect's leg (Büschges et. al, 2008). The sensory organs, *femoral* and *trochanteral campaniform sensilla*, provide information to the different CPGs about load and force (Bässler, 1977; Akay et al., 2001; Bässler and Büschges, 1998; Akay et al., 2004). The information about the position of the leg relative to the stick insect's body is provided by *hair plates* and *hair rows* (Wendler, 1964; Bässler, 1977). The movement and angular velocity of the leg are encoded by the *femoral chordotonal* organ (Bässler, 1967).

The sensory information deriving from these organs does not only provide proper coordination of a single leg, but also the coordination of adjacent legs in order to ensure coordinated walking (Cruse, 1990; Büschges et al., 1995; Dürr et al., 2004; Ludwar et al., 2005; Borgmann et al., 2007, 2009, 2011). Previous studies of inter-segmental coordination in stick insects have shown that a single stepping front leg induces rhythmic in-phase protractor and retractor motoneuron activity in the second thoracic ganglion, the mesothoracic ganglion (Borgmann et al., 2009). It also results in a general tonic increase in protractor and retractor motoneuronal activity of the last thoracic ganglion, the metathoracic ganglion (Ludwar et al., 2005; Borgmann et al., 2007). Furthermore, in a semi-intact preparation, where all legs except ipsilateral front and middle legs were amputated, the presence of a single stepping middle leg results in a general increase in tonic motoneuron activity in the first thoracic ganglion, the prothoracic ganglion, and the metathoracic ganglion. Experiments, where a front and a middle leg were both stepping, showed rhythmic protractor and retractor motoneuron activity in the metathoracic ganglion. This activity was in phase with front leg steps (Borgmann et al., 2009). Concerning the influence of the posterior segments on the anterior segments, the results show that in two thirds of the experiments backward stepping in a single hind leg induces a general increase in protractor and retractor motoneuron activity and in one third of the experiments rhythmic activity in the mesothoracic ganglion. The influence of a forward or backward stepping hind leg on the prothoracic ganglion remains unknown (Borgmann et al., 2009).

In the case of locomotion, many experimental approaches were made in the past to describe walking motor outputs of vertebrate and invertebrate model animals (reviews: Büschges et al., 2008; Büschges, 2005; Dürr et al., 2004; Orlovsky et al., 1999). Biological phenomena, such as neuronal basis of inter- and intra-segmental coordination or the neuromechanical network of the stick insect, for instance, can be described by mathematical models in order to learn about the functionality of the system, or about the relevance of specific parameters. In general, mathematical models aim to answer questions, and formulate hypotheses about the function of the system under investigation.

Existing mathematical models can describe different aspects of locomotion, such as the biomechanical properties in walking and running in cockroaches (Holmes et al., 2006), the centrally coupled oscillators in locomotion (Ijspeert et al., 2007), the behavioral analysis of coordination (Cruse, 1990), and the role of sensory signals contributing to the transition from stance to swing phase (Eckeberg et al., 2004).

Especially in animals that have a decentralized walking system and that mainly walk very slowly, as it is the case in stick insects, for instance, the sensory feedback that is provided through sensory organs situated in the insect's leg plays a crucial role (Cruse, 1990; Büschges et al., 1995; Akay et al., 2001, 2004; Ludwar et al., 2004; Borgmann et al., 2007, 2009, 2011). In addition, it was shown that the stick insect does not only have one controlling CPG for each leg as it was proposed in models for the cockroach (Holmes et al., 2006), but one controlling CPG for each leg joint (Büschges et al., 1995). The CPGs of the single joints of one leg are modulated by sensory feedback in order to produce a coordinated single leg step (Bässler and Büschges, 1998).

For the purpose of investigating the aforementioned, mathematical models based on experimental data on inter- and intra-segmental influences in the stick insect were constructed that not only could reproduce single leg stepping by connecting the three CPGs of the three stick insect leg joints via sensory pathways, but also the protractor-retractor CPGs (3-CPG-MN network model) of the three adjacent legs (Daun et al., 2009; Daun-Gruhn, 2011; Daun-Gruhn and Tóth, 2011). The model networks consisted of Hodgkin-Huxley-type neuron models (Hodgkin and Huxley, 1952). This neuron model comprises biophysical properties of neurons that contribute to motor activity during walking. Using a network model that comprises the leg joint CPGs and by connecting these by means of specific sensory pathways, which mediate sensory information about the position, movements, and load of the leg, coordinated stepping of the single leg could be reproduced (Daun-Gruhn, 2011). A second network model, the inter-segmental 3-CPG-MN network model, is capable of simulating all regular coordination patterns, observed in stick insects, namely the tripod, tetrapod, and wave coordination patterns. This is achieved solely by adjusting parameters like the phase shift between the (periodic) sensory signal, gating the excitatory inter-segmental pathway and the (periodic) activity of the affected protractor-retractor CPG module or the tonic excitatory drive deriving from higher centers to increase or decrease the oscillation frequency of the CPGs (Daun-Gruhn and Tóth, 2011). Moreover, they could simulate continuous transitions between the regular coordination patterns (Daun-Gruhn and Tóth, 2011). In a different model, they

propose a mechanism that contributes to forward and backward movements (Tóth et al., 2012) and simulate curve walking in the stick insect (Knops et al., 2012). These models implement the knowledge of intra- and inter-segmental coordination and are based on experimental results on the stick insect. However, in order to describe certain walking behaviors, such as the transition between coordination patterns in the stick insect, additional hypothetical connections had to be added to complete the inter-segmental 3-CPG-MN network model. One of these hypothetical connections that proved to be crucial for the simulation of stick insect coordination patterns, and for stable and continuous transitions between the tetrapod and tripod coordination pattern, as it is observed in behavioral walking studies of the stick insect, was a sensory pathway providing excitation arising from the third segment (metathoracic protractor-retractor CPG) at a specific phase within the oscillation period of the first segment (prothoracic protractor-retractor CPG) (Daun-Gruhn and Tóth, 2011; Graham, 1972). In this case, the mathematical model leads to new hypotheses regarding the neuronal network of the animal, which can now be tested in experiments.

As mentioned previously, coordinated walking emerges from an interaction of neural networks (CPGs), sensory feedback, and the activity of antagonistic muscle groups in the animal's legs. Therefore, some basic actions of coordination, such as stopping, starting, and leg movements, cannot solely be described by the network properties controlling the rhythmic MN activity of theses muscles. In these basic actions of walking it is also important to consider the specific properties of the musculo-skeletal system.

It is known that there are two muscle groups that are responsible for the performance of walking, fast movements, and posture control. These are the slow and fast muscle fibers. The two types show different contraction kinetics and histochemical properties (Bässler et al., 1996; Bässler and Stein, 1996; Godlewska, 2012). Godlweska (2012) showed that the presence of fast and slow muscle fibres can not only be found in the *extensor tibiae* muscles of the stick insect (Bässler et al., 1996; Bässler and Stein, 1996), but also in other muscle groups within a stick insect's leg (Godlewska, 2012). One can therefore assume an analogous function of those muscles.

To construct a mathematical model, describing the neuromuscular properties of the stick insect's leg, and the sensory feedback at start and stop of this leg would be appropriate to understand the neuronal control of the musculo-skeletal system during different walking behaviors.

Various arthropod species show high variability in the number of legs, from six legs in insects up to 750 legs in millipedes. Nevertheless, these animals show close similarities in their neuroanatomy and muscular systems. Hence, it is reasonable to assume similarities in the inter-segmental coordination in these animals.

It seems challenging to design a network model that can serve as a basis for the simulation of walking behavior in these animals with different numbers of legs.

The previously mentioned network model of Daun-Gruhn and Tóth (2011) can reproduce stick insect locomotion and is based on experimental data of the stick insect. It might, thus, be a good candidate for the aforementioned basic module. Consequently, it could be used to first construct a model that replicates eight-legged locomotion of crustaceans.

The leg muscles of crustaceans are known to have approximately the same innervations as those of stick insects (Elson, 1966). Due to their greater number of legs, namely eight walking legs, crustaceans are capable of using a larger variety of coordination patterns than insects (Wilson, 1966; Graham, 1985; Ritzmann and Büschges, 2007; Cruse et al., 2009; Barnes, 1975; Parrack, 1964; Ross, 2013).

In analogy to stick insects, sensory feedback plays an important role in intra- and inter-segmental coordination of forward walking crayfish and crabs (Cruse, 1990; Sillar, Clarac and Bush, 1987; Cruse and Müller, 1986; Chasserat and Clarac, 1983; Clarac and Barnes, 1985; Bowermann, 1977; Clarac, 1982; Jamon and Clarac, 1995). Sensory feedback from proprioceptors, such as the *thoraco-coxal* muscle receptor organ (TCMRO), a single receptor at the base of each limb in crayfish and crabs, affects the timing as well as the intensity of the rhythmic output of two or more thoracic ganglia (Sillar, Clarac and Bush, 1987). Other sensory organs that contribute to the modulation of rhythmic output and that are comparable to chordotonal organs of stick insects are the cuticular stress detectors (CSDs). These are stimulated by deformations of the cuticle and provide information about loading of the legs during walking (Clarac, Wales and Laverack, 1971; Klärner and Barth, 1986; Klärner and Barnes, 1986). Also, contralateral coupling, as in the stick insect, is known to be weaker than the ipsilateral coupling of the segments (Jamon and Clarac 1995).

Walking speed is very important in the development of different coordination patterns. In crabs, stick insects, and other insects an increase in walking speed can lead to a phase shift of the CPG activities and, therefore, to different coordination patterns. Also, the ratio of the duration of protraction and retraction of one leg during a step, changes from 1:3 in the metachronal wave pattern to nearly 1:1 in the alternating tetrapod coordination pattern (Barnes, 1974; Müller and Cruse, 1991; Ross, 2013).

The resemblance of the neuronal functions and anatomy of the thoracic ganglia and the legs make forward walking crustaceans an appropriate model organism, on which generalizations of the 3-CPG-MN network by Daun-Gruhn and Tóth (2011) can be investigated with regard to their suitability, to describe basic and more general modes of arthropod locomotion.

In the present thesis, I will discuss works that investigate important aspects of intra- and inter-segmental coordination, using three different levels of investigation: behavioral, electrophysiological, and theoretical.

The first publication (Grabowska et al., 2012) shows, what effects, changes in the walking environment and leg amputations have on the locomotor output of the adult stick insect *Carausius morosus*. In this study, video analysis was used to analyse the walking behavior of intact stick insects and ones with amputated front, middle, or hind legs, while they were walking on different slopes or were climbing. This paper stresses the role of the front legs, which can be used, either, as part of the coordinated regular locomotor behavior, or as tactile sense organs. In addition, it shows that amputation of the middle legs leads to loss of coordinated walking.

The second publication (Tóth et al., 2013), presents a neuro-mechanical model that focuses on the physiological role of fast and slow muscle fibres of the three antagonistic muscle groups of a stick insect's leg at stop and start of stepping. This model was used for study putative neuronal and muscular processes that are not accessible in experiments. This includes sensory signals that encode position and velocity of the leg joints as observed in experiments. The simulation results are in good agreement with observed data from the stick insect. This model can thus be regarded as physiologically relevant. It has led to testable hypotheses that point to details of starting and stopping processes during walking and the interaction between the neuromuscular networks of a single leg.

In the third publication (Grabowska et al. 2014, under review), I investigated the suitability of the 3-CPG-MN network model of Daun-Gruhn and Tóth (2011), which was developed based on stick insect data, to serve as a basic module for eight-legged locomotion in walking crustaceans. By using two different topologies, I could predict specific walking behavior of crustaceans only by changing the timing of the excitatory sensory signals. Basic structural properties of the 3-CPG-MN network model were preserved. In addition, I showed that the output of a 4-CPG-MN network model variant with fully cyclical connection from the last to the first CPG, as it is the case in the 3-CPG-MN model, is not stable, and its usefulness is limited, when simulating crustacean locomotion. However, viewing the topology of the 3-CPG-MN network model as one, in which every second CPG is connected caudal-rostrally, a model extension could be constructed which could reproduce all coordination patterns observed in forward walking crabs and crayfish. This network predicts the importance of the excitatory inter-segmental pathways that can now be tested in experiments.

The last chapter (Grabowska et al., in prep) validates the hypothetical connection from the metathoracic to the prothoracic ganglion in the 3-CPG-MN network model by Daun-Gruhn and Tóth (2011) in the stick insect *Carausius morosus*. It shows that in a semi-intact preparation an intact forward or backward walking hind leg is able to entrain a pilocarpine-induced rhythm in the prothoracic protractor and retractor motoneurons. This is the first time that evidence for a long range inter-segmental connection, spanning across two ganglia, is shown in the stick insect. In addition, it stresses the role of mathematical models that may lead to new hypotheses concerning the structure and functionality of a system. The hypotheses can then be tested in experiments as in the presented case, where I established the existence of an investigated inter-segmental influence from the metathoracic CPGs to the prothoracic CPGs.

4. Published Studies

4.1 Quadrupedal gaits in hexapod animals- inter-leg coordination in free-walking adult stick insects

Martyna Grabowska, Elzbieta Godlewska, Joachim Schmidt and Silvia Daun-Gruhn

Published in the Journal of Experimental Biology (215, 4255-4266, 2012)

Author contributions

Conceived and designed the experiments
Martyna Grabowska, Elzbieta Godlewska
Joachim Schmidt, Silvia Daun-Gruhn

Performed the experiments
Martyna Grabowska, Elzbieta Godlewska

Analyzed the data
Martyna Grabowska, Elzbieta Godlewska
Joachim Schmidt, Silvia Daun-Gruhn

Figure preparation:
Martyna Grabowska, Elzbieta Grabowska

First version of manuscript
Martyna Grabowska

Wrote the paper
Martyna Grabowska, Elzbieta Godlewska
Joachim Schmidt, Silvia Daun-Gruhn

Contributed reagents/materials/analysis tools
Joachim Schmidt, Silvia Daun-Gruhn

The Journal of Experimental Biology 215, 4255-4266

doi:10.1242/jeb.073643

RESEARCH ARTICLE

Quadrupedal gaits in hexapod animals – inter-leg coordination in free-walking adult stick insects

Martyna Grabowska[1,*], Elzbieta Godlewska[1,*], Joachim Schmidt[2,†] and Silvia Daun-Gruhn[1,†,‡]

[1]Emmy Noether Research Group of Computational Biology, Department of Animal Physiology, Institute of Zoology, University of Cologne, Cologne, Germany and [2]Department of Animal Physiology, Institute of Zoology, University of Cologne, Cologne, Germany

*These authors contributed equally to this work
†Shared senior authorship
‡Author for correspondence (sgruhn@uni-koeln.de)

SUMMARY

The analysis of inter-leg coordination in insect walking is generally a study of six-legged locomotion. For decades, the stick insect *Carausius morosus* has been instrumental for unravelling the rules and mechanisms that control leg coordination in hexapeds. We analysed inter-leg coordination in *C. morosus* that freely walked on straight paths on plane surfaces with different slopes. Consecutive 1.7 s sections were assigned inter-leg coordination patterns (which we call gaits) based on footfall patterns. Regular gaits, i.e. wave, tetrapod or tripod gaits, occurred in different proportions depending on surface slopes. Tetrapod gaits were observed most frequently, wave gaits only occurred on 90 deg inclining slopes and tripod gaits occurred most often on 15 deg declining slopes, i.e. in 40% of the sections. Depending on the slope, 36–66% of the sections were assigned irregular gaits. Irregular gaits were mostly due to multiple stepping by the front legs, which is perhaps probing behaviour, not phase coupled to the middle legs' cycles. In irregular gaits, middle leg and hindleg coordination was regular, related to quadrupedal walk and wave gaits. Apparently, front legs uncouple from and couple to the walking system without compromising middle leg and hindleg coordination. In front leg amputees, the remaining legs were strictly coordinated. In hindleg and middle leg amputees, the front legs continued multiple stepping. The coordination of middle leg amputees was maladapted, with front legs and hindlegs performing multiple steps or ipsilateral legs being in simultaneous swing. Thus, afferent information from middle legs might be necessary for a regular hindleg stepping pattern.

Supplementary material available online at http://jeb.biologists.org/cgi/content/full/215/24/4255/DC1

Key words: locomotion, walking, gait, inter-leg coordination, stick insect.

Received 23 April 2012; Accepted 20 August 2012

INTRODUCTION

Obviously, the analysis of insect terrestrial locomotion is the analysis of hexapedal walking. Aside from some apparent specialists, e.g. praying mantis, mole cricket or locust, in insect imagines all three leg pairs mainly serve the purpose of walking. Consequently, descriptions of leg coordination during walking consider six legs. Just like legged animals in general, hexapeds use different inter-leg coordination patterns during walking to meet different behavioural demands.

Commonly, inter-leg coordination patterns are grouped into gaits. Insect gaits range from a tripod coordination in fast walkers to a metachronal or wave gait in slow walkers. Between these extremes, intermediate gaits occur (Hughes, 1952) (for reviews, see Wilson, 1966; Graham, 1985; Delcomyn, 1981; Ritzmann and Büschges, 2007). In the tripod gait, 'two mirror-image tripods step in an alternating pattern such that the animal always has at least three feet touching the ground' (Bender et al., 2011). In other words, in a tripod gait three legs swing together (Cruse et al., 2009). When insects walk slowly, a pattern is often observed in which only one leg swings together with a leg located diagonally on the other side. Here, the term tetrapod gait is occasionally used and in this gait 'at least four legs are on the ground at any moment of time' (Cruse et al., 2009).

For insects, the concept of gaits is not without controversy (Cruse et al., 2009) because, under certain conditions, gaits do not appear to be separable. Wendler found a gliding coordination of leg movements in mounted adult stick insects, walking on a passive treadwheel (Wendler, 1964; Wendler, 1965). Coordination ranged from metachronal waves alternating between the left and right side at very low speeds of walking to a tripod coordination at high speeds (7 cm s^{-1}). Dürr stated that 'gaits may not be a helpful concept for describing leg coordination in all walking arthropods' because gaits in mounted stick insects that walk straight on a Styrofoam sphere cannot be identified unequivocally as a result of considerable variation of stepping patterns over time (Dürr, 2005). Of course, insect inter-leg coordination patterns depend on the behavioural context and environmental conditions such as surface structure, slopes, orientation of the body or specifics of an experimental setup (e.g. Spirito and Mushrush, 1979; Delcomyn, 1981; Graham, 1985; Duch and Pflüger, 1995; Dürr, 2005; Gruhn et al., 2009; Bender et al., 2011). And thus, in contrast to walks on the sphere, Graham reported that free-walking adult stick insects (*Carausius morosus*) on a horizontal surface almost exclusively use a 'bi-quadruped'; that is, a tetrapod gait (Graham, 1972). These patterns appear to be regular. However, Graham mentions incidental occurrences of errors in the normal metachronal sequence; for example, extra protractions of a front leg during walking. In sharp

contrast to Graham is the notion by Cruse (Cruse, 1976) that stick insects (*C. morosus*) walking on a horizontal plane use their front legs mainly as sensors. However, this view of front leg function does not appear to have received further attention although it implies consequences for models of the control of hexapedal locomotion. We therefore attempted to deepen the insight into inter-leg coordination in adult untethered stick insects (*C. morosus*). Specifically, we wished to answer the following questions. Is the behaviour of front legs in principle different from that of the other legs? Does front leg behaviour change depending on the actual inter-leg coordination pattern and surface slope? If yes, what are the effects of amputation of a segment's legs on the coordination patterns of the remaining legs?

We show here that in horizontal surface walking the front legs often perform a multiple stepping or probing behaviour that is independent of the adjacent legs' walking cycles and that is not seen in the other legs. Inter-leg coordination patterns and the occurrence of multiple stepping depend on surface slopes. The regularity of middle leg and hindleg coordination is not compromised by front leg multiple stepping or probing. Amputation of front leg or hindleg pairs has an impact on inter-leg coordination but not on the regularity of middle leg and hindleg coordination or multiple stepping behaviour in front legs. In contrast, amputation of middle leg pairs severely hampers the formation of a functional walking pattern in front legs and hindlegs. We conclude that front legs can be coupled to or decoupled from the locomotor system to generate multiple stepping or contribute to regular hexapedal walking. Furthermore, our data imply that middle leg stepping is a robust behaviour that contributes to the coordination of hindleg stepping. The different functionality of legs and the resulting flexibility of the walking system need therefore to be considered in modelling studies of insect locomotion.

MATERIALS AND METHODS

Experiments were performed with adult female stick insects *C. morosus*, Sinety 1901, from a colony maintained at the University of Cologne. The walking behaviour of seven to nine animals was investigated under different walking conditions. Animals were filmed while walking on a plain black fabric surface (160×90 cm). A white 18 mm tape was attached along the mid-line of this arena and a white board with a black stripe was positioned at the end of the arena to give animals orientation for straight walks. In addition, the white stripe served as a reference to determine walking direction. Only straight walks were used for evaluation. Animals that did not start walking voluntarily were briefly touched on the abdomen to trigger walking. To avoid the potential effect of this touch on the walking pattern, the first four steps of those walking sequences were excluded from the analysis. To obtain a 15 or 90 deg slope, the arena was elevated on one side.

Stick insects were filmed from above with an AVT Pike Camera (Allied Vision Technologies, Stadtroda, Germany) at 60 frames s^{-1}. The camera was mounted on a jointed articulated boom stand that allowed the moving insect to be followed continuously. The setup was illuminated by a halogen lamp. The camera was controlled by an AVT-Active-Cam-Viewer (Allied Vision Technologies; configurations: 640×480, monochrome, 8-bit; brightness 36, shutter 250, sharpness 2, digital zoom 1000, 60 frames s^{-1}). For recording, the lens was set to 8 mm and the aperture to f-number 5.6. Movies were analysed frame by frame using AVI edit (AM Software).

Identification of coordination patterns

To identify coordination patterns or gaits, foothold pattern diagrams (e.g. Fig. 1) were constructed in Excel (Microsoft Office 2007) by identification of the posterior extreme position (PEP, lift-off) and the anterior extreme position (AEP, touch-down). Black bars indicate the swing phase of a leg. Frame by frame analysis accounts for an error of ±1 frame (i.e. 16.6 ms) when determining PEP and AEP. Sequences of continuous walking were segmented into sections of 100 frames (1.7 s) to determine a gait for each section. An alternative approach in which 100 frame sections were moved step by step yielded no difference in results and was not applied. We continued with the segmentation of sections of 100 frames. A sequence contained a mean of seven sections. Depending on walking speed, each section contained two to five steps by each leg.

A gait could be assigned to each section of 100 frames. To determine gaits, phase relationships were calculated as the onset of swing with respect to the stepping period of the right middle leg (R2) or right hindleg (R3) in the case of amputated middle legs. Fig. 1 shows idealized step patterns (see also Wilson, 1966) for a tripod gait in which three legs swing in synchrony (Fig. 1A) and two types of tetrapod gait – mirror images of one another – in which two diagonal legs swing in synchrony (Fig. 1B,C). These ideal patterns result in phase relationships of leg movements as given in Table 1. In our experiments, however, we never observed perfectly synchronous swing movements in either gait. Therefore, we tolerate a deviation from ideal phase relationships during swing by ±0.12. When assigning a gait, we allowed one erroneous step of a single leg per section.

In some experiments, a pair of front legs, middle legs or hindlegs was amputated at the coxa–trochanteral joint. To quantify the resulting quadrupedal gaits in front leg or hindleg amputees, phase relationships of the remaining legs were calculated with respect to the stepping period of the right middle leg (R2). In middle leg

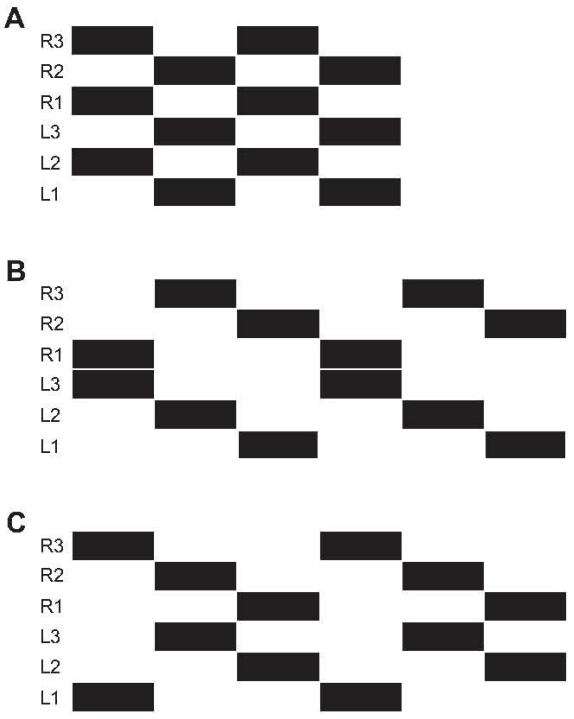

Fig. 1. Schematic drawing of different stereotypic hexapedal walking patterns. Black bars indicate leg swing. In tripod gait, three legs swing in synchrony (A), while in tetrapod gait, two diagonal legs swing synchronously (B,C).

Table 1. Stereotypic phase relationships of all legs within a cycle period of the right middle leg (R2) or the right hindleg (R3) for the different gaits

	R2				R3			
	Tetrapod 1	Tetrapod 2	Tripod	Circular mean	Tetrapod 1	Tetrapod 2	Tripod	Circular mean
R3	0.66	0.66	0.5	0.61	–	–	–	–
R2	–	–	–	–	0.33	0.33	0.5	0.34
R1	0.33	0.33	0.5	0.34	0.66	0.66	0	0.73
L3	0.33	0	0	0.14	0.66	0.33	0.5	0.52
L2	0.66	0.33	0.5	0.52	0	0.66	0	0.91
L1	0	0.66	0	0.88	0.33	0	0.5	0.26

Right (R) and left (L) legs are designated 1 (front) 2 (middle) or 3 (hind). Gaits were tetrapod 1, tetrapod 2 and tripod.
Circular means of phases of the individual legs obtained in our experiments are also given.

amputees, the right hindleg (R3) was taken as the reference. Four different quadrupedal gaits were observed: in trot gait, two diagonal leg pairs always swing together (Fig. 2A); in the two walk gaits (canter gait coordination), synchronous swing of a diagonal pair is followed by two single leg swing phases (see Fig. 2B,C for walk 1 and 2, respectively); and in wave gait, only a single leg swings (Fig. 2D).

It was not always possible to assign a gait to a section. These cases were due to irregularities, like a continuous gait transition or multiple steps by legs; for example, 'probing' of front legs. A section with such irregularities was classified as irregular gait (see Fig. 3C and Fig. 5A for typical examples). To determine the frequency of occurrence of gaits and corresponding phase relationships, data from different animals were pooled. Before pooling, data were weighted according to the number of walking sequences that were performed by each animal.

Walking speed

Walking speeds of intact and amputated animals were evaluated for sections with StickTracker, a customized Matlab program (The MathWorks, Inc., Natick, MA, USA) by Dr Till Bockemühl. StickTracker calculates velocity by frame-to-frame movements of the point defined by the intersection of the lateral axis through both hindleg coxae and the longitudinal axis in relation to ground markers.

Statistics

Circular statistics were performed using the circular statistics toolbox for Matlab (The MathWorks, Inc.) (Berens, 2009). The Rayleigh test (Batschelet, 1981) was used to test whether phases were randomly distributed or whether a predominant directionality is present. The Watson–Williams F-test (Batschelet, 1981) was used to test for differences in length of the mean resulting phase vectors. The length of the mean resulting vector is a crucial quantity for the measurement of circular spread. The closer it is to one, the more concentrated the data sample is around the mean direction. This test was performed using ORIANA 4 (Kovach Computing Services, Anglesey, UK). For the statistical evaluation of the phases, all steps within a sequence were taken into account. To test whether the multiple steps of the front legs were randomly distributed in phase with respect to the stepping period of R2, only the sections in which multiple stepping occurred were considered.

Differences between the mean number of steps performed across all animals for different legs in different walking situations were tested in Matlab using a one-tail ANOVA (see Fig. 4E, Fig. 7B, Fig. 8B and Fig. 9B).

The occurrences of different gaits in different walking situations were compared and tested for significance using the Wilcoxon rank sum test in Matlab (see Fig. 4A–D, pooled weighted data). In the experiments with animals with amputated legs, we put all regular gaits together (trot, walk 1, walk 2 and wave) and compared their occurrence with that of irregular gaits (Fig. 7A, Fig. 8B and Fig. 9B). The Wilcoxon rank sum test in Matlab was also used to determine differences in walking speed between groups.

RESULTS

Hexapedal walking

Stick insects (*C. morosus*) that walked a straight path on a horizontal surface adopted a tetrapod gait in 43.7% of 32 sections from 9 animals. A typical example of a tetrapod gait section is shown in Fig. 3B. Generally, both mirror-image tetrapod gaits were used by the animals (Fig. 1B,C; see Materials and methods for details).

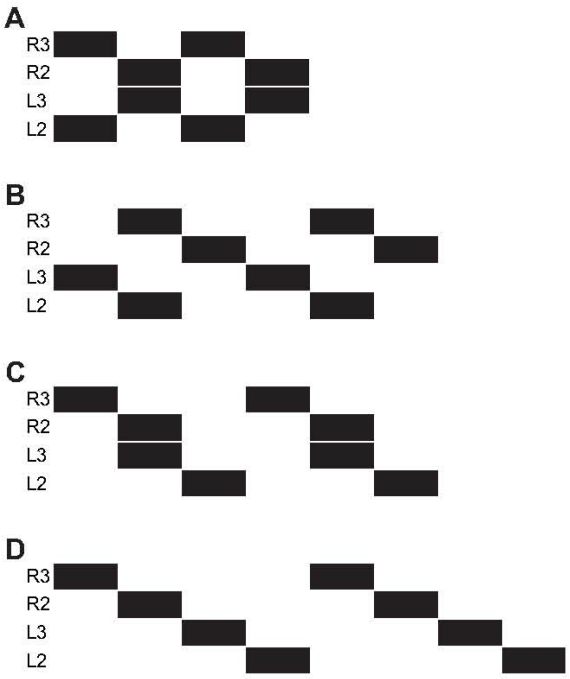

Fig. 2. Schematic drawing of different stereotypic quadrupedal walking patterns. In trot, two diagonal legs swing in synchrony (A). In walk, synchronous swing of a diagonal pair of legs is followed by two single leg swing phases (B,C) and in wave gait, only a single leg swings (D). The stereotypic patterns are shown for the case of stick insect front leg amputees.

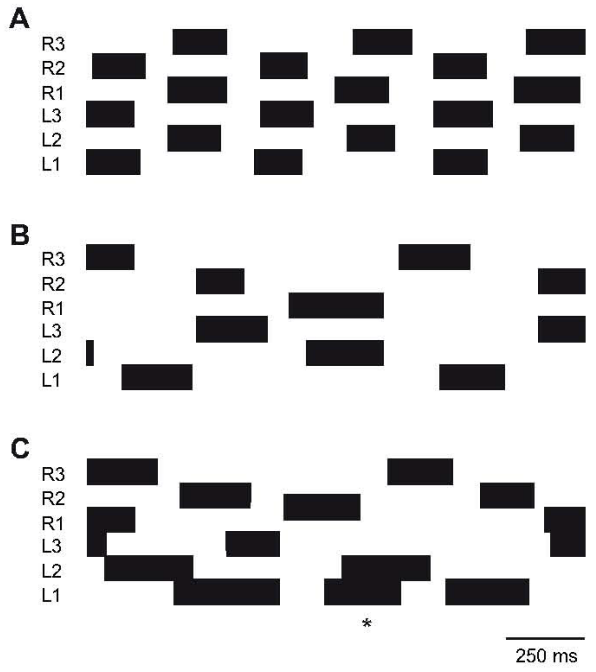

Fig. 3. Examples of tetrapod (A), tripod (B) and irregular (C) walking patterns observed in the adult stick insect. *Simultaneous swing of adjacent legs.

Animals adopted the tripod gait significantly less often (16.6%) (Fig. 3A). Occasionally, an animal switched gaits within a walking sequence. These switches were not abrupt but rather smooth transitions.

The occurrence of regular gaits was reduced in upward slope walking. On a 15 deg upward slope, tetrapod gait was adopted in 32.1% and tripod gait in 8.7% of all sections (N=8 animals, n=36 sequences of continuous walking). On a 90 deg upward slope, tetrapod gait was adopted in 28.1% and tripod gait in 5.7% of the sections (N=7, n=21). Only on the 90 deg slope did animals occasionally use the wave gait (9% of sections). In all three walking situations, a tetrapod gait was adopted significantly more often than a tripod gait. In contrast to this, in downward slope walking the relative number of tripod gait sections increased as tetrapod gaits were observed in 23.9% and tripod gaits in 40.3% of sections (N=7, n=36; differences between occurrences of gaits were not significant, P>0.05).

Besides the regular tetrapod and tripod gaits, we frequently observed irregular non-stereotypic walking patterns in all four walking conditions (example footfall patterns are shown in Fig. 3C, Fig. 5A). These irregular walking patterns, or irregular gaits, occurred even though we allowed a certain variability when assigning a tetrapod or tripod gait to a section (see Materials and methods for details). Irregular gaits occurred in 39.7% of sections recorded on the horizontal surface, and in 35.8% in walks on the 15 deg downward slope. They occurred more often in upward slope walking: in 56.4% and 66.3% of the cases on 15 and 90 deg slopes, respectively. Data are summarized in Fig. 4A–D (grey bars). Closer inspection of irregular gait sections revealed that, on a horizontal surface, the number of steps, i.e. the swing movements, performed by the front legs (R1, n=200; L1, n=253), was significantly higher (P<0.05) than the number of steps by the hindlegs (R3, n=149; L3, n=156) or middle legs (R2, n=156; L2, n=152; Fig. 4E). Step numbers of the hindlegs and middle legs were not significantly different (P>0.05). Similarly, in slope walking, the front legs performed significantly more steps than the middle legs or hindlegs (P<0.001) (Fig. 4E). Therefore, if no switching between the different gaits occurred, inconsistencies in irregular gaits were mainly due to more frequent stepping of the front legs. Sometimes, the animals showed rocking behaviour during walking (up to 22% on the horizontal surface and less in the other walking situations). Rocking behaviour is a side-to-side movement usually performed by stick insects that do not locomote. Occasionally, this behaviour is apparent in animals approaching the end of a walk (Pflüger, 1977). Rocking behaviour was equally distributed among gaits. We therefore conclude that rocking behaviour does not affect the distribution of the occurrence of the different gaits.

When ignoring front legs in the analysis of irregular gait sections, more regular stereotypic walking patterns of the middle legs and hindlegs became obvious. Leg coordination was comparable to that of the quadrupedal gaits walk and trot (Fig. 2, see Materials and methods for details). Fig. 5A shows such a regular middle leg and hindleg walk-like pattern (black bars) with irregular stepping of the front legs (grey bars). Phases of multiple steps of both front legs were randomly distributed with respect to the reference leg (R2 and R3) cycles. Mean direction vectors in circular plots (Fig. 5B; data not shown for reference leg R3) did not indicate a significant directionality (Rayleigh test). The relative occurrence of quadrupedal gaits on the horizontal surface with a walk-like pattern was 76.3% (7% wave gait), with a trot-like pattern was 17.3%, and with an irregular pattern was 6.4% (N=9, n=32); on a 15 deg upward slope the values were: walk-like 67.5%, trot-like 5.5%, irregular 27% (N=8, n=36); on a 90 deg upward slope the values were: walk-like 75.9%, trot-like 0.5%, irregular 23.6% (N=7, n=21); and on a 15 deg downward slope the values were: walk-like 42.8%, trot-like 43.3%, irregular 13.9% (N=7, n=36). The relative occurrence of different gaits with and without the front legs in the different walking situations is illustrated in Fig. 4A–D. The occurrence of irregular gaits significantly decreased when ignoring the front legs in walks on a horizontal surface and on upward slopes. The remaining irregular gaits were mainly due to gliding transitions between gaits. In contrast to irregular gaits, the relative occurrence of walk-like gaits was significantly higher than the amount of the corresponding tetrapod gaits in all walking situations except for downward slopes. The relative occurrence of the trot-like and corresponding tripod gait was comparable in all four walking situations. Wave gaits only occurred in 90 deg upward slope walks.

Walking in leg amputees

Multiple stepping performed by the front legs during walking suggests that front legs not only function as locomotor organs but also serve an additional function, for example to probe the environment (Cruse, 1976). Because this function is performed during walking, we were interested in whether front legs are necessary at all for the establishment of a regular gait in middle legs and hindlegs. We were also interested in whether front legs assume a more regular walking pattern in animals that lack support by either both middle legs or both hind legs. Therefore, we amputated leg pairs and subsequently allowed the animals to walk on a horizontal surface. From these walks we determined gaits, and calculated phases of the individual legs with respect to R2 or R3 cycles.

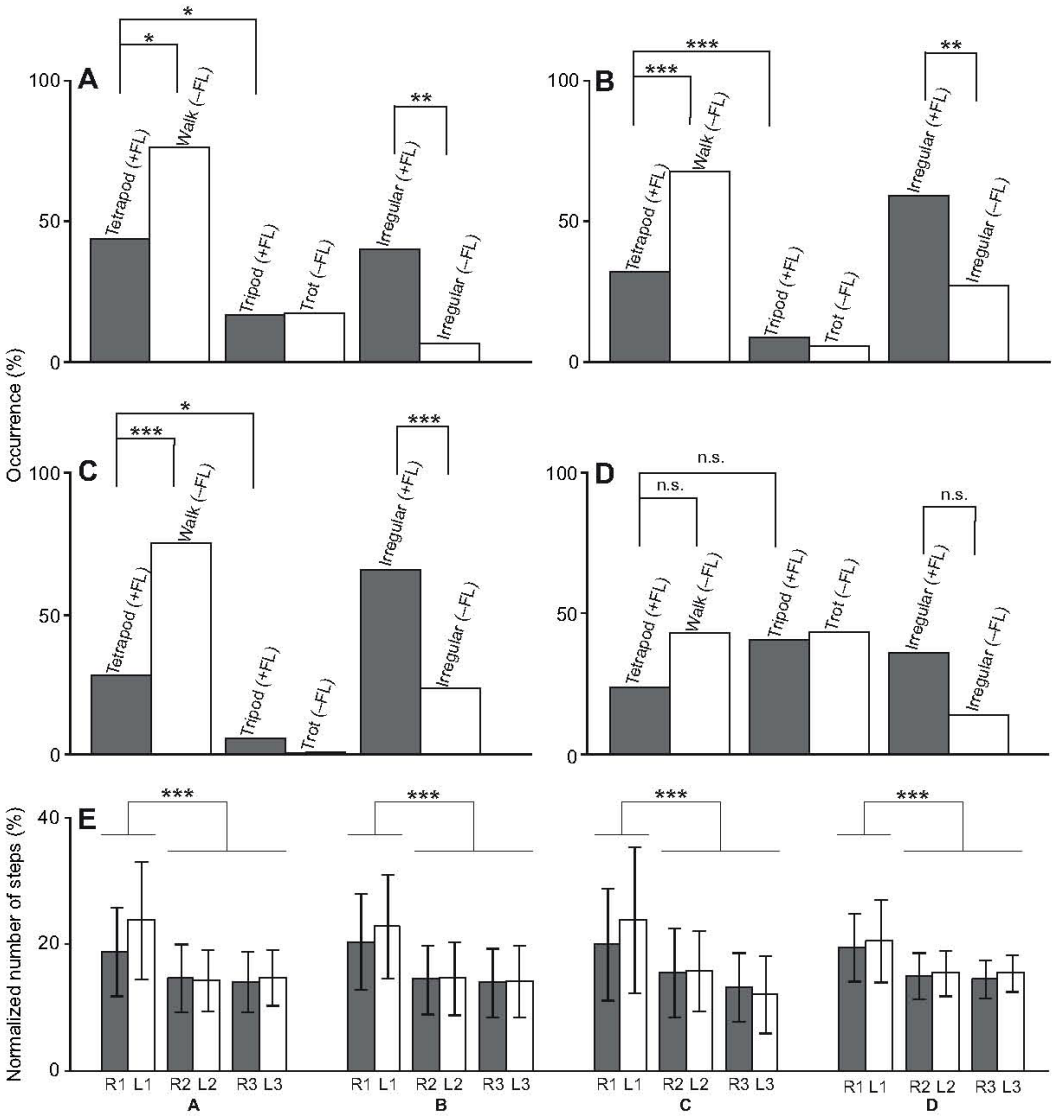

Fig. 4. Frequency of occurrence of different gaits in the different walking situations: (A) horizontal surface; (B) 15 deg upward slope; (C) 90 deg upward slope; and (D) 15 deg downward slope. Grey bars indicate hexapedal gaits; +FL, front legs were considered when assigning a gait. White bars indicate quadrupedal gaits; –FL, front legs were not considered when assigning a gait. Significance in the difference of occurrence of the different gaits was tested using the Wilcoxon rank sum test (*P<0.05, **P<0.01, ***P<0.001; n.s., not significant). The tetrapod gait was performed significantly more often than the tripod gait in A–C. When ignoring the front legs, the occurrence of irregular gaits significantly decreased in comparison to when all legs were considered. In parallel, the occurrence of walks when front legs were ignored was significantly higher than the occurrence of tetrapod gait when all legs were considered (A–C). (E) Normalized number of steps by the different legs in A–D. The front legs R1 and L1 performed a significantly greater number of steps than the other legs in all four walking situations (***P<0.001). Significance was tested using a one-tail ANOVA.

Phase relationships in intact stick insects

As a reference for the phase relationships between legs in amputation experiments, we determined the phases of swing movements in intact animals that walked on the horizontal surface. Phases of L3, L2, R3 and R1 were calculated with respect to the stepping period of R2 [Φ(R2–L3), Φ(R2–L2), Φ(R2–R3) and Φ(R2–R1), respectively] and phases of L3, L2, R2 and R1 with respect to the R3 period [Φ(R3–L3), Φ(R3–L2), Φ(R3–R2) and Φ(R3–R1), respectively]. The results are shown in Fig. 6. Animals used a tetrapod gait in 43.7% of the sections (see above). The two mirror-image tetrapod gaits were used equally often. When the front legs were ignored, 76.3% of the sections were classified as walk-like gaits (see above). Therefore, we expected phases to be most frequently near Φ(R2–L3)=0 and 0.33, Φ(R2–L2)=0.33 and 0.66, Φ(R2–R1)=0.33 and Φ(R2–R3)=0.66 and at Φ(R3–L3)=0.33 and 0.66, Φ(R3–L2)=0 and 0.66, Φ(R3–R1)=0.66 and Φ(R3–R2)=0.33 (see also stereotypic phases in Table 1).

When R2 was the reference leg, phases had the following circular means: Φ(R2–L3)=0.14 (n=407), Φ(R2–L2)=0.52 (n=418), Φ(R2–R1)=0.34 (n=474) and Φ(R2–R3)=0.61 (n=408)

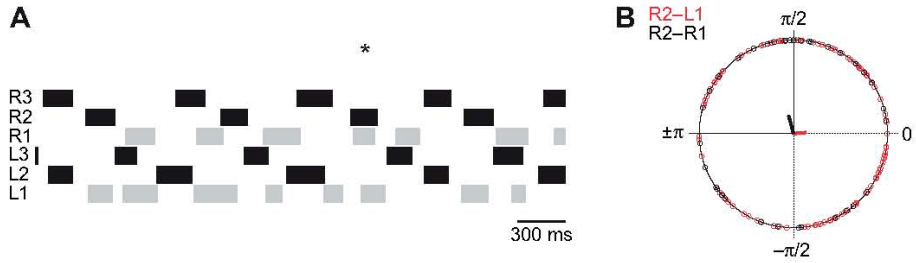

Fig. 5. (A) Example of an irregular walking pattern observed in an adult stick insect walking on a horizontal surface. Middle legs and hindlegs are coordinated in a regular quadrupedal walking pattern. Grey bars indicate that front legs were not considered. (B) Phase distributions of R1 (black) and L1 (red) in the R2 stepping cycle, only for irregular walking patterns. Phases for both front legs are randomly distributed and the resultant mean vectors (black and red) show no significant directionality (in both cases $P>0.05$). *Simultaneous swing of adjacent legs.

(N=9; Fig. 6A, Table 1). The data meet the expectations as phases for L3 and L2 lie well within the two phases that these legs adopt in an ideal tetrapod gait, and the phases of R3 and R1 are very close to their expected values. In addition, as expected, distributions for L3 and L2 phases were broader than those for R3 and R1 (Fig. 6A). This observation was corroborated by calculating the length of the mean direction vectors for the four legs. Vectors for L3 and L2 were significantly shorter than vectors for R3 and R1 ($P<0.001$, data not shown). The data generally met the expectations when R3 was the reference leg. Circular means of the phases were Φ(R3–L2)=0.91, Φ(R3–L3)=0.52, Φ(R3–R1)=0.73 and Φ(R3–R2)=0.34 (n=417). Also, a broader distribution for L3 and L2 phases in comparison to R2 and R1 phases was indicated by the significantly different lengths of the mean direction vectors ($P<0.001$, data not shown; see also Fig. 6B).

Gaits and phase relationships in front leg amputees

It is striking that front leg amputees almost exclusively used regular gaits (Fig. 7A). Irregular gaits were observed in only in 5.7% of the sections (N=7, n=161). Usually, animals walked with a wave gait (61%). Less often, the two mirror-image walk gaits were observed (20% walk 1, 18% walk 2; see Fig. 2 for ideal footfall patterns). Rarely, animals walked with trot gait (1%). The average number of steps (14–19 steps per leg) by individual legs in irregular gait sections did not significantly differ (Fig. 7B, $P>0.05$).

The circular means of the phases of R3 and L3 with respect to the R2 step cycle were Φ(R2–R3)=0.73 (n=202) and Φ(R2–L3)=0.22 (n=202), respectively (Fig. 7C). This was expected as they are close to the ideal phases in the observed quadrupedal gaits [Φ(R2–R3)=0.66 (walk) or 0.75 (wave gait) and Φ(R2–L3)=0 and 0.33 (walk) or 0.25 (wave gait); see Fig. 2B–D). Also, the phase relationship Φ(R2–L2)=0.47 was as expected for a typical wave gait (not shown).

To compare the phase distributions of the left and right hindleg (L3, R3) with respect to the R2 cycle in intact animals and in front leg amputees, we calculated mean resultant phase vectors and their lengths (Fig. 7D,E). All four vectors had significant directionality (Rayleigh test; $P<0.001$). Mean direction vectors of phase distributions of L3, L2 and R3 with respect to the R2 cycle in front leg amputees were significantly longer than corresponding vectors from intact animals ($P<0.05$; Fig. 7D,E). This means that phase distributions of L3, L2 and R3 with respect to the R2 cycle become narrower and thus more distinct in front leg amputees (compare also green and blue distributions in Fig. 6A and Fig. 7C).

Gaits and phase relationships in hindleg amputees

In hindleg amputee walking, the percentage of irregular gaits was about three times that of front leg amputee walking, i.e. 17.2% (N=8, n=30; Fig. 8A); 42% of the regular gait sections were wave gaits and 58% were walk gaits (40% walk 1, 18% walk 2). Trot was not observed. In irregular gaits, the number of front leg steps was significantly higher than the number of middle leg steps ($P<0.001$); 28% of all leg steps were L1 steps, 34% were R1 steps, 20% were L2 steps and 18% were R2 steps (Fig. 8B). This result indicates that irregular gaits are mainly due to multiple stepping or probing of the front legs as observed in intact animals.

The circular means of the phases of L2 and R1 with respect to the R2 cycle were Φ(R2–L2)=0.52 (n=253) and Φ(R2–R1)=0.25 (n=344) (see grey and red distributions in Fig. 8C). These phases were comparable to respective phases in the intact animal (compare with Fig. 6A). Mean phase vectors from hindleg amputees and intact animals had a significant directionality (Rayleigh test; $P<0.001$). Mean direction vectors of phase distributions of L2 and R1 with respect to the R2 cycle, however, were not significantly longer than corresponding vectors from intact animals ($P>0.05$; Fig. 8D,E). The phase distribution of L2 was significantly broader in hindleg amputees than in front leg amputees ($P<0.001$, data not shown). Thus, the distribution of the phases of L2 and R1 with respect to the R2 cycle did not become narrower and thus more distinct in hindleg amputees (compare also distributions for L2 and R1 in Fig. 6A and Fig. 8C).

In hindleg amputees, the abdomen was on the ground in 67.5% and in the air in 32.5% of the sections. However, the percentage of irregular sections was not significantly different between conditions (17.5% in animals with abdomen on the ground and 16.9% in animals with abdomen in the air). Thus, the position of the abdomen does not appear to affect the additional stepping activity in front legs.

Gaits and phase relationships in middle leg amputees

The percentage of irregular gaits was 27.7% in middle leg amputees (N=7, n=47; Fig. 9A); 56% of the regular gait sections were wave gaits and 44% were walk gaits (27% walk 1, 16% walk 2). Only 1% of all regular walking sections were trot. Interestingly, the average step number of individual legs in irregular gait sections did not significantly differ (Fig. 9B). Closer inspection revealed that, in contrast to all walking situations described above, irregular gaits did not mainly result from multiple front leg stepping. We observed multiple front leg steps in 22% of the irregular gait sections. In 12%, we observed multiple hindleg steps that were never observed in our other experimental situations. Of the irregular gait sections, 14%

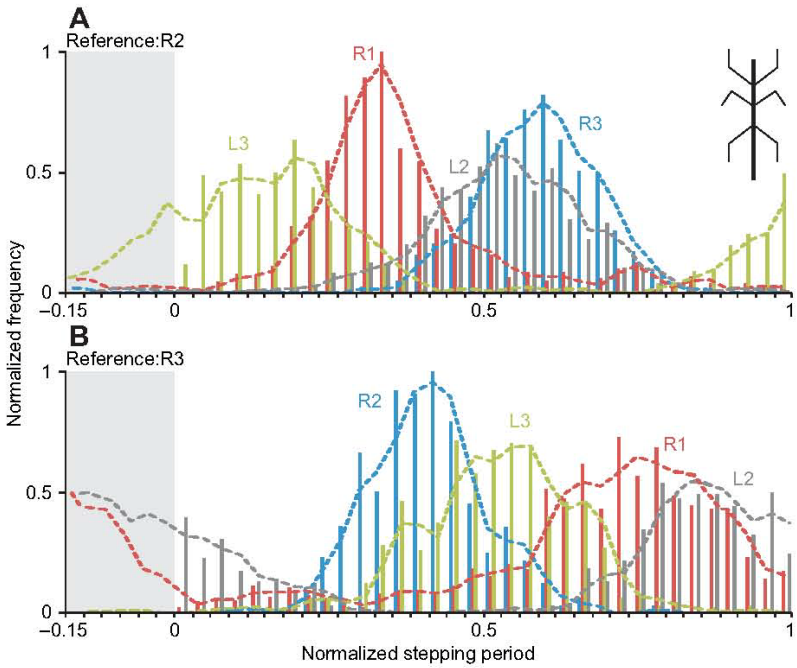

Fig. 6. Phases in intact animals walking on a horizontal surface. (A) Phase distributions of the right front leg (R1, red), right hindleg (R3, blue), left middle leg (L2, grey) and left hindleg (L3, green) with respect to the phase of the right middle leg (R2). (B) Phase distributions of the right front leg (R1, red), right middle leg (R2, blue), left middle leg (L2, grey) and left hindleg (L3, green) with respect to the phase of the right hindleg (R3).

were due to fast, simultaneous protraction of three legs (R3, L3, L1 or L3, R3, R1) and 16% to simultaneous swing movements of the two ipsilateral legs (R3, R1 or L3, L1; see supplementary material Movies 1–6). In 36% of irregular gait sections, switching between gaits or other irregular patterns occurred.

In this walking situation, we used R3 as the reference leg to calculate the phases of the three remaining legs. The circular means of the phases of R1, L3 and L1 with respect to the R3 cycle were Φ(R3–R1)=0.31, Φ(R3–L3)=0.51 and Φ(R3–L1)=0.76 (see Fig. 9C; note, only distributions of R1 and L3 are shown). As expected from the predominant quadrupedal wave and walk gaits (see above), the R1 swing starts far earlier in the R3 cycle than in the intact animal [Φ(R3–R1)=0.73; compare with Fig. 6B]. The respective mean direction vectors clearly indicate the difference in phase (Fig. 9D). Mean phase vectors from middle leg amputees and intact animals had a significant directionality (Rayleigh test; P<0.001; Fig. 9D,E).

The lengths of the mean direction vectors of R1 and L3 phase distributions with respect to the R3 cycle differed significantly between middle leg amputees and intact animals (P<0.05). The distribution of the R1 phases with respect to the R3 cycle became narrower in middle leg amputees (mean direction vector is longer). In contrast, the L3 phase distribution became broader, as indicated by the much shorter vector (compare the red and black vector in Fig. 9E).

To investigate whether irregular walking is primarily a consequence of a reduction in walking speed, we compared walking speeds in intact animals and middle leg amputees. As shown in Fig. 10, in intact animals (red box plots, N=9), the velocities of irregular (n=59) and tetrapod (n=76) gaits were not significantly different. The velocities of animals using these two gaits were significantly slower than the velocities of animals using tripod (n=29) gait. In middle leg amputees (black box plots, N=7), the velocities of animals using irregular (n=81), walk/wave (n=168) or trot (n=4) gaits did not differ significantly. Middle leg amputees that used irregular and walk/wave gaits were significantly slower than intact animals using irregular and tetrapod gaits. Thus, irregular gaits occur at slow velocities. However, not all animals that walk slowly necessarily use an irregular gait.

DISCUSSION

We investigated the leg coordination patterns of stick insects (*C. morosus*) walking freely along a straight path on a plane horizontal surface as well as on inclining and declining surfaces. We showed that, on horizontal and on inclining surfaces, tetrapod gaits occur significantly more often than a tripod walking pattern. On the horizontal surface, for example, tetrapod gaits occurred about 2.6 times more often than a tripod gait. On the 15 deg declining surface, there was no significant difference between the occurrence of tripod and tetrapod gaits. While Graham (Graham, 1972) states that a tripod gait is relatively rare in adult stick insects (he does not give quantitative data), our data show that the occurrence of a tripod gait in adult stick insects is not generally rare but rather context dependent. Generally, gaits in animals are correlated with walking speed (Alexander, 1989). It is thus reasonable to assume that the higher probability of tripod gaits on the declining surface is due to an increase in speed. This conclusion is supported by our observation that tripod gaits occur at higher speeds and by a previous finding that in stick insects walking on a treadmill, phase relationships of different legs change in gliding coordination as a function of walking speed (Wendler, 1965). In Wendler's experiments, a phase relationship corresponding to a tripod gait was obtained at higher walking speeds than those for the phase relationship corresponding to a tetrapod gait. Our results from walking on slopes suggest that load conditions may matter in determining gait. Nothing is known about this in stick insects yet. However, it has been reported in the locust (Duch and Pflüger, 1995) that 'motor patterns are relatively constant for a given walking situation, but are markedly altered under different conditions, such as horizontal walking, vertical climbing and upside down walking'.

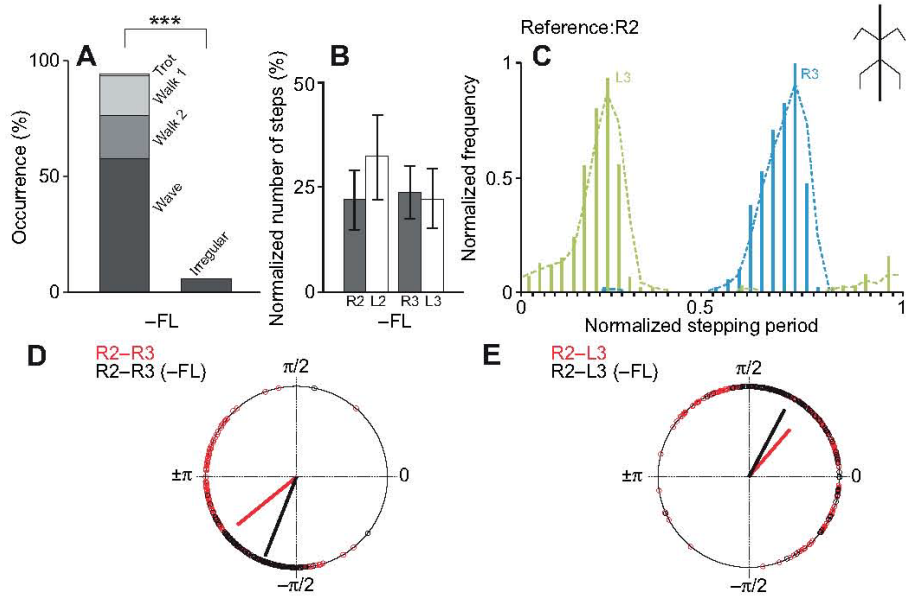

Fig. 7. Frequency of occurrence of different gaits (A), normalized number of steps by the middle legs and hindlegs (B), and phase distribution of legs (C–E) in front leg amputees. (A) Normalized occurrence of regular gaits (trot, walk 1, walk 2 and wave; left bar) and irregular gaits (right bar), which are rare occurrences. Within the regular gaits, the wave gait is the most common (***P<0.001). The two walk patterns (1 and 2) are used equally often. (B) There is no significant difference between the number of steps of the hindlegs and middle legs. (C) Phase distributions of the right hindleg (R3, blue) and the left hindleg (L3, green) with respect to the phase of R2. (D,E) Phase distributions of R3 and L3 for intact animals (red) and front leg amputees (black, –FL) shown as circles on the unit circle. Red and black lines indicate the direction and magnitude of the mean resultant vector in intact animals and amputees, respectively. In all four cases, significant predominant directionality of the mean resultant vectors is given (P<0.001). Mean resultant vectors for front leg amputees (black in D and E) are significantly longer than those for intact animals (red in D and E; P<0.05). These data indicate that distributions become narrower if the front legs are amputated.

Another interesting finding of our experiments is that animals often performed 'irregular' walking patterns that drastically differed from the classical gaits. These irregular gaits were most often observed on inclining slopes. On the horizontal surface, 39.7% of walking sections qualified as irregular gaits. In general, these gaits were a result of the occurrence of multiple front leg steps in the reference leg's (usually R2) cycle. A small amount of coordination irregularity is due to transitions between gaits. Our finding does not concur with that of Graham (Graham, 1972), who observed only eight 'extra' protractions in 400 leg cycles in adult stick insects walking on a horizontal surface for both front legs. However, our data are corroborated by Cruse's observation (Cruse, 1976) that *C. morosus* walking on a horizontal plane 'often make groping movements'. Cruse concluded, 'In a walk on the horizontal plane: the forelegs mainly have feeler function'. Judging from our data, this statement appears to be a slight exaggeration. However, the appearance of front leg multiple stepping is indeed context dependent. In our experiments, for example, the appearance of irregular coordination patterns increased during upward slope walking (Fig. 4), and Cruse (Cruse, 1976) mentions that front legs are much more regularly moved when animals walk a 30 mm wide horizontal path. We will avoid using the term feeler, although the behaviour suggests that the legs are used for probing the ground. Multiple stepping or probing is worthy of receiving further attention. First, stick insect legs do perform stereotypic searching movements in the context of loss of ground contact when reaching a gap (Dürr, 2001), although we do not know whether the multiple stepping that we observed is related to searching. Second, afferent feedback during ground contact in probing behaviour is likely to be different from feedback during ground contact in stance phase, in which the leg supports the body or provides a propulsive force (Zill et al., 2012). Such feedback does matter for inter-leg coordination (Wendler, 1965) and may be different during irregular gaits *versus* regular ones.

The multiple front leg steps were never phase coupled to the reference leg's cycle (Fig. 5B). When this behaviour occurred, middle legs and hindlegs continued to perform regular stereotypic walking patterns. These patterns relate to the two quadrupedal mirror-image walk gaits and the wave gait (Fig. 2B–D). It thus appears that the front legs can be uncoupled from the walking system without compromising the coordination of the other legs. The occurrence of front leg multiple stepping is limited to walk and wave gaits. This limitation is functional as tetrapod gaits with only one leg on each side in swing provide more stability during multiple stepping than a tripod gait.

Obviously, multiple stepping of the front legs during the step cycle of the right middle leg (R2) implies simultaneous protraction of ipsilateral front and middle legs (Fig. 3C, Fig. 5A). Cruse and co-workers identified six rules for leg coordination that operate between adjacent legs in the stick insect (Dean, 1989; Cruse, 1990). These rules do not consider multiple stepping of the front legs. In particular, rule 1, which establishes that swing prevents lift-off in the next anterior leg through forward-directed inhibition, is not always obeyed. However, context-dependent changes in the strength and efficacy of leg coordination mechanisms in stick insects have been described by Dürr (Dürr, 2005). Dürr concludes that 'the coordination rules that are thought to underlie many adaptive

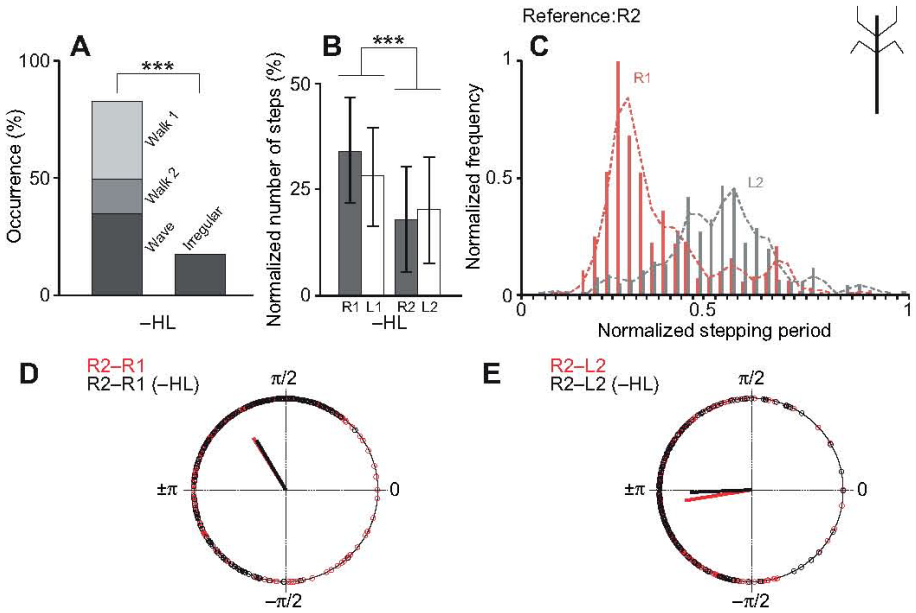

Fig. 8. Frequency of occurrence of different gaits (A), normalized number of steps by the front and middle legs (B), and phase distribution of legs (C–E) in hindleg amputees. (A) Regular gaits (walk 1, walk 2 and wave) are adopted significantly more often than irregular gaits (***P<0.001). No trot gait was observed. In most cases animals used the walk 1 and wave gait. (B) Normalized number of steps of the front and middle legs. Both front legs step significantly more often than the middle legs (P<0.001). (C) Phase distributions for the right front leg (R1, red) and the left middle leg (L2, grey) with respect to the phase of R2. (D,E) Phase distributions of R1 and L2 for intact animals (red) and hindleg amputees (black, –HL). Red and black lines indicate the direction and magnitude of the mean resultant vector in intact animals and amputees, respectively. In all four cases, significant predominant directionality of the mean resultant vectors is given (P<0.001). Mean resultant vectors for amputees (black in D and E) do not significantly differ in length from those for intact animals (red in D and E; P>0.05). These data indicate that the distributions become neither broader nor narrower if the hindlegs are amputated.

properties of the walking system, themselves adapt in a context-dependent manner'.

The general layout of the insect nervous system appears to be well suited to allow functionally specialized legs to be uncoupled from or coupled to the locomotor system. For example, the praying mantis, which has front legs designed for catching prey, normally walks with its middle legs and hindlegs using wave or walk gaits, like the front leg-amputated stick insect. During fast walking, however, the front legs may be used as 'walking legs' as well, leading to a tetrapod or tripod gait (Roeder, 1937). In locusts walking on a flat surface, hindlegs that are specialized for jumping may step such that it is not possible to define a hexapod gait, or may be well coordinated with front and middle legs. However, a front leg and its contralateral middle leg are always precisely coordinated in-phase (Pearson and Franklin, 1984).

Intact animals *versus* front leg amputees

In front leg amputees, phase distributions of both hindlegs and the left middle leg with respect to the right middle leg were less broad than in the intact animal. Also, the number of steps performed by the remaining legs did not differ significantly from one another (Fig. 7). These results suggest that inter-segmental information from the front legs is not necessary to coordinate and stabilize regular walking in the middle legs and hindlegs. Rather, the presence of front legs appears to cause a weaker coupling of the middle legs and hindlegs. In addition, the onset of hindleg swing in the ipsilateral middle leg cycle of front leg amputees is shifted from 0.61 in the intact animal to 0.73 in amputees. This shift is due to the appearance of the wave gait.

We do not know whether front leg multiple stepping generates intersegmental signals that are transmitted from the prothoracic ganglion to the mesothoracic ganglion. Generally, single front leg stepping in stick insects is able to modulate the membrane potential of ipsilateral middle leg motoneurons: middle leg protractor and retractor motoneurons in the deafferented mesothoracic ganglion become rhythmically active and phase coupled to ipsilateral front leg stepping on a treadmill (Ludwar et al., 2005; Borgmann et al., 2007). Borgmann and colleagues (Borgmann et al., 2009) have shown that middle leg sensory signals from campaniform sensilla could overcome front leg step-induced entrainment. Such local dominance might also adjust the effects of potential intersegmental signals transmitted during front leg multiple stepping.

Intact animals *versus* hindleg amputees

In hindleg amputees, 17.2% of walking sections were assigned to the category of irregular gaits based on the occurrence of multiple front leg steps (Fig. 8A,B). This observation is surprising because front leg multiple stepping is likely to compromise stability in the four-legged animal. And after all, multiple front leg stepping appears to be a context-dependent and therefore modifiable behaviour.

As the phase distribution of the left middle leg (L2) with respect to the phase of R2 did not change significantly, the regularity of middle leg movements remained unchanged in hindleg amputees. We therefore suggest that regular stepping of the middle legs does not depend on inter-segmental information from the hindlegs. Although middle leg stepping is quite regular, there might be an effect of multiple front leg stepping on middle leg stepping because

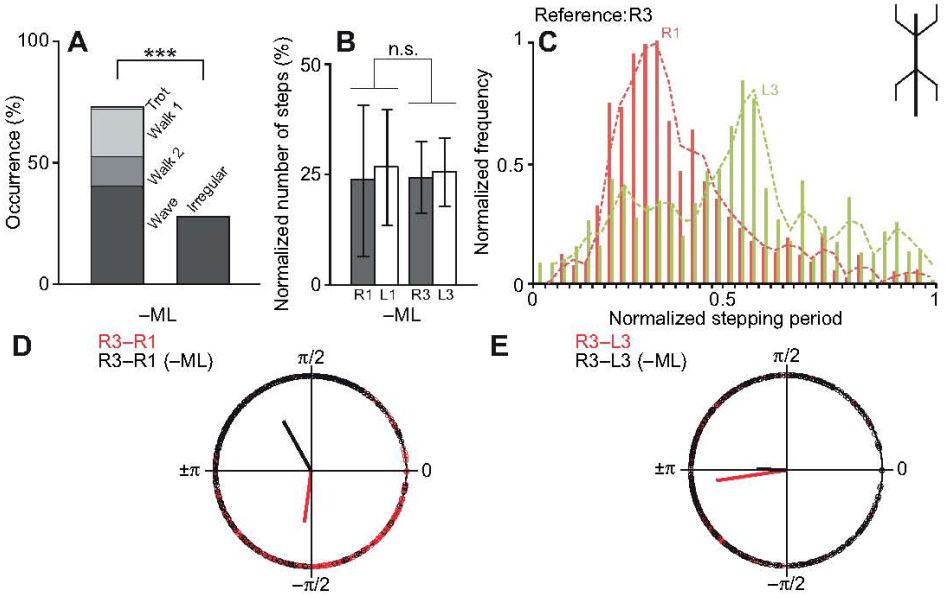

Fig. 9. Frequency of occurrence of the different gaits (A), normalized number of steps by the front legs and hindlegs (B), and phase distribution of the legs (C–E) in middle leg amputees. (A) Regular gaits (trot, walk 1, walk 2 and wave) are adopted significantly more often than irregular gaits (***P<0.001). Animals mostly used the wave gait. (B) There is no significant difference between the normalized number of front and middle leg steps. (C) Phase distributions for the right front leg (R1, red) and the left hindleg (L3, green) with respect to the phase of R3. (D,E) Phase distributions of R1 and L3 for intact animals (red) and middle leg amputees (black, –ML). Red and black lines indicate the direction and magnitude of the mean resultant vector in intact animals and amputees, respectively. In all four cases significant predominant directionality of the mean resultant vectors is given (P<0.001). The mean resultant vector of the phase distribution of L3 in the case of amputated middle legs (black in E) is significantly shorter than that for intact animals (red in E) (P<0.05). Mean resultant phase vector for R1 is significantly longer in amputees than in intact animals (P<0.05; D). These data indicate that the phase distribution of L3 with respect to the phase of R3 becomes significantly broader if the middle legs are amputated, whereas the broadness of the phase distribution of R1 decreases.

the L2–R2 phase distribution was broader in intact animals and hindleg amputees than in front leg amputees.

Intact animals *versus* middle leg amputees

In middle leg amputees, the percentage of irregular gait sections (~28%) was higher than in front leg or hindleg amputees. In contrast to all other cases described here, in middle leg amputees, multiple stepping of the front legs was not the main cause of irregular gaits. In 12% of all irregular sections, we observed multiple hindleg steps that almost never appeared in other conditions. Also, unstable coordination patterns occurred with both hindlegs and a front leg (14%) or two ipsilateral legs in swing phase (16%). Altogether, middle leg amputation destabilizes the walking system more than amputation of any other leg pair. A similar unstable coordination in middle leg amputees has been observed in cockroaches and in the grasshopper *Romalea* (Wilson, 1966). If regular gaits occurred in middle leg amputees, the wave gait and walk gaits were observed most often (Hughes, 1957; Wilson, 1966). The irregular gaits cannot exclusively be characterized by walking speed because walk and wave gaits occurred at the same average speed as irregular gaits (Fig. 10).

First instar stick insect amputees change their regular tripod gait into a gait similar to gait II (Graham, 1976), a walk gait (the corresponding figure in Graham's paper actually shows a wave gait). Graham did not report unstable situations for instars. However, we can assume that the walking system becomes less rigidly coordinated in the course of ontogenesis. In this context, it is interesting that the model Walknet, a biologically inspired network to control six-legged locomotion that is based on the previously mentioned rules for coordination (Dürr et al., 2004) (see also Cruse, 1990), failed to produce a coordinated walking pattern after 'amputation' of both middle legs (Schilling et al., 2007). A stable coordination was regained after introducing a rule that prevents a front leg swing when the ipsilateral hindleg is swinging. If such a mechanism is present in the adult stick insect, it appears to be weakly developed.

Our experiments indicate that in stick insects the presence of middle legs is important for the organization of a regular functional activity pattern in the hindlegs as seen in intact animals and front leg amputees. The mechanisms for such influences are unclear, especially as Borgmann and colleagues (Borgmann et al., 2007) have shown that in a single middle leg preparation the stepping middle leg is not able to induce rhythmic alternating activity in either hindleg or front leg protractor and retractor motoneurons (Borgmann et al., 2007). Thus, under their experimental conditions, the effects of middle leg stepping on the adjacent ipsilateral legs were quite weak. In contrast, single front leg walking does induce rhythmic activity in middle leg protractor and retractor motoneurons and is even able to produce in-phase coupling of pharmacologically induced alternating activity in hindleg protractor and retractor motoneurons (Borgmann et al., 2009). While the effect of front leg walking on the hindlegs is weak, the effect on middle leg protractor/retractor motoneuron activity is quite strong (Ludwar et al., 2005; Borgmann et al., 2007). Again, such a strong effect is not seen in our

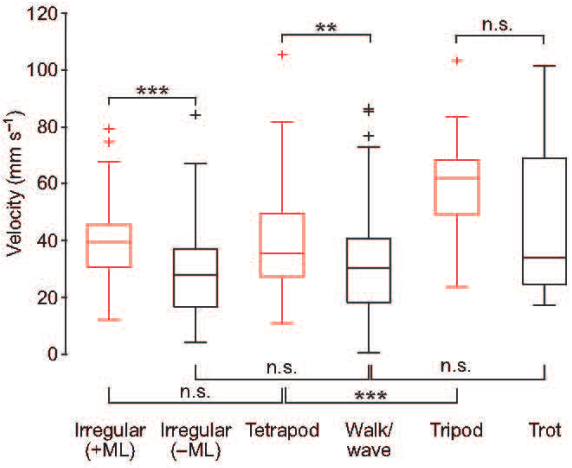

Fig. 10. Walking velocities in intact animals (red, +ML) and middle leg amputees (black, –ML). Box–whisker plots are shown for irregular, tetrapod, walk/wave, tripod and trot gaits (**P<0.01, ***P<0.001).

experiments, where the middle legs in hindleg amputees show a more regular pattern than the front legs. In addition, the in-phase coupling of retractor and protractor motoneurons in ipsilateral legs observed by Borgmann and colleagues (Borgmann et al., 2007; Borgmann et al., 2009) does not match our data. However, the importance of local load signals and their ability to overcome intersegmental entrainment has already been mentioned and may also be responsible for our observations in middle leg amputees. In a stick insect walking on a treadmill, the impact of such load signals is likely to be the cause of the ~180 deg phase shift in protractor and retractor activity after ground contact was regained by mounting a peg leg to a partly amputated middle leg (Wendler, 1965). Middle leg afferents appear to be essential not only for an adequate middle leg phasing but also for intersegmental coordination. For a proper coordination of ipsilateral legs, phasic afferent input induced by the normal motions of the middle legs appears to be important because in tethered stick insects walking on a treadmill, ipsilateral front leg and hindleg movements are not phase locked to one another when the middle legs rest on a platform (Wendler, 1965). Such uncoupling of front legs and hindlegs might destabilize walking in untethered middle leg amputees.

Gaits in amputees and inter-leg control

Our experiments corroborate the observation that, after amputation, arthropods generally adopt a functional gait with phase relationships different from those for six-legged locomotion. Amputees in our experiments often adopted the wave gait, which was rarely observed in intact animals. Such adaptivity has been reported for spiders (Wilson, 1967; Foelix, 1996), cockroaches (Hughes, 1957; Delcomyn, 1971), stick insects (von Buddenbrock, 1921; von Holst, 1943; Wendler, 1965; Graham, 1977) and other arthropods (see review by Wilson, 1966). The adaptations provide stability and are probable means of reducing energy expenditure, like gait changes in intact animals that adapt to changing speed (Alexander, 1989; Nishii, 2000). A rare example of a non-adaptive behaviour is escape running in cockroaches that carry an extra load. The startled animals use a tripod gait that is not functional because it does not compensate for the increased load (Quimby et al., 2005).

At first glance, the notion that inter-leg coordination depends on sensory feedback appears to be trivial. In locusts, it has been shown that signals from leg sense organs are largely conveyed by intersegmental interneurons to other ganglia and only rarely do sense organs have intersegmental projections (Hustert, 1978). The intersegmental interneurons can be descending (Laurent, 1987; Laurent and Burrows, 1989a; Laurent and Burrows, 1989b) or ascending (Laurent and Burrows, 1988). Some mesothoracic intersegmental interneurons make connections with ipsilateral metathoracic non-spiking interneurons and motoneurons (Laurent and Burrows, 1989b). However, the role of sense organs in inter-leg coordination is poorly understood (for review, see Büschges and Gruhn, 2007). For example, the neuronal basis of the coordination rules identified by Cruse and co-workers (Cruse, 1990; Dürr et al., 2004) is still largely unknown. So far, only a few interneurons in the stick insect have been identified that could mediate intersegmental coordination between middle legs and hindlegs (Brunn and Dean, 1994). This lack of knowledge is in sharp contrast to the wealth of information we have for local feedback control of a single leg stepping cycle (for review, see Büschges, 2005; Büschges and Gruhn, 2007). Cruse (Cruse, 1985a; Cruse, 1985b) provides evidence that swing phase starts upon a small initial forward movement of the leg followed by a decrease in load, which also reinforces swing phase muscle activity as shown by Akay and colleagues (Akay et al., 2001; Akay et al., 2004). Such mechanisms are also effective in inter-leg control. In cockroaches, triggering activity in campaniform sensilla of the middle leg by mechanical action of the hindleg could facilitate the onset of swing in the middle leg through local reflex effects (Zill et al., 2009). Such an emergent mechanism of inter-leg control that results from mechanical forces should be effective whenever legs are mechanically coupled through the substrate. Interestingly, however, lasting stable functional coordination of leg movements was rarely achieved by middle leg amputees, but was often found in front leg and hindleg amputees (we do not consider multiple stepping in front legs). Therefore, inter-leg coordination appears to depend largely on intersegmental neural pathways that are most effective between adjacent legs.

CONCLUSIONS

(1) Front legs have a special role during walking as they show multiple stepping, independent of the walking cycles of the adjacent legs. At the same time, coordination in middle legs and hindlegs is organized in gaits typical for quadrupeds. Inter-segmental information from the front legs is not necessary to coordinate and stabilize these patterns. However, front legs can be coupled to the locomotor system and then regular hexapedal walking is generated. This would correspond to a strengthening of the inter-segmental connections at least between the front and middle legs. (2) Afferent information from the middle legs seems to be necessary to produce regular stepping in the hindlegs. This assumption implies a special role for middle leg afferent signals in inter-leg coordination. (3) Hindleg afferent signals, in contrast, do not seem to be necessary for middle legs to produce regular stepping.

The different functionality of the legs and the resulting flexibility of the walking system need therefore to be considered in modelling studies of insect locomotion.

ACKNOWLEDGEMENTS

We thank Drs A. Borgmann, A. Büschges, M. Gruhn, S. Hooper, T. I. Toth and S. Zill for stimulating discussions in the course of this work and Dr T. Bockemühl for his Matlab program for analysing walking speed.

FUNDING

This study was supported by Deutsche Forschungsgemeinschaft [grant DA1182/1-1] and by generous start-up support from the University of Cologne, Department of Animal Physiology, Cologne, Germany.

REFERENCES

Akay, T., Bässler, U., Gerharz, P. and Büschges, A. (2001). The role of sensory signals from the insect coxa-trochanteral joint in controlling motor activity of the femur-tibia joint. *J. Neurophysiol.* **85**, 594-604.

Akay, T., Haehn, S., Schmitz, J. and Büschges, A. (2004). Signals from load sensors underlie interjoint coordination during stepping movements of the stick insect leg. *J. Neurophysiol.* **92**, 42-51.

Alexander, R. M. (1989). Optimization and gaits in the locomotion of vertebrates. *Physiol. Rev.* **69**, 1199-1227.

Batschelet, E. (1981). *Circular Statistics in Biology* (ed. R. Sibson and J. E. Cohen). London, UK: Academic Press.

Bender, J. A., Simpson, E. M., Tietz, B. R., Daltorio, K. A., Quinn, R. D. and Ritzmann, R. E. (2011). Kinematic and behavioral evidence for a distinction between trotting and ambling gaits in the cockroach *Blaberus discoidalis*. *J. Exp. Biol.* **214**, 2057-2064.

Berens, P. (2009). CircStat: A Matlab Toolbox for Circular Statistics. *J. Stat. Softw.* **31**, Issue 10.

Borgmann, A., Scharstein, H. and Büschges, A. (2007). Intersegmental coordination: influence of a single walking leg on the neighboring segments in the stick insect walking system. *J. Neurophysiol.* **98**, 1685-1696.

Borgmann, A., Hooper, S. L. and Büschges, A. (2009). Sensory feedback induced by front-leg stepping entrains the activity of central pattern generators in caudal segments of the stick insect walking system. *J. Neurosci.* **29**, 2972-2983.

Brunn, D. E. and Dean, J. (1994). Intersegmental and local interneurons in the metathorax of the stick insect *Carausius morosus* that monitor middle leg position. *J. Neurophysiol.* **72**, 1208-1219.

Büschges, A. (2005). Sensory control and organization of neural networks mediating coordination of multisegmental organs for locomotion. *J. Neurophysiol.* **93**, 1127-1135.

Büschges, A. and Gruhn, M. (2007). Mechanosensory feedback in walking: from joint control to locomotor patterns. *Adv. Insect Physiol.* **34**, 193-230.

Cruse, H. (1976). The function of legs in the free walking stick insect, *Carausius morosus*. *J. Comp. Physiol. A* **112**, 235-262.

Cruse, H. (1985a). Which parameters control the leg movement of a walking insect? I. Velocity control during the stance phase. *J. Exp. Biol.* **116**, 343-355.

Cruse, H. (1985b). Coactivating influences between neighbouring legs in walking stick insects. *J. Exp. Biol.* **114**, 513-519.

Cruse, H. (1990). What mechanisms coordinate leg movement in walking arthropods? *Trends Neurosci.* **13**, 15-21.

Cruse, H., Dürr, V., Schilling, M. and Schmitz, J. (2009). Principles of insect locomotion. In *Spatial Temporal Patterns for Action-Oriented Perception in Roving Robots* (ed. P. Arena and L. Patanè), pp. 1-57. Berlin: Springer.

Dean, J. (1989). Leg coordination in the stick insect *Carausius morosus*: effects of cutting thoracic connectives. *J. Exp. Biol.* **145**, 103-131.

Delcomyn, F. (1971). The locomotion of the cockroach *Periplaneta americana*. *J. Exp. Biol.* **54**, 453-496.

Delcomyn, F. (1981). Insect locomotion on land. In *Locomotion and Energetics in Arthropods* (ed. C. F. Herreid and C. R. Fourtner), pp. 103-125. New York: Plenum Press.

Duch, C. and Pflüger, H. J. (1995). Motor patterns for horizontal and upside-down walking and vertical climbing in the locust. *J. Exp. Biol.* **198**, 1963-1976.

Dürr, V. (2001). Stereotypic leg searching movements in the stick insect: kinematic analysis, behavioural context and simulation. *J. Exp. Biol.* **204**, 1589-1604.

Dürr, V. (2005). Context-dependent changes in strength and efficacy of leg coordination mechanisms. *J. Exp. Biol.* **208**, 2253-2267.

Dürr, V., Schmitz, J. and Cruse, H. (2004). Behaviour-based modelling of hexapod locomotion: linking biology and technical application. *Arthropod Struct. Dev.* **33**, 237-250.

Foelix, R. F. (1996). *Biology of Spiders*, pp. 130-135. Oxford: Oxford University Press.

Graham, D. (1972). A behavioural analysis of the temporal organisation of walking movements in the 1st instar and adult stick insect (*Carausius morosus*). *J. Comp. Physiol. A* **81**, 23-52.

Graham, D. (1977). The effect of amputation and leg restraint on the free walking coordination of the stick insect *Carausius morosus*. *J. Comp. Physiol. A* **116**, 91-116.

Graham, D. (1985). Pattern and control of walking in insects. *Adv. Ins. Physiol.* **18**, 31-140.

Gruhn, M., Zehl, L. and Büschges, A. (2009). Straight walking and turning on a slippery surface. *J. Exp. Biol.* **212**, 194-209.

Hughes, G. M. (1952). The co-ordination of insect movements. I. The walking movements of insects. *J. Exp. Biol.* **29**, 167-285.

Hughes, G. M. (1957). The co-ordination of insect movements. II. The effect of limb amputation and the cutting of commissures in the cockroach (*Blatta orientalis*). *J. Exp. Biol.* **34**, 306-333.

Hustert, R. (1978). Segmental and interganglionic projections from primary fibres of insect mechanoreceptors. *Cell Tissue Res.* **194**, 337-351.

Laurent, G. (1987). The morphology of a population of thoracic intersegmental interneurones in the locust. *J. Comp. Neurol.* **256**, 412-429.

Laurent, G. and Burrows, M. (1988). A population of ascending intersegmental interneurones in the locust with mechanosensory inputs from a hind leg. *J. Comp. Neurol.* **275**, 1-12.

Laurent, G. and Burrows, M. L. (1989a). Intersegmental interneurons can control the gain of reflexes in adjacent segments of the locust by their action on nonspiking local interneurons. *J. Neurosci.* **9**, 3030-3039.

Laurent, G. and Burrows, M. L. (1989b). Distribution of intersegmental inputs to nonspiking local interneurons and motor neurons in the locust. *J. Neurosci.* **9**, 3019-3029.

Ludwar, B. C., Göritz, M. L. and Schmidt, J. (2005). Intersegmental coordination of walking movements in stick insects. *J. Neurophysiol.* **93**, 1255-1265.

Nishii, J. (2000). Legged insects select the optimal locomotor pattern based on the energetic cost. *Biol. Cybern.* **83**, 435-442.

Pearson, K. G. and Franklin, R. (1984). Characteristics of leg movements and patterns of coordination in locusts walking on rough terrain. *Int. J. Robot. Res.* **3**, 101-112.

Pflüger, H.-J. (1977). The control of the rocking movements of the phasmid *Carausius morosus* Br. *J. Comp. Physiol. A* **120**, 181-202.

Quimby, L., Amer, A.S., Zill, S.N. (2005). Effects of increased body load in cockroach walking and running. *Society for Neuroscience Abstracts* **31**, program no. 54.18.

Ritzmann, R. E. and Büschges, A. (2007). Adaptive motor behavior in insects. *Curr. Opin. Neurobiol.* **17**, 629-636.

Roeder, K. D. (1937). The control of tonus and locomotor acivity in the praying mantis (*Mantis religiosa* L.). *J. Exp. Zool.* **76**, 353-374.

Schilling, M., Cruse, H. and Arena, P. (2007). Hexapod walking: an expansion to walknet dealing with leg amputations and force oscillations. *Biol. Cybern.* **96**, 323-340.

Spirito, C. P. and Mushrush, D. L. (1979). Interlimb coordination during slow walking in the cockroach. *J. Exp. Biol.* **78**, 233-243.

von Buddenbrock, W. (1921). Der rhythmus der schreitbewegungen der stabheuschrecke dixippus. *Biol. Zblt.* **41**, 41-48.

von Holst, E. (1943). Über relative Koordination bei Arthropoden. *Pflügers. Arch.* **246**, 847-865.

Wendler, G. (1964). Laufen und stehen der stabheuschrecke carausius morosus: sinnesborstenfelder in den beingelenken als glieder von regelkreisen. *Z. Vgl. Physiol.* **48**, 198-250.

Wendler, G. (1965). The co-ordination of walking movements in arthopods. *Symp. Ssc. Exp. Biol.* **20**, 229-249.

Wilson, D. M. (1966). Insect walking. *Annu. Rev. Entomol.* **11**, 103-122.

Wilson, D. M. (1967). Stepping patterns in tarantula spiders. *J. Exp. Biol.* **47**, 133-151.

Zill, S. N., Keller, B. R. and Duke, E. R. (2009). Sensory signals of unloading in one leg follow stance onset in another leg: transfer of load and emergent coordination in cockroach walking. *J. Neurophysiol.* **101**, 2297-2304.

Zill, S. N., Schmitz, J., Chaudhry, S. and Büschges, A. (2012). Force encoding in stick insect legs delineates a reference frame for motor control. *J. Neurophysiol.* **108**, 1453-1472.

4.2 A Neuro-Mechanical Model Explaining the Physiological Role of Fast and Slow Muscle Fibers at Stop and Start of an Insect Leg.

Tibor Istvan Toth, Martyna Grabowska, Joachim Schmidt, Ansgar Büschges, Silvia Daun-Gruhn

Published in PLoS ONE (8(11): e78246, 2013)

Author contributions

Conceived and designed the experiments
Tibor Istvan Toth, Silvia Daun-Gruhn

Performed the experiments
Tibor Istvan Toth, Martyna Grabowska

Analyzed the data
Tibor Istvan Toth, Martyna Grabowska
Joachim Schmidt, Ansgar Büschges
Silvia Daun-Gruhn

Figure preparation:
Tibor Istvan Toth, Martyna Grabowska

First version of manuscript
Tibor Istvan Toth

Wrote the paper
Tibor Istvan Toth, Martyna Grabowska
Joachim Schmidt, Ansgar Büschges
Silvia Daun-Gruhn

Contributed reagents/materials/analysis tools
Ansgar Büschges, Silvia Daun-Gruhn

OPEN ACCESS Freely available online

PLOS | ONE

A Neuro-Mechanical Model Explaining the Physiological Role of Fast and Slow Muscle Fibres at Stop and Start of Stepping of an Insect Leg

Tibor Istvan Toth[1], Martyna Grabowska[1], Joachim Schmidt[2], Ansgar Büschges[2], Silvia Daun-Gruhn[1]*

1 Emmy Noether Research Group of Computational Biology, Department of Animal Physiology, University of Cologne, Cologne, Germany, **2** Department of Animal Physiology, University of Cologne, Cologne, Germany

Abstract

Stop and start of stepping are two basic actions of the musculo-skeletal system of a leg. Although they are basic phenomena, they require the coordinated activities of the leg muscles. However, little is known of the details of how these activities are generated by the interactions between the local neuronal networks controlling the fast and slow muscle fibres at the individual leg joints. In the present work, we aim at uncovering some of those details using a suitable neuro-mechanical model. It is an extension of the model in the accompanying paper and now includes all three antagonistic muscle pairs of the main joints of an insect leg, together with their dedicated neuronal control, as well as common inhibitory motoneurons and the residual stiffness of the slow muscles. This model enabled us to study putative processes of intra-leg coordination during stop and start of stepping. We also made use of the effects of sensory signals encoding the position and velocity of the leg joints. Where experimental observations are available, the corresponding simulation results are in good agreement with them. Our model makes detailed predictions as to the coordination processes of the individual muscle systems both at stop and start of stepping. In particular, it reveals a possible role of the slow muscle fibres at stop in accelerating the convergence of the leg to its steady-state position. These findings lend our model physiological relevance and can therefore be used to elucidate details of the stop and start of stepping in insects, and perhaps in other animals, too.

Citation: Toth TI, Grabowska M, Schmidt J, Büschges A, Daun-Gruhn S (2013) A Neuro-Mechanical Model Explaining the Physiological Role of Fast and Slow Muscle Fibres at Stop and Start of Stepping of an Insect Leg. PLoS ONE 8(11): e78246. doi:10.1371/journal.pone.0078246

Editor: Vladimir Brezina, Mount Sinai School of Medicine, United States of America

Received April 29, 2013; **Accepted** September 10, 2013; **Published** November 22, 2013

Funding: This work was supported by DFG Emmy-Noether Programme (http://www.dfg.de/en/research_funding/programmes/individual/emmy_noether/index.html). The funders had no role in study design, data collection and analysis, decision to publish, or preparation of the manuscript.

Competing Interests: The authors have declared that no competing interests exist.

* E-mail: sgruhn@uni-koeln.de

Introduction

When legged animals stop or start stepping, a transition between posture and locomotion takes place. Thus stop and start of stepping are essential basic actions of the musculo-skeletal system of a leg. There is experimental evidence [1] that a leg does not stop randomly during its step cycle. Rather it stops or starts stepping in a systematic way depending on its position within the stepping cycle [1]. It is therefore reasonable to assume that both processes require coordinated actions of the leg muscles. This is presumably achieved by the interactions of the local neuronal networks that control the activity of the leg muscles. For a deeper understanding of the underlying neurophysiological mechanisms of locomotion in insects, it is thus quite important to study and analyze its elementary processes such as stop and start of stepping. This may open up the way for tackling more complex processes of walking in various conditions.

To be specific, in the stick insect, 3 pairs of antagonistic muscles play the major part in locomotion: the m. protractor and retractor coxae at the thorax-coxa (ThC) joint, the m. levator and depressor trochanteris at the coxa-trochanter (CTr) joint, and the m. flexor and extensor tibiae at the femur-tibia (FTi) joint. The coordination of their activity within a leg is achieved by means of proprioceptive sensory signals. They report load or position, or position and (angular) velocity to the nervous system. The load signals are generated in the campaniform sensilla (CS) [2], the position signals in specialized hairfields [3 5], and the position and (angular) velocity signals in the chordotonal organs [6,7]. Chordotonal organs are present in other insects, as well [8,9]. Their sensory signals are conveyed between the local neuronal networks controlling the activity of the muscle pairs. On the efferent side, one can distinguish between slow and fast muscle fibres constituting each of the above muscles according to their contraction kinetics [10,11], or histochemical properties [12]. [10] and [11] showed that the two types are anatomically separated in the extensor tibiae muscle of the stick insect but more importantly that they also have different physiological function: fast muscle fibres are active during stepping, only, whereas slow muscle fibres are responsible for maintaining the static position (posture) of the stick insect. Since [12], in a recent work, showed the existence of slow and fast fibres in the other, aforementioned muscles, too, it seems reasonable to assume that they have analogous function in those muscles, as well.

The question now arises whether and how the neuro-muscular system just described can bring about the stop and start of stepping of an insect leg. One suitable way to try to answer this question is to use appropriate mathematical models. In the accompanying paper [34], we presented a neuro-mechanical model that included slow and fast muscle fibres and their dedicated controlling

neuronal networks. In this paper, we apply an extended version of this model in an attempt to unveil and elucidate the details of the stopping and starting of stepping. We have thus extended the model in [34] to include four important new properties: i) all six muscle types have both slow and fast fibres; ii) the slow muscle fibres possess residual stiffness, and iii) are controlled by the activity of the common inhibitor motoneuron CI1 (for the flexor tibiae muscle CI2 and CI3); iv) the effects of the position and (angular) velocity sensory signals are implemented. As a result, we can suggest neuro-mechanical mechanisms that might exist in insects at stop and start of stepping. More generally, we hope to have helped gain a deeper understanding of elementary mechanisms of locomotion in insects, and perhaps in other animals, too.

Methods

The model comprising all three neuro-muscular systems

The model introduced in this paper is an extension of the models in [13] and the accompanying paper [34]. Fig. 1 shows the network with all three neuro-muscular systems. Each of them is now equipped with slow muscles, too, and with motoneurons (MNs) that innervate the slow muscles (in short slow MNs), as well as with the corresponding interneurons (INs). The three systems are coupled via position and load signals [2] represented by the levation angle β (hexagon with β in Fig. 1). If β exceeds, or falls below, a critical value ($\beta_{cr} = 38^o$ for the protractor-retractor system and $\beta_{cr} = 50^o$ for the extensor-flexor system), it will initiate a new (swing or stance) phase of a stepping cycle. For a more detailed explanation, see [13].

The activation kinetics of a muscle fibre during a contraction initiated by the excitation of its MN determine its type. Thus fast muscle fibres have fast activation kinetics and slow fibres much slower ones compared to those of the fast muscle fibres. The slow kinetics of the slow muscle fibres are therefore characterized by small rate constants, which apply during an incoming action potential. The specific values of the activation rate constants of the fast muscle fibres are listed in Table 1 for each muscle type. These values were chosen in earlier versions of the model [13,14] such as to fit the movements of the femur and the tibia during the swing and the stance phase of the stepping leg as seen in the experiments [15].

The values of the activation rate constants of the corresponding slow muscle fibres were set to be 100 times smaller. The relaxation rate constants (b values) were chosen to be identical in both muscle types ($b = 0.01$ ms^{-1} for all muscle types). Details of the properties of the neuron and muscle models and the neuro-muscular coupling can be found in [14] and in the accompanying paper [34].

However, the elastic properties of the slow muscle fibres differ substantially from those of the fast ones. All types of the slow fibres are assumed to have a positive residual stiffness, while the fast ones are not. Formally that means that the actual value, $k(t)$, of the stiffness (spring constant) of the *slow* muscles in the absence of an action potential is now calculated as

$$k(t) = k_\infty - [k_{res} - k(t_0)]\exp[-b(t - t_0)] \qquad (1)$$

(cf. eqns 1 2 in the accompanying paper [34]). Here is k_{res}, the actual value of the residual stiffness. This value can be affected by the activity of the CI1 (and CI2-CI3) (see below). The residual stiffness ensures that static positions of the stick insect are maintained over a longer period of time with virtually no driving activity of the motoneurons innervating these fibres [16]. The value of the residual stiffness is controlled by the activity of common inhibitory MNs. The common inhibitory MN CI1 innervates slow fibres of five of the six muscles named above. (The slow flexor tibiae muscle is innervated by CI2 and CI3.) [17] performed experiments on the locust and showed that the residual stiffness of the slow muscles is abolished during locomotion (stepping) by the activity of CI1. He suggested that the main physiological role of CI1 (and of the synchronously active CI2 and CI3 in the m. flexor tibiae [18]) is to ensure fast movements of the limbs, especially during the swing phase (e.g. during protraction in the protractor-retractor muscle system). Similar results were obtained in the crab [19] and in the cockroach [20,21]. We implemented the residual stiffness of the slow muscle fibres in accordance with these findings and hypotheses. Table 2 lists its value for each muscle type. The values in Table 2 were chosen such that the stationary position, i.e. the angles β and γ at the coxa-trochanter and the femur-tibia joint, respectively, be in the range of angles measured in the stick insect in its standing resting position (Fig. 2). Thus, β in a small range around 30^o ($\beta \approx 30^o$), and γ in the range of 80^o to 90^o ($\gamma \approx 84^o$) [22]. The position of the femur in the horizontal plane is determined by the angle α. Its stationary value was set to 90^o, and the values of the residual spring constants of the slow protractor and retractor muscles were calculated accordingly (Table 2). These "basic" stationary values can, of course, be modified by making use of the recruitment properties of the model (cf. Results and the accompanying paper [34]).

In the present version of the model, we implemented the function of CI1 implicitly. We did not model the mechanism itself that produces the changes in the residual stiffness of the slow muscle fibres during activity of CI1 but the effect, i.e. the changes, only. Hence, the residual values of the spring constants assume their stationary (nonzero) values during inhibition of the innervating CI1. During stepping, when CI1 is active, the residual values vanish in the swing phase and are small in the stance phase of the stepping. To be more specific, CI1 affects the actual value of the residual stiffness k_{res} of a slow muscle in the following way:

$$k_{res} = \begin{cases} k_{res0} & \text{in steady state : } t \in [t_{stop}, t_{start}] \\ 0 & \text{during stepping if } V_{CN}(t) < V_{th} \\ k_{res0}/10 & \text{during stepping if } V_{CN}(t) \geq V_{th} \end{cases} \qquad (2)$$

In this eqn, k_{res0} is the value of the residual stiffness k_{res} which it assumes during steady state. Furthermore, t_{stop} is the onset of the stop command, and t_{start} is the onset of the command for re-start. $V_{CN}(t)$, with $N = 1,\mathbf{4},5$, denotes the actual value of the membrane potential of the 'retractor' (C1), 'depressor' (C4) and 'extensor' (C5) CPG neurons' (cf. Fig. 1). V_{th} is a threshold value (set to $-25mV$ in the simulations). It is used to decide whether the CPGs are in phases corresponding to the swing phase of the stepping cycle, in particular, whether the protractor-retractor CPG is in the protraction phase. That is, if the neurons CN, $N = 1,\mathbf{4},5$ are sufficiently hyperpolarized, the leg is in the swing (protraction) phase. The third condition in eqn 2 means that the stepping movement is in the stance phase. Obviously, during stepping: $t \notin [t_{stop}, t_{start}]$. The lack of residual stiffness in the swing phase increases the speed of the leg movement, in accordance with the experimental findings [17,19,21]. In the model, we lumped together CI1, which innervates five of the six muscle types, CI2 and CI3, which innervate the flexor tibiae muscle. This simplification is not likely to cause noticeable errors in the simulations, since, as experiments showed, the activities of CI1, CI2 and CI3 are synchronous with good approximation [18,21].

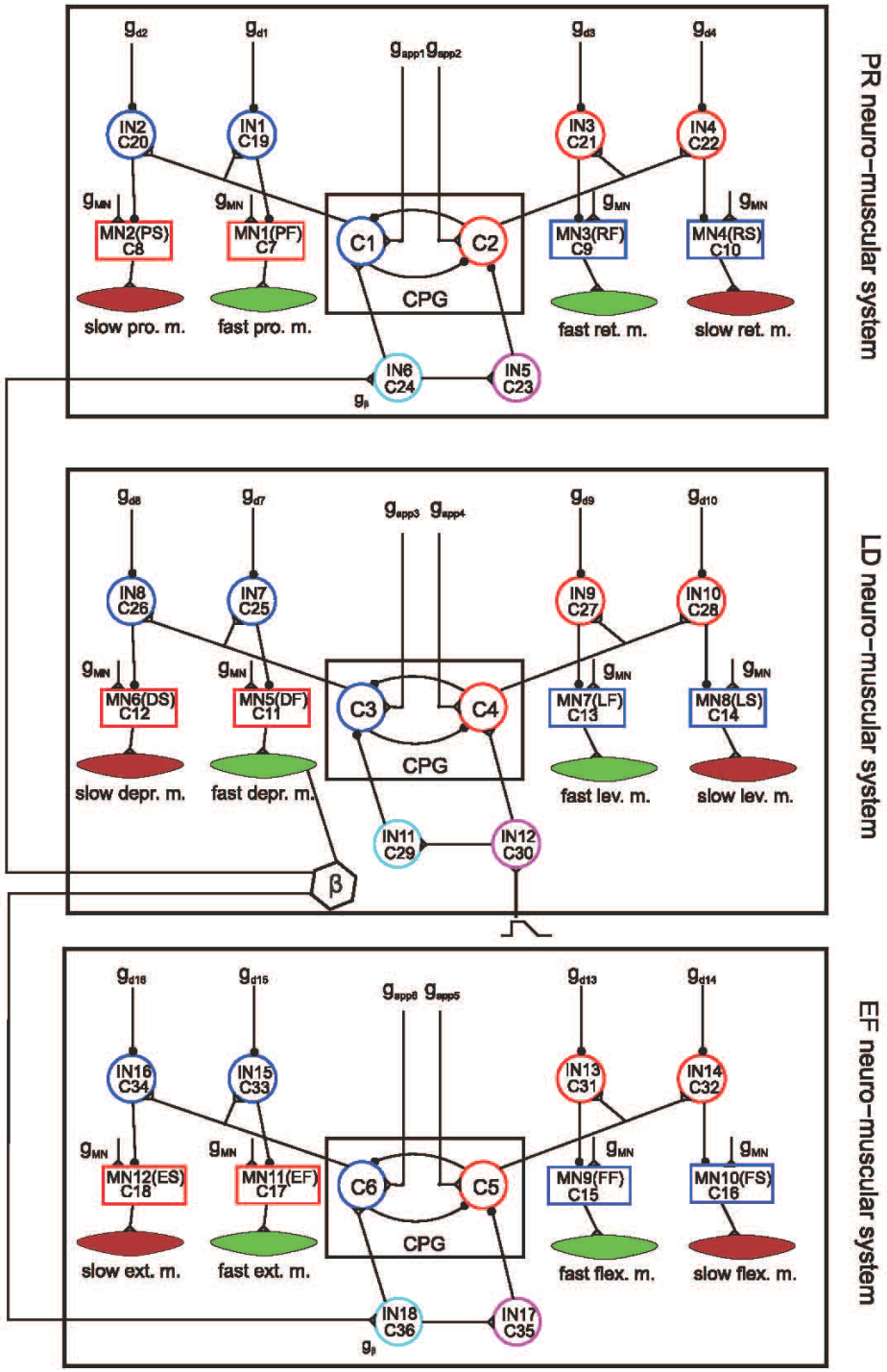

Figure 1. The extended model comprising all three neuro-muscular systems equipped with fast and slow muscle fibres. The **protractor-retractor** (PR) neuro-muscular system consists of a central pattern generator: CPG, slow and fast protractor and retractor muscles as indicated (slow pro. m. etc.), the corresponding motoneurons: MN(PS) etc., 4 inhibitory interneurons (IN1–IN4) connecting the CPG to the motoneurons, and two additional interneurons (IN5–IN6), which convey neuronal signals to the CPG from sense organs of other joints of the same leg, or possibly of other legs. g_{app1}, g_{app2} are conductances of the driving currents to C1 and C2, respectively. g_{d1}–g_{d4} are conductances of the inhibitory currents to IN1–IN4, respectively. g_β is the conductance of the sensory input current from the levator-depressor muscle system. The **levator-depressor** (LD) neuro-muscular system consists of a central pattern generator: CPG, slow and fast levator and depressor muscles as

indicated (slow depr. m. etc.), the corresponding motoneurons: MN(DS) etc., 4 inhibitory interneurons (IN7–IN10) connecting the CPG to the motoneurons, and two additional interneurons (IN11–IN12), which convey neuronal signals to the CPG from peripheral sense organs of the leg (ramp symbol). g_{app3}, g_{app4} are conductances of the driving currents to C3 and C4, respectively. g_{d7}–g_{d10} are conductances of the inhibitory currents to IN7–IN10, respectively. The **extensor-flexor** (EF) neuro-muscular system consists of a central pattern generator: CPG, slow and fast extensor and flexor muscles as indicated (slow ext. m. etc.), the corresponding motoneurons: MN(ES) etc., 4 inhibitory interneurons (IN13–IN16) connecting the CPG to the motoneurons, and two additional interneurons (IN17–IN18), which convey neuronal signals to the CPG from sense organs of other joints of the same leg, or possibly of other legs. g_{app5}, g_{app6} are conductances of the driving currents to C5 and C6, respectively. g_{d13}–g_{d16} are conductances of the inhibitory currents to IN13–IN16, respectively. g_β is the conductance of the sensory input current from the levator-depressor muscle system. g_{MN} is the conductance of the common (central) input current to all motoneurons. Empty triangles are excitatory synapses; filled black circles on neurons are inhibitory synapses. The tiny black circles on synaptic paths are branching points. The three neuro-muscular systems have been put in frames with reference to Fig. 7 for the sake of their easier identification in that figure.
doi:10.1371/journal.pone.0078246.g001

The various sensory, in particular position (angle) and (angular) velocity, signals were also implicitly modelled. The sense organs that produce such signals do exist for each joint of each leg in insects [6,8]; for a survey, see [7]. In the model, these signals were treated as physical quantities and were not encoded in neuronal signals. Their effects were therefore implemented as abstract logical decisions or operations (see Results below). Nevertheless, we have endeavoured to make these effects and functions physiologically viable by providing a putative neuronal network that, at least qualitatively, is capable of reproducing them (cf. Discussion).

A technical note on the usage of muscle fibre recruitment in the model

If the recruitment levels of the slow muscle fibres and the contraction forces in the recruited fibres of a pair of antagonistic muscles are given, they determine a unique stationary position of the leg joint (cf. the accompanying paper [34]). It is however more practical to define the stationary angle (e.g. the horizontal position of the femur by the angle α) and to determine the recruitment levels in the appropriate muscles (e.g. in the protractor and retractor muscles).

Here is a short description of the calculation of the angle $\alpha = \alpha_0$, which yields the horizontal resting position of the femur. At the stationary angle α_0, we have [14,34]

$$a = \frac{k_{R,eff}}{k_{P,eff}} = \frac{l_R(\alpha_0)(l_P(\alpha_0) - l_{P,min})^2}{l_P(\alpha_0)(l_R(\alpha_0) - l_{R,min})^2} \quad (3)$$

where k_{eff} (omitting here and in the subsequent formulae the subscripts indicating the specific muscle type for the sake of simplicity) is the so-called effective spring constant, which is the value corrected for the actual level of recruitment r_a; $l(\alpha)$ is the muscle length at the angle α, l_{min} denotes the minimal length of the corresponding muscle (at which the muscle is completely relaxed). Now, $k_{eff} = r_a k_0 / r_c$, where r_c is the control (or reference) recruitment level, and k_0 is computed in the model for the recruitment level r_c in the first place (cf. the accompanying paper [34]). In the stationary state, we have $k_0 = k_{res}$, the latter being the residual value of the spring constant k. Hence,

$$a = \frac{k_{R,res}}{k_{P,res}} \frac{r_{aR}}{r_{cR}} \frac{r_{cP}}{r_{aP}} \quad (4)$$

according to [34]. From this eqn, we obtain

$$\frac{r_{aR}}{r_{aP}} = a \frac{k_{P,res}}{k_{R,res}} \frac{r_{cR}}{r_{cP}} = \bar{a} \quad (5)$$

If $\bar{a} < 1$, we set $r_{aP} = r_{cP}$ and $r_{aR} = \bar{a} r_{cP}$. If $\bar{a} > 1$, then analogously $r_{aP} = r_{aR}/\bar{a} = r_{cR}/\bar{a}$. (At $\bar{a} = 1$ trivially $r_{aP} = r_{cP}$ and $r_{aR} = r_{cR}$.)

When the stick insect is standing in the usual (normal) position (cf. Fig. 2), then no calculation of the recruitment levels is needed for the other two muscle pairs. The stationary values of the two corresponding angles β and γ are namely predefined by the normal standing position. That is, we have $\beta \approx 30^o$ and $\gamma \approx 84^o$. It is, of course, not difficult to apply the reasoning we have just used for the protractor-retractor system to the other two neuro-muscular systems, if required.

Table 1. Activation rate constants of the different fast muscle types.

Muscle type	activation rate constant (1/ms)	
	stance phase	swing phase
Protractor	2.01	0.81
Retractor	5.01	0.71
Levator	15.01	8.01
Depressor	5.01	5.01
Extensor	5.01	5.01
Flexor	8.01	8.01

doi:10.1371/journal.pone.0078246.t001

Results

In the model, we assumed that sensory signals reflecting the positions (angles) and the (angular) velocities of the joints of the middle leg were used to coordinate the movements of the femur and tibia both at stopping and starting the locomotion (stepping). According to our hypothesis, both processes were triggered by mutually exclusive command signals of central origin. First, we deal with the stop of stepping.

Stop of stepping

We recall the definitions of the angles α, β and γ [13,14]: α increases during retraction, i.e. moving the femur backward in the horizontal plane; β increases during levation, i.e. lifting the femur off the ground; and γ increases during flexion, i.e. moving the tibia towards the body in the vertical plane.

With these conventions in mind, we assumed that the stopping process must start with α and γ both in the decreasing phase, i.e. with protraction and extension of the femur and the tibia, respectively. This constraint ensured that the leg movement never finished with a protraction in the stance phase. Such a situation was never observed in experiments ([1], and Grabowska, unpublished data). It is however self evident that the last phase before steady state is always a stance phase [1], since ground contact must have been established before, or at, a complete still stand. This means that the central command signal to stop became

Table 2. Residual values of the spring constants k_{res} of the different slow muscle types.

Muscle type	k_{res} (mN/mm²)
Protractor	15.0
Retractor	25.5
Levator	10.0
Depressor	8.8
Extensor	34.0
Flexor	4.3

doi:10.1371/journal.pone.0078246.t002

effective only after $d\alpha/dt<0$ and $d\gamma/dt<0$ had been fulfilled. More formally, we have

$$g_{di}=g_{di,red} \quad \text{if}(d\alpha/dt<0)\wedge(c_{STOP}=TRUE)\wedge(g_{di}\neq g_{di,red}) \quad (6)$$

$$g_{di}=g_{di,n} \quad \text{during stepping} \quad (7)$$

for $i=1,3$ (cf. Fig. 1). In these eqns, $g_{di,n}=1.6nS$ is the value of g_{di} during stepping ('normal' value), and $g_{di,red}=1.0nS$ is its value during steady state ('reduced' value). c_{STOP} is the boolean variable for the stop command, and '$\wedge$' is the boolean 'and' operator. The last inequality condition in eqn 6 means that the switch in the value of g_{di} occurs only once while the stop command is on. If we set $i=13,15$, substitute γ for α in eqn 6, we obtain a completely analogous condition for stopping the fast MNs of the extensor-flexor neuro-muscular system. Once these conditions were met, the activity of the fast MNs was inhibited via the inhibitory INs. Consequently, the fast muscle fibres in all four muscles: protractor, retractor and extensor, flexor relaxed and did not exert any torque on the thorax-coxa and femur-tibia joints, respectively. As far as the corresponding slow MNs are concerned, their activity was enhanced upon onset of the stop command due to the inhibition of their inhibitory INs: Again, expressing this in form of equations, we have

$$g_{di}=g_{di,incr} \quad \text{if}(c_{STOP}=TRUE)\wedge(g_{di}\neq g_{di,incr}) \quad (8)$$

$$g_{di}=g_{di,n} \quad \text{during stepping} \quad (9)$$

for $i=2,4$ and $i=14,16$ in the protractor-retractor and the extensor-flexor neuro-muscular system, respectively. In eqn 8, $g_{di,incr}=10nS$ is the enhanced conductance of the (central) inhibitory current to the IN (cf. Fig. 1). The disinhibition of the corresponding slow MNs resulted, of course, in stronger activity of the slow muscles innervated by these MNs.

The negative angular velocities above were preconditions for establishing and maintaining permanent ground contact by the levator-depressor neuro-muscular system. However, they had to be complemented by one condition on the angular signal β, which had to reach the value at ground contact ($\approx 30^o$) in order that both *fast and slow* levator and depressor MNs became inhibited. In equation form, these conditions read

$$g_{di}=g_{di,red} \quad \text{if}(Boole=TRUE)\wedge(g_{di}\neq g_{di,red}) \quad \text{with}$$

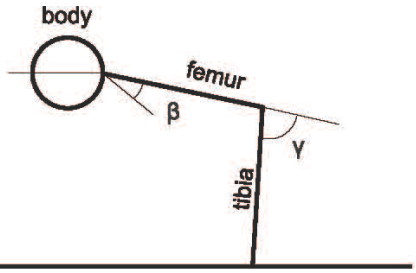

Figure 2. Illustration of the standing position of the middle leg of the stick insect as a projection into the vertical plane. β: levation angle $\approx 30^o$, γ: flexion angle $\approx 84^o$. Note that the reference axis of the angle β is not horizontal because the longitudinal axis of the coxa is tilted from the horizontal direction by an angle of $\psi=41.1^o$ [22].
doi:10.1371/journal.pone.0078246.g002

$$Boole=(c_{STOP}=TRUE)\wedge(|\beta-30^o|<\varepsilon)\wedge(g_{dj}=g_{dj,red})\wedge(g_{dk}=g_{dk,red}) \quad (10)$$

$$g_{di}=g_{di,n} \quad \text{during stepping} \quad (11)$$

for $i=7,8,9,10$, $j=1,3$, and $k=13,15$; *Boole* is a boolean variable, and ε is a sufficiently small value ($\varepsilon=1^o$). Thus, once the conditions in eqn 10 were fulfilled, a permanent ground contact was established. The (middle) leg came to a complete rest, having performed a retraction in the stance phase, while approaching the stationary angle α_0. The activity of slow muscle fibres of both the protractor-retractor and the extensor-flexor system was only stopped when the angles α and γ were close enough ($\pm 3^o$) to their stationary values (α_0 and $\gamma_0=84^o$) and the angular velocities $d\alpha/dt$ and $d\gamma/dt$ were nearly zero. These conditions, like the previous ones, can also be expressed as equations.

$$g_{di}=g_{di,red} \quad \text{if}(c_{STOP}=TRUE)\wedge(|\alpha-\alpha_0|<\varepsilon_1)\wedge(|d\alpha/dt|<\varepsilon_3)\wedge(g_{di}\neq g_{di,red}) \quad (12)$$

$$g_{di}=g_{di,n} \quad \text{during stepping} \quad (13)$$

for $i=2,4$ (cf. Fig. 1). Here, ε_1 and ε_3 are small values (3^o and $0.5s^{-1}$, respectively). Setting $i=14,16$ and substituting γ for α, we obtain analogous conditions for stopping the activity of the slow MNs of the extensor-flexor neuro-muscular system.

Fig. 3 illustrates the result of these interacting processes. The top panel shows the three angular movements $\alpha(t)$ (red), $\beta(t)$ (black), and $\gamma(t)$ (green), and their phase relations. The arrow indicates the central stop command. As it arrives at the start of a retraction (stance) phase, this phase of the stepping cycle is completed before the stopping process becomes effective at the beginning of the next protraction (swing) phase. Then a permanent ground contact is established (black trace). Finally, the complete steady state is preceded by a retraction (stance) phase. The middle and the bottom panel display intracellular activity of the slow and the fast protractor MNs, respectively. Note that whereas the fast MNs are rhythmically active, the slow ones show tonic activity, especially after the inhibition of the fast MNs. This happens, because we additionally assumed that, in the model, the central stop command

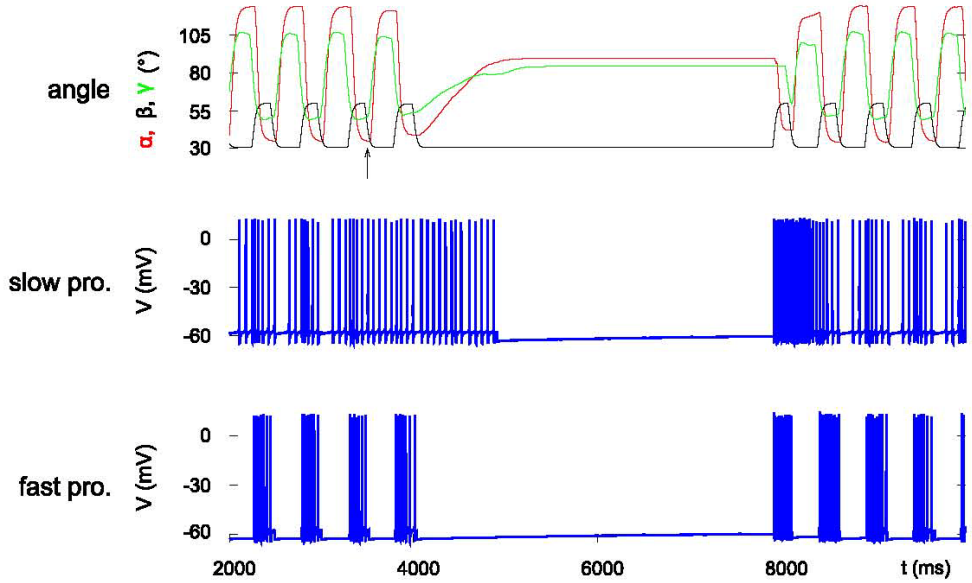

Figure 3. Simulation results illustrating the stop and start of stepping in the model. Top panel: time evolution of the three joint angles α (retraction, red), β (levation, black), and γ (flexion, green). Middle and bottom panel: activity of the slow and fast protractor motoneuron, respectively. The arrow in the top panel indicates the onset of the central stop command. The ground contact is, as during stepping, established by activation of the depressor muscle at the end of the swing phase, and the steady state is attained in the subsequent stance phase. Note that the activity of the fast protractor motoneuron is stopped only at the end of the last protraction (swing) phase but the slow one has a prolonged and enhanced tonic activity that lasts until the steady-state α_0 of the angle α is reached. At start, as shown in the top panel, the levator muscle is activated first initiating a swing phase (protraction and extension, respectively, in the other two neuro-muscular systems). The motoneurons start with a high firing frequency (middle and bottom panel).
doi:10.1371/journal.pone.0078246.g003

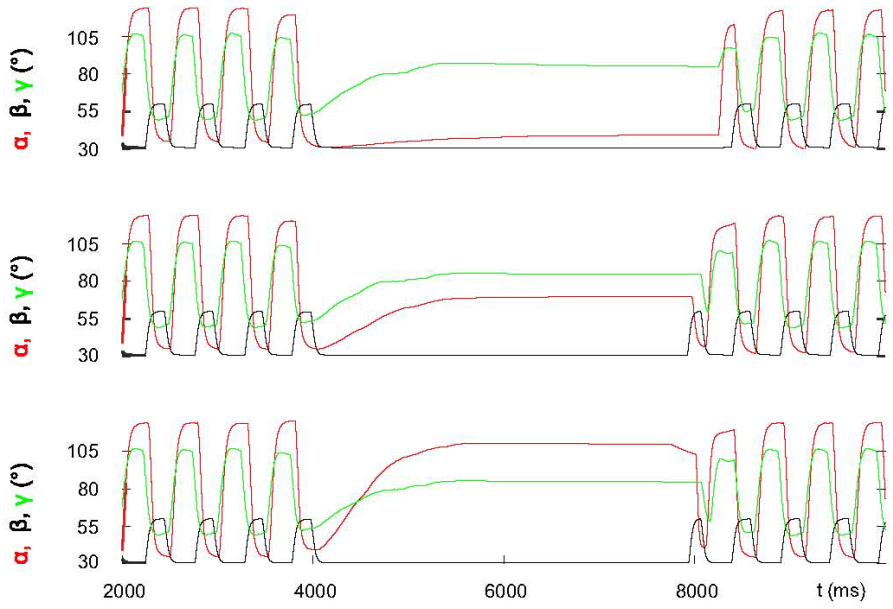

Figure 4. Steady state at three different angles α_0 α: red trace. Top panel: $\alpha_0 = 40°$, middle panel: $\alpha_0 = 70°$, bottom panel: $\alpha_0 = 110°$. The steady-state values of β and γ are always the same (cf. text). The central stop command occurs at the same time as in Fig. 3. The stepping starts with a swing phase when $\alpha_0 = 70°$ (middle panel) and when $\alpha_0 = 110°$ (bottom panel) like in Fig. 3 but when $\alpha_0 = 40°$, the stepping commences with a stance phase (top panel). See subsection Start of stepping.
doi:10.1371/journal.pone.0078246.g004

also enhanced the activity of the slow protractor, rectractor, extensor and flexor MNs (via inhibition of their inhibitory INs by increasing the corresponding g_d values, see eqn 8 above and Fig. 1). There is only weak indirect experimental evidence for the prolonged tonic activity of the slow MNs. Records in [10] show tonic activity of the slow extensor MN (SETi) in the stick insect and in the locust in the absence of the fast MN activity at fixed middle leg, that is a prolonged tonic activity of the slow MNs can be seen.

The process of stopping described above in detail is independent of the steady-state angle α_0 to which α converges. Fig. 4 demonstrates this result. The different steady-state values of α were set by making use of the recruitment property of the model (cf. Methods and [34]). The steady-state values of β ($\beta_0 = 30^o$) and γ ($\gamma_0 = 84^o$) were always the same since the projection of the standing position into the vertical plane is unchanged in all cases (cf. Fig. 2). The cases depicted in Fig. 4 do have experimental correlates. In [1], they correspond well to the steady-state horizontal position of the femur of the front, middle and hind leg, respectively (cf. [1], Fig. 2). Moreover, some unpublished observations (Grabowska, unpublished data) also appear to be in agreement with our simulation results.

Fig. 5 demonstrates an important putative physiological role, as mimicked by the model, of the slow muscle fibres and of the slow MNs innervating them during the stopping process. It shows that the convergence of the angle α to its steady-state value is markedly faster when the slow protractor and retractor MNs exhibit prolonged and enhanced tonic firing activity (compare the corresponding angular movements: red, blue in Fig. 5). Although this result is shown here for the protractor-retractor neuro-muscular system only, it is also valid for the extensor-flexor neuro-muscular system. That is, the slow MNs of the latter system work according to the same time schedule during the stopping process as their counterparts in the protractor-retractor system. However, the situation is different in the levator-depressor neuro-muscular system. We found in the simulations that when the slow MNs of this system were tonically firing, a stable and permanent ground contact in the stance phases could not be produced because of the tonic firing of these very MNs. Hence, we attributed the slow MNs in the levator-depressor system the same rhythmic activity as that of the fast MNs, i.e we made no difference between the activities of the slow and fast MNs.

Finally, we show in Fig. 6 that the behaviour of the system remains basically unaffected by the time of onset of the central stop command. In the simulations, we chose a number of different occurrence times of the central stop command that fell within the same stepping cycle (of ≈ 500 ms), i.e. occurred at different phases of that cycle, in each case. Every time, the levator-depressor system behaved exactly the same way, whereas the protractor-retractor system showed qualitatively the same behaviour by performing a retraction (in the stance phase) before reaching its stationary position (the angle α approaching its steady-state value α_0 from below). The extensor-flexor system, however, did not always exhibit exactly the same behaviour. Occasionally, as shown in the bottom panel of Fig. 6 (green trace), it carried out first a flexion followed by a partial extension during which the angle γ monotonically converged to its steady-state value. This happened because the central stop command arrived just when the flexion started. Note that the extension during stepping finishes a bit earlier than the corresponding protraction (Fig. 6), like in the stick insect [15]. This is why the protractor-retractor system is still in the protraction phase when the extensor-flexor system has already completed its extension phase.

Start of stepping

Theoretically, there are two possible ways of starting from a standing, stationary position: performing first a swing phase (protraction) or a stance phase (retraction). We implemented both possibilities in the model. Indeed, the stick insect seems to make use of both of these possibilities [1] and (Grabowska, unpublished data). Whether a swing phase or a stance phase would be produced first by a (middle) leg depends on the actual steady-state value of α in the standing position. In the model, we defined a critical angle that separates these two cases. We set its value to be 60^o. In the extensor-flexor system of the stick insect, it was found that the relative frequency of the middle leg starting with a swing or a stance phase monotonically depended on the angle γ [23]. Our assumption of a critical α angle seems therefore reasonable, even though the choice of the specific value of 60^o remains somewhat arbitrary.

The simulations show examples for both cases. In Fig. 4, top panel in which $\alpha_0 = 40^o$, the protractor-retractor system starts with a retraction, accompanied by a flexion in the extensor-flexor system, while the leg has still ground contact ($\beta = 30^o$), i.e. the leg is in the stance phase. Only when both retraction and flexion are completed will the levator-depressor system be enabled to lift the leg off the ground. This appears to be in good agreement with findings in [1] and (Grabowska, unpublished data). In the model, the stepping starts at a well-defined phase of the activity of the protractor-retractor CPG (C1 and C2 in Fig. 1): when the "retractor" CPG neuron (C1 in Fig. 1) is about to reach its maximal depolarization by exceeding a threshold value $V_{thr} = 15$ mV. Note that all three CPGs are active and synchronized, because the load and position sensory signals represented by the angle β are active, i.e. β is below its critical value (38^o for the protractor-retractor system, and 50^o for the extensor-flexor system; cf. Fig. 1 and Methods). Summarizing the starting conditions in this case in form of equations, we have

$$g_{di} = g_{di,n} \text{ if } (c_{START} = TRUE) \wedge (V_{C1}(t) > V_{thr}) \wedge (g_{di} \neq g_{di,n}) \quad (14)$$

$$g_{dj} = g_{dj,n} \quad \text{if} \quad (g_{di} = g_{di,n}) \wedge (g_{dj} \neq g_{dj,n}) \quad (15)$$

$$g_{dk} = g_{dk,n} \quad \text{if} \quad (g_{di} = g_{di,n}) \wedge (g_{dj} = g_{dj,n}) \wedge (g_{dk} \neq g_{dk,n}) \quad (16)$$

for $i = 1,2,3,\mathbf{4}$, $j = 13,\mathbf{14},15,16$, and $k = 7,8,9,10$. The boolean variable c_{START} represents the central start command. These eqns also show that after the protractor-retractor system is activated, in a retraction (stance) phase, the extensor-flexor neuro-muscular system is activated next with a flexion, provided that the protractor-retraction system is already active. The levator-depressor neuro-muscular system is finally activated, once both of the other systems are already active. Because of the synchronization between the three CPGs, the leg's next lift-off will only occur when the retraction and the flexion have been completed. Note that in all three systems the slow and fast MNs are activated at the same time.

In the two other panels of Fig. 4 in which $\alpha_0 > 60^o$, the stepping starts with lifting the leg off the ground. This kind of start was also observed in the animal [1] and (Grabowska, unpublished data). In the model, the mechanical movement is triggered when the "levator" CPG neuron (C3 in Fig. 1) reaches the depolarization level of $V_{thr} = 15$ mV. The corresponding equation reads

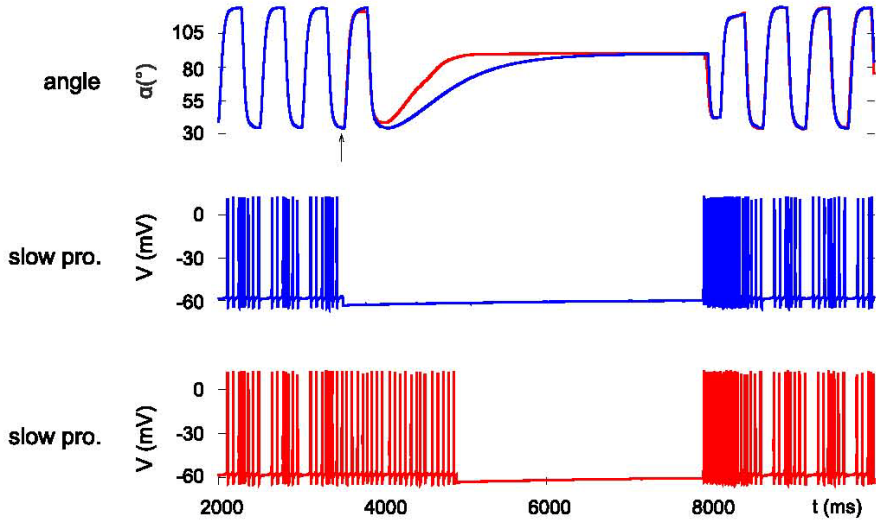

Figure 5. The role of the prolonged activity of the slow protractor and retractor motoneurons and muscle fibres. Top panel: time evolution of the retraction angle α; middle panel: activity of the protractor (and retractor motoneuron – not shown) is stopped at the occurrence of the central stop command; and bottom panel: prolonged and enhanced activity of the protractor (and retractor motoneuron – not shown). In the top panel, the colour of angular movements corresponds to that of the motoneuron activity in the two other panels. Note that prolonged and enhanced activity of the slow motoneurons (bottom panel) results in an accelerated convergence of α to its steady-state value (red curve, top panel).
doi:10.1371/journal.pone.0078246.g005

$$g_{di} = g_{di,n} \quad \text{if} \quad (c_{START} = TRUE) \wedge (V_{C3}(t) > V_{thr}) \wedge (g_{di} \neq g_{di,n}) \quad (17)$$

for $i = 7,8,9,10$. Then the angle β increases by activation of the levator muscles in the levator-depressor system. The levation induces protraction and extension, respectively, in the two other neuro-muscular systems via the load and position sensory signals represented by the angle β (Fig. 1). Here, too, in all neuro-muscular systems, the slow MNs and muscles are simultaneously activated with the fast ones. Note that the extension starts

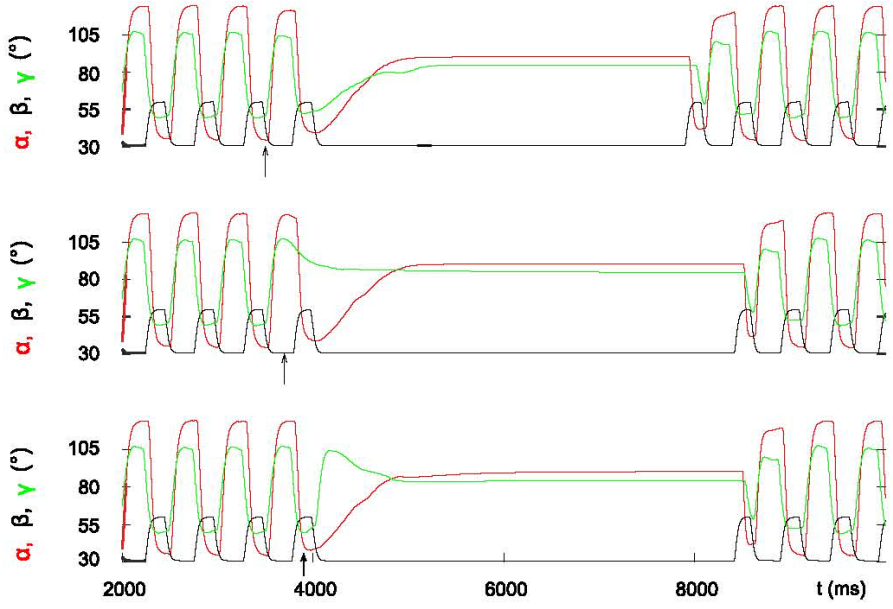

Figure 6. Central stop command evoked in three different phases of the stepping cycle. Top panel: at the start of the retraction phase ($t = 3500ms$); middle panel: at the end of the retraction phase ($t = 3700ms$); bottom panel: towards the end of the protraction phase ($t = 3900ms$). Note that the qualitative behaviour of the model remains the same in all three cases both at stop and start, except for the extensor-flexor system which occasionally shows an extra (partial) extension (bottom panel). For further explanation, see text.
doi:10.1371/journal.pone.0078246.g006

later than the protraction due to the different thresholds of β in the two systems (cf. Methods and [13]).

Discussion

In this paper, we set out to provide an explanation of how locomotion in the stick insect is stopped and started by making use of a suitable neuro-mechanical model. This model is based on our one in the accompanying paper [34]. We complemented it by making physiologically plausible assumptions with regard to the stopping and starting of stepping. Among these assumption two are of fundamental importance. The first one is on the coordinating roles of sensory signals reflecting position and velocity of the leg's main joints. The existence of such sensory signals has been well established in experiments [7 9]. Our assumption, more precisely a set of assumptions, relates to their crucial role in coordinating the activities of the leg's neuro-muscular systems during locomotion, standing, and during the transition processes between these states. These sensory signals can thus trigger sub-processes in the same or in a different neuro-muscular system. For example, the negative value of the angular velocity $d\alpha/dt$ results in the inhibition of the fast MNs in the protractor-retractor neuro-muscular system at stopping; the activity of the levator-depressor can only be blocked at stopping, once the fast MNs of both the protractor-retractor and the extensor-flexor system have been inhibited. A model not incorporating the specific set of assumptions we used here would have to have quite different properties and mechanisms of intra-

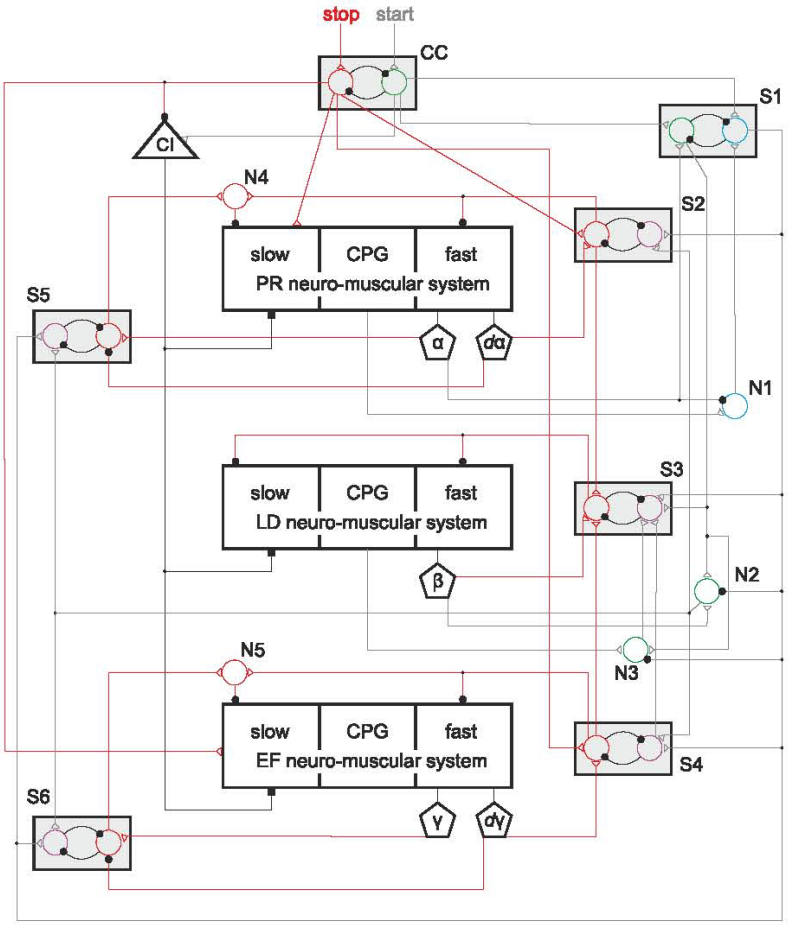

Figure 7. The physiological viability of the model. Active pathways at stopping. The three large boxes in the centre of the figure are the three neuro-muscular systems as indicated from Fig. 1. Their existence is physiologically well established [15,27]. Their inner structure has been partially confirmed in experiments [10,11,24,27–31]. The small boxes CC and S1–S6 are CPG-like functional units consisting of mutually inhibitory neurons. Such small networks of mutually inhibitory neurons do exist in the nervous system of athropods [32] and other animals [33]. However, such units with the specific roles assigned to them in the present model have not been identified. Triangle CI represents the common inhibitory motoneuron. Its existence is proven in experiments [17–19,21]. N1-N5 are neurons whose existence with the specific function they have in the present model has not yet been established. Pentagons α, β, γ are sense organs where signals reflecting the position (angle) are generated; pentagons $d\alpha$, $d\gamma$ are sense organs where signals reflecting the (angular) velocity are generated. Such sense organs do exist in insects (e.g. [6–8]). Small empty triangle on neurons or on system boxes are excitatory synapses. Filled black squares symbolize inhibition by CI of the slow muscle fibres. Filled black circles are inhibitory synapses. Very small black circles along paths (neuronal connections) are branching points. Red pathways are the connections that are active at stop of stepping. Grey pathways are the connections that are active at start of stepping (see. Figs. 8–9). For more explanation as to the workings of this network, see text.
doi:10.1371/journal.pone.0078246.g007

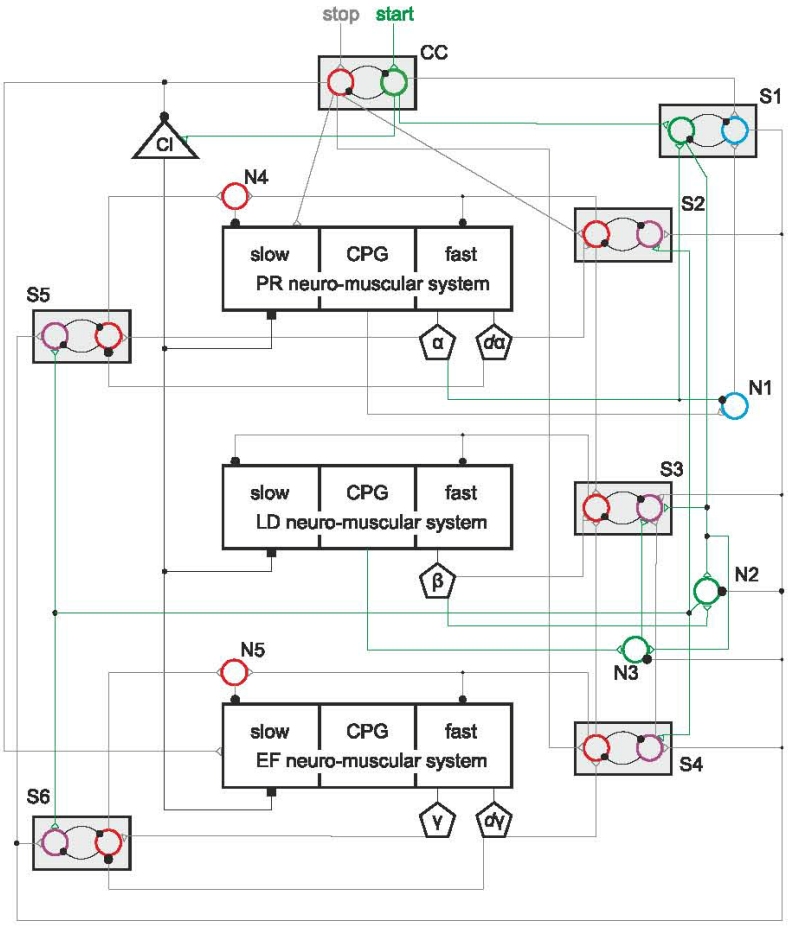

Figure 8. The physiological viability of the model. Active pathways at start. The same network as in Fig. 7: Here, the pathways that are active when the starting process commences with a protraction (swing phase) are highlighted in green. The other pathways are suppressed by having been drawn in grey. For explanation of how the network works in this case, see text.
doi:10.1371/journal.pone.0078246.g008

leg coordination. The second fundamental assumption was not made explicitly, since we used it in our earlier work [13,14]. Its main claim is that neither stopping nor starting of stepping requires any direct interference with the activity of any of the three CPGs. As it should be clear from the Results, and the eqns describing the actions of the sensory signals, the driving currents (the conductances g_{appk}) to the CPGs were at no point changed. That means that the CPGs ran autonomously all the time without direct interference. All actions on the MNs, hence on muscles, were conveyed via the inhibitory INs connecting the CPGs to the MNs. Thus all transient signals that would arise by directly changing the activity of the CPGs (i.e. changing the conductances g_{appk}) could be avoided. Equipped with this property, our model is capable of responding to unexpected changes (e.g. sudden stop or start) much faster than models in which the activity of the CPGs is directly manipulated. Quite recently, experimental evidence has arisen that the CPG is not affected during change in the MN activity. It has been shown by Rosenbaum et al. (unpublished results) that the activity of the protractor-retractor CPG remains unaffected during a switch from forward to backward walking of the stick insect when, however, the protractor and retractor muscles, hence MNs, exchange roles. We also successfully modelled this phenomenon the same way, i.e. without changing the activity of the protractor-retractor CPG in the model [14].

We also assigned the slow muscle fibres residual stiffness and took the effects of the common inhibitory MNs on the function of slow muscle fibres into account [17 19,21]. Having incorporated these properties into the new version of the model, we could mimic both stopping and starting of locomotion (stepping). It turned out that both processes, though basic elements of locomotion, required precise coordination of the three main neuro-muscular systems of a leg. The simulations with the model highlighted the details of the coordination between those neuro-muscular systems. The constituent processes are physiologically plausible. They are i) sensory signals representing position (angle) or (angular) velocity at the individual joints as well as load signals, represented by the angle β); ii) neuronal signals driving the MNs of the system; iii) activities of the MNs driving the fast or slow muscles they innervate; and iv) contractions of the slow and fast muscles producing the mechanical movement of the individual leg joints. Gradual muscle recruitment in the model ensures that any stationary position (angle α) of the femur can be attained. The steady state, posture, is

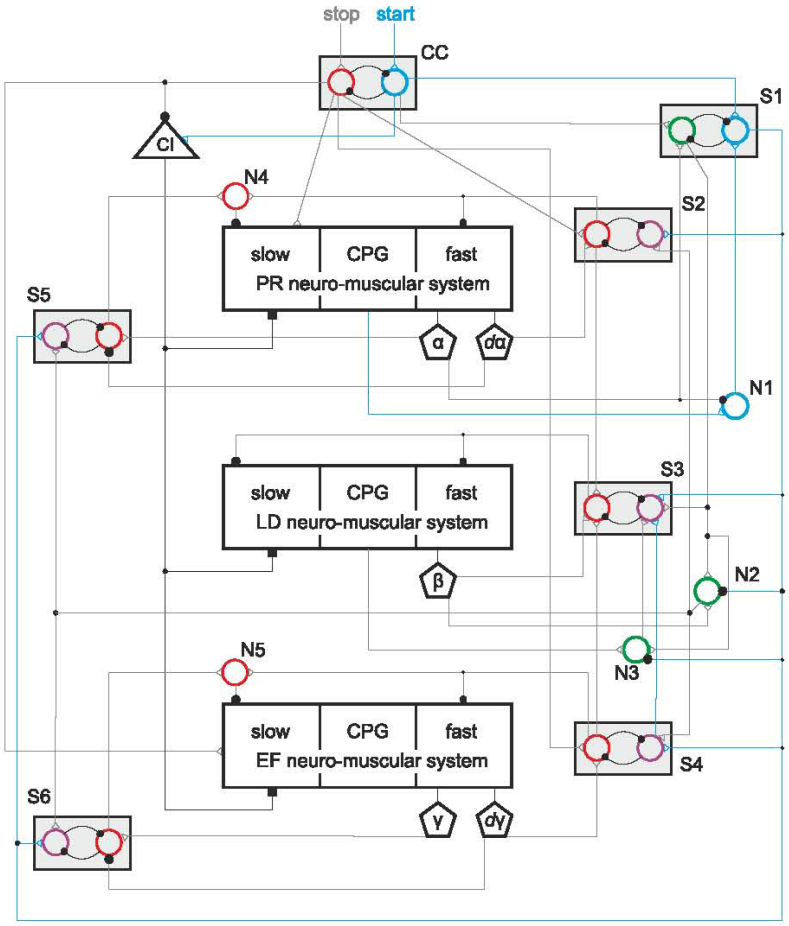

Figure 9. The physiological viability of the model. Active pathways at start. The same network as in Figs 7–8: Here, the pathways that are active when the starting processes commences with a retraction (stance phase) are highlighted in blue. The other pathways are suppressed by having been drawn in grey. For explanation of how the network works in tin this case, see text.
doi:10.1371/journal.pone.0078246.g009

maintained in the model by the residual stiffness of the slow muscle fibres, in agreement with experimental findings [16,17]. This property of the model does not contradict the result in the accompanying paper [34] that steady state is maintained by enhanced tonic firing of the slow MNs, hence co-contractions of the slow muscle fibres in the protractor-retractor system. There, the slow muscle fibres did not possess any residual stiffness, and the co-contraction of the slow muscle fibres was thus required to maintain a stable steady state. In reality, both possibilities are likely to exist and co-exist [10,16].

There are important experimental results that underpin the assumption made when constructing the model. First of all, it is well established that slow and fast muscle fibres have their dedicated MNs driving them, and that the fast muscle fibres do not contribute to maintaining the steady state (posture) in insects [10,11]. It has also been experimentally confirmed that there are position-, velocity- and load-dependent sensory signals in the animals [2,7 9]. The existence of residual stiffness in the slow muscle fibres, and the related function of the common inhibitory MNs (CI1-CI3) to remove it, was demonstrated [10,11,17 19,21]. It was also observed that stop of stepping does not occur randomly during a step cycle, and a leg grinds to a halt when it has ground contact, i.e. in the stance phase [1]. The model presented in this paper incorporates all these properties, and, as far as we are aware of, it is the first one to do so.

The model behaviour is in good agreement with the experimental findings. In the simulations, the time evolution of the angles at the leg joints produced coordinated movement of the whole leg both at stop and start of stepping, similar to the observed ones in the stick insect [1] (Grabowska, unpublished data). In particular, our model is capable of reproducing the preferred steady-state positions of the front, middle and hind leg in the stick insect: the front leg (femur) being near to its anterior extreme position, the hind leg near to its posterior extreme position, and the middle leg somewhere between them. (Compare the three panels in our Fig. 4 with Fig. 2 in [1].) The fast MNs fire rhythmical bursts during locomotion due to their rhythmic inhibition by the associated CPG [24]. The slow MNs, by contrast, produce tonic firing, at least in the case of the extensor muscle [10]. In the model, we applied these firing modes both in the protractor-retractor and the extensor-flexor system. In the levator-depressor system, however, we found that tonic firing of

the slow MNs resulted in incomplete ground contact in the stance phases. In the levator-depressor system, we therefore implemented identical rhythmic firing of both the fast and the slow MNs. The experimental evidence, we could find is inconclusive as to the activity of the slow MNs in the levator-depressor system [25,26]. Hence this part of the model remains highly hypothetical. However, we succeeded in identifying a putative physiological role of the slow muscle fibres at stopping. The prolonged and enhanced tonic activity of the slow protractor and retractor MNs driving the corresponding slow muscle fibres substantially accelerated convergence of the angle α to its stationary value (Fig. 5). The same is true for the slow MNs and muscle fibres of the extensor-flexor system. This is a hitherto unidentified function of the slow MNs and muscle fibres in both systems, and it is thus an important prediction of our model. It should be mentioned here that there is some uncertainty in the physiological interpretation of the apparent "stop" and "start" commands in the model. Currently, there is no experimental way to find out whether such single command signals are produced by the brain, and if so when and in which part of the brain they exactly arise.

As pointed out in the Methods and Results, the sensory signals representing position (angle) and (angular) velocity (e.g. α, $d\alpha/dt$) were not implemented in the model as neuronal signals but only formally, by computing their effects on the neuronal and muscular activity in an abstract way. This is also true for the role of the common inhibitor MNs CI1-CI3. Their effect: removing the residual stiffness of the slow muscle fibres during locomotion and restoring it at stopping was implemented only, as an abstract mathematical function obeying logical conditions.

Physiological viability of the model

Now, we show that our model is, at least in qualitative terms, physiologically viable. We present, in Figs. 7 9, a neuronal network that could be regarded as a physiologically meaningful implementation of our model. The network structure and its elements are not entirely hypothetical. The existence of the three main building blocks (neuro-muscular systems) has reliably been established in experiments [15,27]. Basic properties of the local networks of the neuro-muscular systems could also be gleaned from experimental data [10,11,24,27 31]. In addition, it is known that pairs of mutually inhibitory (nonspiking) neurons or groups of neurons capable of exhibiting bistability do exist in the nervous system of athropods [32] and other animals [33]. All these facts lend the network in Fig. 7 a sufficient physiological basis.

We did not implement this network as a quantitative model to be used in simulations, since there are too many unknown parameter values, especially synaptic weights, in it, hence the attribute "qualitative". Nevertheless, we believe that presenting it does make a contribution to bringing an abstract model and a physiological system closer to each other, and to furthering a better understanding of how the model works.

Here we give an account of how the network works at stop and start of locomotion (stepping), respectively. The stop is initiated by a central stop command: red path labelled with "stop" into unit CC. When the stop command arrives CC, it inhibits its alternative, the "start", command (green neuron). The stop command enhances the activity of the slow MNs in the protractor-retractor and the extensor-flexor system (see red pathways starting at the red neuron in unit CC and ending in red empty triangles on the boxes representing these two systems). The fast MNs of the protractor-retractor system are inhibited, the activation of the fast muscle fibres innervated by them stopped, as soon as $d\alpha/dt<0$ (cf. Results), because the red neuron in S2 is activated and sends an inhibitory signal to the MNs of the fast protractor-retractor system. It also inhibits the other (magenta) neuron in S2. An analogous cascade of events takes place in the extensor-flexor system (unit S4). Now, if the red neurons in the units S2 and S4 are excited, they send a signal each to their red counterpart in unit S3. In order to enter the excited state, the red neuron in S3 also needs an excitation from the sense organ sensing position (angle β) in the levator-depressor system. This sensory signal is evoked, if β is in a close neighbourhood of its steady-state value (30^o). Then the red neuron in S3 is activated and inhibits both the fast and slow MNs of the levator-depressor system. By this, a permanent ground contact of the leg is established. Note that the slow MNs in both the protractor-retractor and the extensor-flexor system are still active. Moreover, their activity has been boosted by the stop command. The slow MNs of the protractor-retractor system are inhibited as soon as the red neuron in S5 is activated. For that to happen, it is required that the angle α be close to its steady-state value, and that $d\alpha/dt\approx 0$. If this is the case, the red neuron in S5 will receive an excitatory signal originating in the sense organ that signals the value of α, and the inhibition coming from the sense organ signalling the value of $d\alpha/dt$ will vanish. Thus the red neuron in S5 becomes excited and sends an excitatory signal to neuron N4, which has already been receiving another excitatory signal from S2. The latter has, on its own, been insufficient to activate neuron N4. Now, it is activated and it inhibits the slow MNs of the protractor-retractor system. The mechanical movement of the femur grinds to a halt. The events in the extensor-flexor system are completely analogous. By inhibiting all MNs in each of the three systems, the leg stops moving. The central stop command inhibits the common inhibitor CI directly, and the excitatory signal to it from unit CC also ceases. This abolishes the inhibition by CI of the slow muscle fibres in all muscles. That is, residual stiffness in the slow muscle fibres becomes active, and it determines the stationary position of the leg. Of course, as soon as the red neurons of the units S2 S6 (and CC) become activated, they inhibit their magenta counterparts in the same unit strongly enough to prevent any signal flow through them.

The start of stepping can occur in the model in two different ways: the leg starting with a swing phase or a stance phase. The steady-state value α_0 of the angle α determines which of the two cases will occur. In any case, the foremost action is that the central start command activates the 'start' neuron (green in Fig. 8 and blue in Fig. 9) in unit CC, hence inhibits the 'stop' (red) one whose excitatory output immediately ceases. Let us consider first the case when $\alpha_0>\alpha_{0thr}=60^o$. That is, the stepping will start with a swing phase. For this variant, the green pathways in Fig. 8 will be used. Because of the condition for α_0 above, the position signal for α (cf. Fig. 8) excites the green neuron in unit S1, together with the start signal, and inhibits neuron N1. In turn, the blue neuron in S1 is inhibited, and, as a consequence, all blue pathways will be blocked (Fig. 9). The green neuron in S1 then excites the neurons N2 and N3 enabling the excitatory pathways through them to become active. The pathway through N3 from the CPG conveys an excitatory signal to the magenta neuron in S3 when the CPG of the levator-depressor system starts the levation phase. This excitatory signal and the start signal conveyed by the green neuron in unit S1 activate the magenta neuron in unit S3, which inhibits the red neuron in the same unit. This, in turn, abolishes the inhibition of both the fast and slow MNs of the levator-depressor system. Since the CPG is in the levation phase, the angle β increases, i.e. the leg is lifted off the ground. To transmit this information to the other neuro-muscular systems, an excitatory signal is sent via neuron N2 to the magenta neurons in the units S2, S4, and S5, S6. The magenta neurons in these units become activated, hence their counterparts (the red neurons) in the same

unit inhibited. Accordingly, the inhibitory signals to the fast MNs disappear directly, whereas the inhibition to the slow MNs indirectly by deactivation of the neurons N4 and N5, respectively. By virtue of the sensory signals represented by the angle β (cf. Fig. 1), the CPGs of the protractor-retractor system and the extensor-flexor system are synchronized to that of the levator depressor system [13,14,34]. The stepping therefore starts with a swing phase (see, for example, Fig. 3 or Fig. 6).

The alternative to this process is one with an initial stance phase. An example is displayed in the top panel of Fig. 4. This process uses the blue pathways in Fig. 9. In this case, the retractor phase of the CPG of the protractor-retractor system triggers the start of the stepping. Since there is now no α-signal to S1 and to neuron N1, the latter is activated, and it activates, together with the central start command, the blue neuron in unit S1. This neuron, in turn, inhibits the neurons N2 and N3, hence no excitatory signal from the β-sensor and the CPG of the levator-depressor system can reach the magenta neurons in units S2 and S4. (The β-signal to unit S3 is irrelevant in this case, because it is present only at the tarsus reaching the ground.) Instead, excitatory signals from S1 arrive these (magenta) neurons, activate them and inhibit the corresponding red neurons simultaneously. This is also true for units S5 and S6, which control the slow MNs in the protractor-retractor and the extensor-flexor system (cf. direct blue pathways to these units from unit S1). The red neurons will also be inhibited in units S5 and S6. This means that the inhibition of both the fast and the slow MNs will be abolished in both the protractor-retractor and the extensor-flexor neuro-muscular system. Since the levator-depressor system is still inhibited, ground contact is maintained, and because the protractor-retractor CPG is in the retractor phase, a stance phase of the stepping cycle ensues. The magenta neuron in unit S3 is activated by simultaneous excitatory signals from S1 and S4, the latter belonging to the extensor-flexor system. The red neuron in S3 is now inhibited, and the inhibition of the fast and slow MNs of the levator-depressor system is abolished. Thus the next swing phase can commence when the CPG of the levator-depressor system reaches the next levation phase of the stepping cycle. Irrespective of whether the stepping starts with a swing or a stance phase, the start signal immediately activates the common inhibitor MN (CI in Figs. 8 9) by inhibiting the red neuron in CC, which has an inhibitory effect on CI and, at the same time sending a permanent excitatory signal to CI (Figs. 8 9).

Conclusions

Having shown that our model is physiologically viable, i.e. it can, at least qualitatively, be implemented by using a neuronal network with physiologically realistic neurons and synapses, we should like to argue that it is physiologically relevant, too. First, it was constructed by using experimental results and physiologically reasonable assumptions. The signals in it are of neuronal origin. Thus there exists a close correspondence between the model and its biological counterpart at several levels of complexity. This makes the interpretation of the simulation results easier and more plausible. Second, our model, in contrast to earlier ones, allows functional differentiation between static and dynamic aspects of movement control. Third, even though our model has been constructed by using experimental findings from the stick insect, the main result achieved with it, namely showing of how intra-leg coordination is organized during stop and start of locomotion (stepping) may be generalized to elucidate analogous processes in other insect species, too. We even venture to suggest that some details of the model could perhaps be used in constructing insect-like robots. In this sense our model might attain a more general relevance and, maybe, significance than just relating to physiological processes in the stick insect.

Acknowledgments

We should like to thank Dr. Guschlbauer for valuable discussions concerning the manuscript.

Author Contributions

Conceived and designed the experiments: TT SDG. Performed the experiments: TT MG. Analyzed the data: TT MG JS AB SDG. Contributed reagents/materials/analysis tools: AB SDG. Wrote the paper: TT MG JS AB SDG.

References

1. Dean J, Wendler G (1984) Stick insect locomotion on a wheel: patterns of stopping and starting. J Exp Biol 110: 203 216.
2. Zill SN, Büschges A, Schmitz J (2011) Encoding of force increases and decreases by tibial campaniform sensilla in the stick insect, *Carausius morosus*. J Comp Physiol A 197: 851 867.
3. Bässler U (1977) Sensory control of leg movement in the stick insect *Carausius morosus*. Biol Cybern 25: 61 72.
4. Schmitz J (1986) The depressor trochanteris motoneurones and their role in the coxatrochanteral feedback loop in the stick insect *Carausius morosus*. Biol Cybern 55: 25 34.
5. Schmitz J (1986) Properties of the feedback system controlling the coxa-trochanter joint in the stick insect *Carausius morosus*. Biol Cybern 55: 35 42.
6. Bässler U (1983) Neural basis of elementary behavior in stick insects. Springer Verlag Berlin-Heidelberg
7. Büschges A, Gruhn M (2008) Mechanosensory feedback in walking: from joint control to locomotor patterns. Advances in Insect Physiology 34: 193 230.
8. Hustert R (1978) Segmental and interganglionic projections from primary fibres of insect mechanoreceptors. Cell Tiss Res 194: 357 351.
9. Bräuning P, Hustert R, Pflüger HJ (1981) Distribution of specific central projections of mechanoreceptors in the thorax and proximal leg joints of locusts. Cell Tiss Res 216: 57 77.
10. Bässler D, Büschges A, Meditz S, Bässler U (1996) Correlation between muscle structure and filter characteristics of the muscle-joint system in three orthopteran insect species. J Exp Biol 199: 2169 2183.
11. Bässler U, Stein W (1996) Contributions of structure and innervation pattern of the stick insect extensor tibiae muscle to the filter characteristics of the muscle-joint system. J Exp Biol 199: 2185 2198.
12. Godlewska E (2012) The histochemical characterization of muscle fiber types in an insect leg. Master Thesis, University of Cologne, Germany.
13. Knops S, Tóth TI, Guschlbauer C, Gruhn M, Daun-Gruhn S (2013) A neuro-mechanical model for the neuronal basis of curve walking in the stick insect. J Neurophysiol 109: 679 691.
14. Tóth TI, Knops S, Gruhn S (2012) A neuro-mechanical model explaining forward and backward stepping in the stick insect. J Neurophysiol 107: 3267 3280.
15. Büschges A (2005) Sensory control and organization of neural networks mediating coordination of multisegmental organs for locomotion. J Neurophysiol 93: 1127 1135.
16. Hooper SL, Guschlbauer Ch, Blümel M, Rosenbaum P, Gruhn M, et al. (2009) Neural control of unloaded leg posture and leg swing in stick insect, cockroach, and mouse differs from that in larger animals. J Neurosci 29: 4109 4119.
17. Wolf H (1990) Activity patterns of inhibitory motoneurones and their impact on leg movement in tethered walking locusts. J Exp Biol 152: 281 304.
18. Schmidt J, Rathmayer W (1993) Central organization of common inhibitory motoneurons in the locust: role of afferent signals of leg mechanoreceptors. J Comp Physiol A 172: 447 456.
19. Ballantyne D, RathmayerW(1981) On the function of the common inhibitory neuron in walking legs of the crab, *eriphia spinifrons*. J Comp Physiol A 143: 111 122.
20. Pearson KG, Iles JF (1971) Innervation of coxal depressor muscles in the cockroach, periplaneta americana. J Exp Biol 54: 215 232.
21. Iles JF, Pearson KG (1971) Coxal depressor muscles of the cockroach and the role of *peripheral inhibition*. J Exp Biol 55: 151 164.
22. Cruse H, Bartling Ch (1995) Movement of joint angles in the legs of a walking insect, *Carausius morosus*. J Insect Physiol 41: 761 771.
23. Bucher D, Akay T, DiCaprio RA, Büschges A (2003) Pharmacological analysis of tonic activity in motoneurons during stick insect walking. J Neurophysiol 89: 1245 1255.

24. Westmark S, Oliveira EE, Schmidt J (2009) Pharmacological analysis of tonic activity in motoneurons during stick insect walking. J Neurophysiol 102: 1049 1061.
25. Fischer H, Schmidt J, Haas R, Büschges A (2001) Pattern generation for walking and searching movements of a stick insect leg. I. Coordination of motor activity. J Neurophysiol 85: 341 353.
26. Rosenbaum P, Wosnitza A, Büschges A, Gruhn M (2010) Activity patterns and timing of muscle activity in forward walking and backward walking stick insect *Carausius morosus*. J Neurophysiol 104: 1681 1695.
27. Büschges A (1995) Role of the local nonspiking interneurons in the generation of rhythmic motor activity in the stick insect. J Neurobiol 27: 488 512.
28. Schmidt J, Fischer H, Büschges A (2001) Pattern generation for walking and searching movements of a stick insect leg. II. Control of motoneuronal activity. J Neurophysiol 85: 354 361.
29. Borgmann A, Büschges A, Toth TI, Daun-Gruhn S (2012) Dominance of local sensory signals over inter-segmental effects in a motor system. Experiments. Biol Cybern 422, 473.
30. Laurent G, Burrows M (1989) Distribution of intersegmental inputs to nonspiking local interneurons and motor neurons in the locust. J Neurosci 9: 3019 3029.
31. Laurent G, Burrows M (1989) Intersegmental interneurons can control the gain of reflexes in adjacent segments of the locust by their action on nonspiking local interneurons. J Neurosci 9: 3030 3039.
32. Mullroney B, Hall WM (2007) Local and intersegmental interactions of coordinating neurons and local circuits in the swimmeret system. J Neurophysiol 98: 405 413.
33. Marder E, Calabrese RI (1996) Principles of rhythmic pattern generation. Physiol Rev 76: 687 717.
34. Toth TI, Schmidt J, Büschges A, Daun-Gruhn S (2013) A Neuro-Mechanical Model of a Single Leg Joint Highlighting the Basic Physiological Role of Fast and Slow Muscle Fibres of an Insect Muscle System. PLoS ONE 8: e78247.

4.3 A network model comprising 4 segmental, interconnected ganglia, and its application to simulate multi-legged locomotion in crustaceans

Martyna Grabowska, Tibor Istvan Toth, Carmen Smarandache-Wellmann, Silvia Daun-Gruhn

Submitted in the Journal of Computational Neuroscience (under review)

Author contributions

Conceived and designed the experiments
Martyna Grabowska, Tibor Istvan Toth, Silvia Daun-Gruhn

Performed the experiments
Martyna Grabowska

Analyzed the data
Martyna Grabowska, Tibor Istvan Toth
Carmen Smarandache-Wellmann, Silvia Daun-Gruhn

Figure preparation:
Martyna Grabowska

First version of manuscript
Martyna Grabowska

Wrote the paper
Martyna Grabowska, Tibor Istvan Toth
Carmen Smarandache-Wellmann, Silvia Daun-Gruhn

Contributed reagents/materials/analysis tools
Silvia Daun-Gruhn

A network model comprising 4 segmental, interconnected ganglia, and its application to simulate multi-legged locomotion in crustaceans

M. Grabowska[1], T.I. Toth[1], C. Smarandache-Wellmann[2], S. Daun-Gruhn[1]

[1]Heisenberg Research Group of Computational Biology
[2]Emmy-Noether Research Group
Department of Animal Physiology, Institute of Zoology, University of Cologne, Zülpicher Str. 47b, 50674 Cologne, Germany

ABSTRACT

Inter-segmental coordination is crucial for the locomotion of animals. Arthropods show high variability of leg numbers, from 6 in insects up to 750 legs in millipedes. Despite this fact, the anatomical and functional organization of their nervous systems show basic similarities. The main similarities are the segmental organization, and the way the function of the segmental units is coordinated.

We set out to construct a model that could describe locomotion (walking) in animals with more than 6 legs, as well as in 6-legged animals (insects). To this end, we extended a network model by Daun-Gruhn and Tóth (2011). This model describes inter-segmental coordination of the ipsilateral legs in the stick insect during walking. Including an additional segment (local network) into the original model, we could simulate coordination patterns that occur in animals walking on eight legs (e.g. crayfish). We could improve the model by modifying its original cyclic connection topology. In all model variants, the phase relations between the afferent segmental excitatory sensory signals and the oscillatory activity of the segmental networks played a crucial role. Our results stress the importance of this sensory input on the generation of different stable coordination patterns. The simulations confirmed that using the modified connection topology, the flexibility of the model behavior increased, meaning that changing a single phase parameter, i.e. gating properties of just one afferent sensory signal was sufficient to reproduce all coordination patterns seen in the experiments.

Keywords

Central pattern generator; inter-segmental coordination; network model; locomotion; sensory feedback; arthropods.

INTRODUCTION

The main goal of this work has been to construct a model that is capable of mimicking coordination patterns of walking observed in crustaceans. Since the model to be introduced here is based on one that simulates coordination patterns of walking in the stick insect, we shall provide first a survey of analogies in the function of the nervous systems of crustaceans and stick insects. These analogies will justify our approach in the model construction.

As in other arthropods, the cyclic movements of walking legs of decapods consist of a power stroke (retraction /stance phase) and a return stroke (protraction/swing phase) (Wilson 1966; Cruse 1990 (review)). The legs are moved by antagonistic muscle pairs, which, in turn, are activated by their individual motoneuron pools. The anatomical properties of the antagonistic muscle pairs and their activities are comparable to those of stick insects (Elson 1996). In turn, in each thoracic ganglion, the motoneurons (MN) receive direct or indirect input from central oscillators (Sillar, Clarac and Bush 1987). Like in stick insects, sensory influences play a crucial role in intra- and inter-leg coordination (stick insect: Büschges 2005; Clarac et al. 2000; Pearson 2000; Zill et al. 2004; Hess and Büschges 1999; Akay et al. 2001; 2004; 2007; Zill et al. 2009; Cruse 1990; Dürr et al. 2004; Borgmann et al. 2007; 2009; crustaceans: Cruse 1990; Sillar, Clarac and Bush 1987; Cruse and Müller 1986; Chasserat and Clarac 1983; Clarac and Barnes 1985; Bowermann 1977; Clarac 1982; Jamon and Clarac 1995). Proprioceptive feedback can modulate the centrally generated rhythm in the walking animal. For example, the thoraco-coxal muscle receptor organ (TCMRO), which is a single receptor at the base of each limb of crayfish and crabs, can affect the timing as well as the intensity of rhythmic output of two or more thoracic ganglia (Sillar, Clarac and Bush 1987). Other important sensory organs that are comparable to those of stick insects are the cuticular stress detectors (CSDs), chordotonal organs, which are stimulated by deformations of the cuticle. The sensory input is therefore produced by the loading of the legs during walking (Clarac, Wales and Laverack 1971; Klärner and Barth 1986; Klärner and Barnes 1986). The next important aspect is the mechanical support of the body during walking. Loading of the legs plays an important role during walking since the animal's weight has to be distributed properly over the legs in order to maintain stability of the animal during walking (Cruse 1990; Sillar et al.1986). Without sensory feedback the legs would all swing nearly at the same time. As in the stick insect, the ipsilateral coupling between the hemiganglia of crustaceans is stronger than the contralateral coupling (Jamon and Clarac 1995). As a result, crabs and crayfish, when walking on a treadweel, are capable of using different coordination patterns on each side of the body (Müller and Cruse 1985). Until now, the observed coordination patterns could be divided in two major groups: a metachronal wave and an "alternating tetrapod pattern" (Jamon and Clarac 1995; Müller and Cruse, 1986; Barnes 1974; Parrack 1964; Ross and Belanger 2013). Similar coordination patterns could be found in other arthropods, such as stick insects and locusta although these animals use six legs for walking (Wilson 1966; Graham 1985; Grabowska et al. 2012; Ritzmann and Büschges 2007; Cruse et al. 2009). Speed of walking plays a crucial role in the development of different coordination patterns. In crabs, as in stick insects, an increase in walking speed can lead to a phase shift of the CPG activities and therefore to different coordination patterns. Also the ratio between the lengths of protraction and retraction changes from 1:3 in the metachronal wave pattern to nearly 1:1 in the alternating tetrapod coordination pattern (Barnes 1974; Müller and Cruse 1991; Ross and Belanger 2013).

In arthropods, like in insects and crustaceans, the muscles have approximately the same innervations, and these animals are capable of using many different coordination patterns and also behave differently during walking, depending on the number of the legs. It is therefore a challenging task to design a network model that simulates the walking behaviour of these different animals. In order to elucidate how locomotor patterns are generated at the neuronal level in the stick insect, Daun-Gruhn and Tóth (2011) constructed a neuronal network model using experimental data from the stick insect (Cruse 1990; Borgmann et al. 2007; 2009; Büschges 2005; Akay et al. 2001; 2004; 2007; Ludwar et al. 2005). Each segment of the model network consists of a central pattern generator (CPG), a protractor and a retractor motoneuron (MN) and two inhibitory interneurons (IINs). The CPG is connected via the IINs to the MNs (Daun-Gruhn 2011; Daun-Gruhn and Tóth 2011). The segmental modules of the network are connected via synaptic pathways that are gated by sensory signals changing the phase relations of the CPG activities on the ipsilateral side of the stick insect (Daun-Gruhn and Tóth 2011). Other simulation studies on stick insect walking also support the idea that sensory feedback from other legs and the same leg serve as gating mechanisms for inter-joint and inter-segmental coordination (Ekeberg et al. 2004; von Twickel et al. 2011). The close analogies in the organization and function of the nervous system of stick insects and crustaceans, just described, sufficiently justify our approach of taking the network model by Daun-Gruhn and Tóth (2011) as the starting point for modelling 8-legged locomotion. We extended this basic model as described in later parts of this paper. The extended model produced simulated coordination patterns that showed close similarity to their biological counterparts.

MATERIALS AND METHODS

The inter-segmental network model

The inter-segmental network model used in the present work is an extension of the model by Daun-Gruhn and Tóth (2011), which we henceforth will also call the 3-CPG-MN model. The extended model is composed of four segmental protractor/retractor neuronal networks (Fig. 1a, b). In each segmental network, two nonspiking Hodgkin-Huxley-type neurons that are connected by mutually inhibitory synapses, form the CPG, a half-center oscillator (Hodgkin and Huxley 1952; Daun-Gruhn 2011; Daun-Gruhn and Tóth 2011). (The four oscillators of this type are: C1-C2, C3-C4, C5-C6, and C7-C8 in Fig. 1a).

The oscillatory properties of the CPGs can be changed by the descending excitatory input currents I_{app} whose strengths are set by the conductances g_{app1} and g_{app2} (Daun-Gruhn 2011; Daun-Gruhn and Tóth 2011). For a detailed description of the model and the analysis of its behaviour, see Daun et al. (2009). In the segmental networks, the values of the g_{app}s were set such that the CPG neurons were tonically active without mutual inhibition (Daun-Gruhn 2011; Grillner et al. 2005). The CPG neurons excite the IINs (IIN1-IIN8), which in turn inhibit the corresponding MNs (MN1-MN8). All MNs receive the same permanent central activation (g_{MN}) (Büschges 1998; Büschges 2004; Westmark et al. 2009). The four CPG-MN units are coupled cyclically with each other in the anterior-posterior direction (Fig. 1a, b).

Sensory signals from the cyclically preceding leg gate the inter-segmental excitatory pathway, and sensory signals from the same leg gate the inhibitory pathway between two neighbouring CPGs. Data on the gating effect of sensory signals on inter-segmental connectivity were mainly gathered from experiments done in the stick insect but the sensory signals appear to be similar to those in crustaceans (Akay et al. 2004; 2007; Cruse 1985; Borgmann et al. 2007; 2009; Büschges 2005; Clarac 1982; Cruse and Müler 1985). In the model, excitation and inhibition between two neighbouring CPGs is gated by abstract sensory signals via the sensory INs (SINFL, SINML1, SINML2, SINHL, pink for excitation and turquoise for inhibition). They represent a combination of ground contact and load signals of the leg, which are lumped together in the model. Thus they mainly originate in the levator-depressor neuro-muscular system of a leg and, hence are themselves periodic. Moreover, they act at a certain phase within the period of the protractor-retractor CPG on the excitatory and the inhibitory descending pathways between two neighbouring CPGs. Accordingly, let ϕ denote the phase shift between the (periodic) sensory signal gating the aforementioned excitatory inter-segmental pathway and the (periodic) activity of the affected protractor-retractor CPG. Similarly, let ψ denote the phase shift between the sensory signal that gates the inhibitory inter-segmental pathway and the activity of the affected CPG. The value of this phase shift for each inhibitory inter-segmental connection is kept constant throughout the whole modelling study.

However, we shall change or vary the value of ϕ at the different segments in order to obtain different coordination patterns that were described to occur in crayfish and forward walking crabs. To specify exactly which segments are meant, ϕ will be subscripted as ϕ_{ij} to indicate that the inter-segmental connection from segment j to segment i is being considered. Changing ϕ thus means that the excitatory influence of the preceding leg on the protractor-retractor system of the following leg was delayed or advanced. As a consequence, this leads to a prolongation or reduction of the retractor activity.

In the course of this work, we shall only display the activities of the protractor CPG neurons (C2, C4, C6 and C8). Graphs of the corresponding retractor activities will not be shown, since these activities strongly overlap. It is thus easier to identify the various (simulated) coordination patterns by just examining the protractor activities.

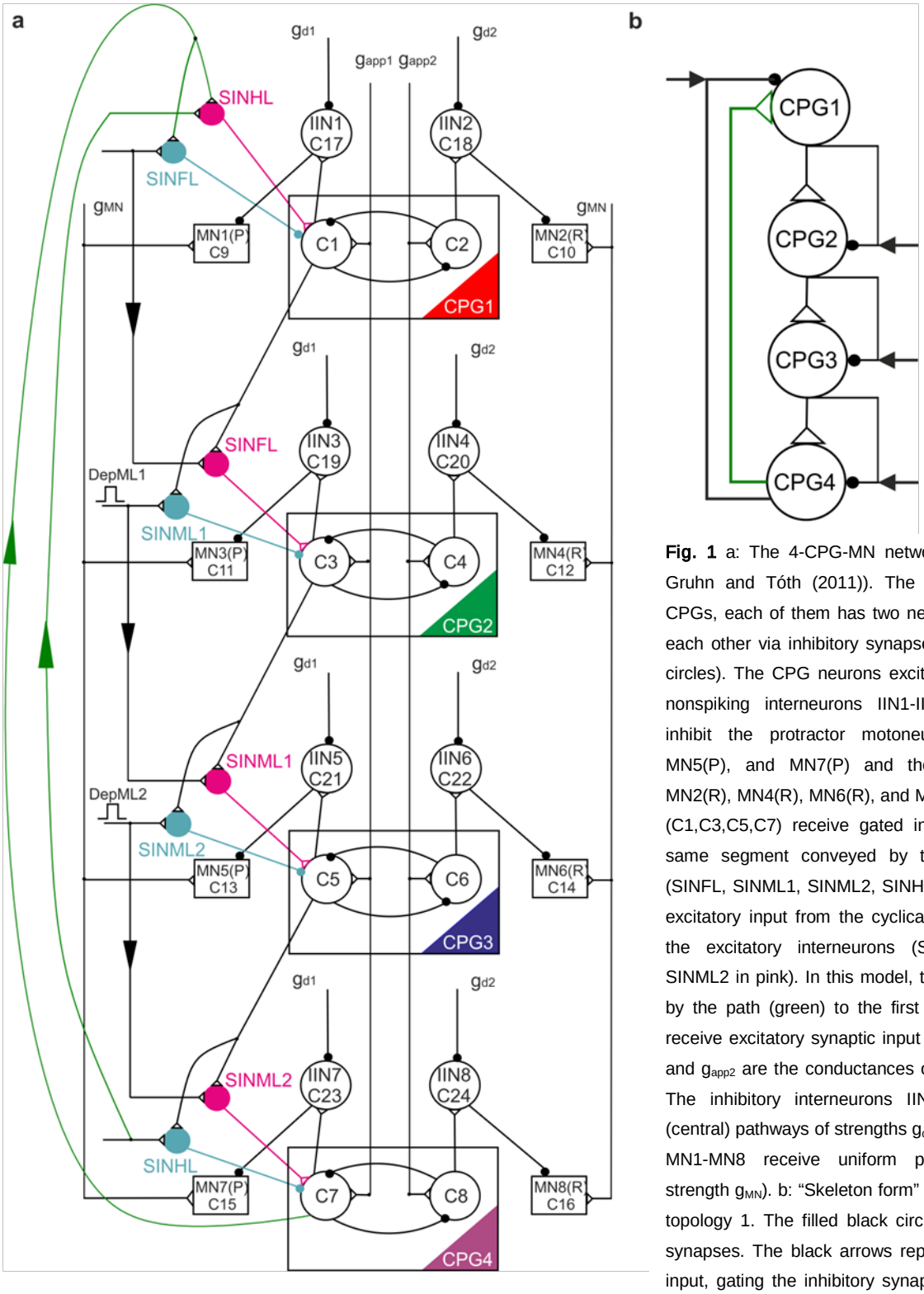

Fig. 1 a: The 4-CPG-MN network (modified after Daun-Gruhn and Tóth (2011)). The network consists of four CPGs, each of them has two neurons (C1-C8) that inhibit each other via inhibitory synapses (connections with filled circles). The CPG neurons excite (empty triangles) other, nonspiking interneurons IIN1-IIN8. These interneurons inhibit the protractor motoneurons MN1(P), MN3(P), MN5(P), and MN7(P) and the retractor motoneurons MN2(R), MN4(R), MN6(R), and MN8(R). The CPG neurons (C1,C3,C5,C7) receive gated inhibitory signals from the same segment conveyed by the sensory interneurons (SINFL, SINML1, SINML2, SINHL in turquoise), and gated excitatory input from the cyclically preceding segment by the excitatory interneurons (SINHL, SINFL, SINML1, SINML2 in pink). In this model, the last CPG is connected by the path (green) to the first CPG. The CPG neurons receive excitatory synaptic input from higher centers (g_{app1} and g_{app2} are the conductances of the excitatory currents). The inhibitory interneurons IIN1-IIN8 are inhibited by (central) pathways of strengths g_{d1} to g_{d8}. The motoneurons MN1-MN8 receive uniform permanent excitation (of strength g_{MN}). b: "Skeleton form" of the 4-CPG-MN network topology 1. The filled black circles represent the artificial synapses. The black arrows represent the local inhibitory input, gating the inhibitory synapses. The empty triangles represent the excitatory synapses. The excitation derives from the cyclically preceding CPG.

Classification of coordination patterns

The classification of the coordination patterns was adopted from, and modified, after Barnes (1975), Parrack (1964), and Ross and Belanger (2013), and is summarized in Table 1. The numbers in Table 1 stand for the single legs, starting with 4, the last walking leg, and ending with 1, the first walking leg. The chelipeds of crabs and crayfish are not counted as legs since, in most cases they don't contribute to walking. The same applies to the swimmeret system in crayfish. The horizontal brackets in Table 1 denote synchronous activity of the enclosed legs. The coordination patterns observed in these animals include Coordination pattern 1 (yellow): a wave coordination pattern with different orders of leg protraction; Coordination pattern 2 (green): a coordination pattern that is characterized by synchronous protractions of two ipsilateral legs followed by alternating protractions of the remaining two legs; and Coordination pattern 3 (blue): a diagonal pattern, also called "alternating tetrapod step pattern" (Barnes 1975) in which two legs are simultaneously in protraction phase followed by the remaining two legs that also move in synchrony.

stepping order	coordination pattern
4 3 2 1	1
4 1 3 2	1
4 1 2 3	1
4 3 1 2	1
4 1 3 2	2
4 1 2 3	2
4 3 2 1	2
4 3 2 1	2
4 2 1 3	2
4 1 3 2	3
4 2 3 1	3
4 3 2 1	3

Table 1 Classes of coordination patterns (modified after Barnes 1974; Parrack 1964; Ross 2013). On the right hand side, the table shows coordination patterns 1, 2, and 3 and the different variants of these coordination patterns observed in crayfish and crabs during forward walking. The left hand side shows the leg numbers 4-1 (hind leg to front leg), and the colour code shown will be used in the subsequent figures. The brackets indicate the simultaneous protractor activities of the individual legs. Coordination pattern 1 (yellow) is a pattern where one leg after another is in protraction phase. Coordination pattern 2 (green) is characterized by simultaneous protractions of two legs followed by alternating protractions of the two remaining legs. Coordination pattern 3 (blue) is a diagonal pattern, also called "alternating tetrapod step pattern" (Barnes 1974) where two pairs of ipsilateral legs alternately protract. The darker the colour is on the right hand side, the more frequently this coordination pattern is observed.

In our model, protracting legs were considered to be synchronously active if the overlap of their swing phases was more than 50%. Examples for different crayfish coordination footfall patterns are shown in Fig. 2, adapted from Cruse and Müller (1986). This figure shows the response of the walking crayfish to perturbations of a single leg during its stance phase. In the following, we shall apply the same method of identification of coordination patterns to our simulation results.

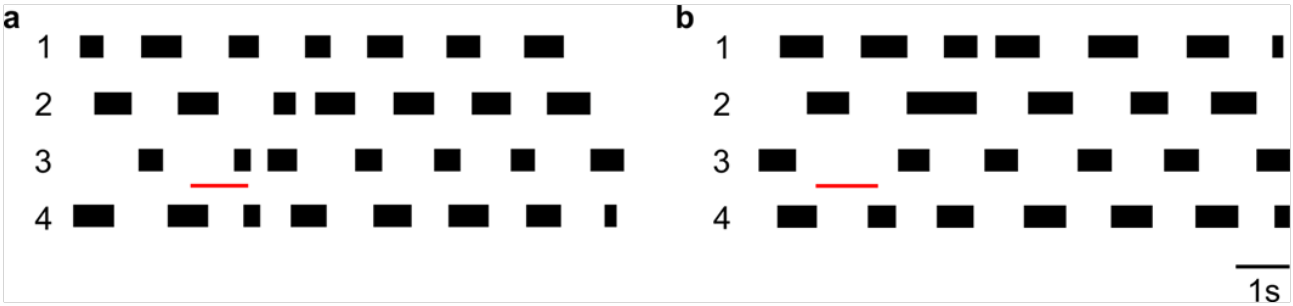

Fig. 2 Coordination of ipsilateral walking legs of a crayfish (modified after Cruse and Müller (1986)). In both panels, the black bars represent the protraction phase. The numbers 1-4 represent the single walking legs, starting with the front leg down to the hind leg. The thin red line indicates the timing of the perturbation, a: shortened retraction phase, and b: prolonged retraction phase. In both cases, the crayfish returned to a stable coordination pattern after a few stepping periods of adjustment.

RESULTS

Simulating different coordination patterns by varying the timing of the sensory signal that gates the inter-segmental excitatory synaptic pathway

In order to be able to simulate 8-legged locomotion, we extended the 3-CPG-MN network, which could reproduce coordination patterns of the stick insect walking, by adding a “second middle leg” to the network. The CPG of this new segment had the same properties as the existing ones. In the 4-CPG-MN network model, like in the 3-CPG-MN one, the most posterior CPG cyclically connects to the most anterior CPG by both excitatory and inhibitory synaptic pathways (Fig. 1a, b). In this extended model, too, the sensory signals encoding for ground contact and load gate the excitatory inter-segmental pathways from the cyclically preceding leg to the subsequent one, especially the synaptic pathway from CPG4 to CPG1 (Fig. 1a, b). We called the topology of this model topology 1. This distinction was necessary since we later introduced a network model with a different topology.

The timing of the gating by the sensory signal, as mentioned earlier (cf. Materials and Methods), is expressed by the value of the phase variable ϕ. Thus ϕ can take values between 0 and 1, and is a periodic variable. We wanted to find values of ϕ for which coordination patterns 1, 2 and 3 could be produced by the extended (4-CPG-MN) network model (Table 1). For this to happen, we systematically varied ϕ and examined the simulated activities of the segmental CPGs. More precisely, we varied ϕ_{ij} locally at each segment i with an increment of 0.1 between 0.02 and 1 and determined whether an experimentally established coordination pattern was produced by the model. We called a coordination pattern 'stable' if it was periodic. As an example of this procedure, Fig. 3 displays a colour-coded plot representing coordination patterns that could be generated by the model when varying ϕ_{14} (vertical axis in Fig. 3) and ϕ_{21} (horizontal axis in Fig 3). The other ϕ values were fixed, i.e. ϕ_{32}=0.82 and ϕ_{43}=0.62.

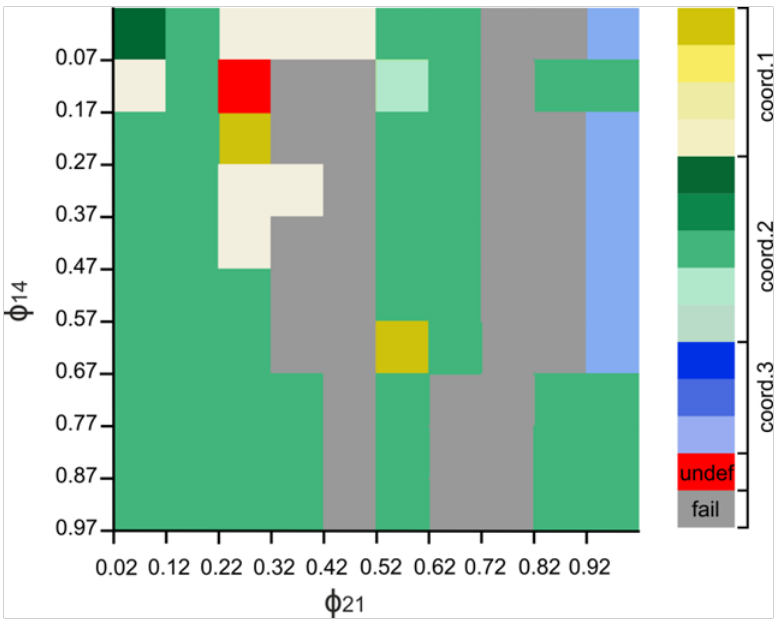

Fig. 3 System output when two segmental ϕ, as indicated, are varied. ϕ_{32} = 0.82 and ϕ_{43} =0.62 were fixed. The y-axis shows the values of ϕ_{14} and the x-axis shows the values ϕ_{21}. The colours in the diagram represent the different coordination patterns in Table 1. The red area represents a stable, but experimentally not observed coordination patterns (observed in 1% of the test cases). The grey areas represent failures (see text). The proportion of failures was about 30% of the test cases. 51% of the test cases resulted in variants of coordination pattern 2 (green). Nevertheless these variants were not the one that was most frequently observed in the animals. Variants of coordination pattern 1 (yellow) occurred in 9% of the test cases. But here, too, the resulting coordination patterns 1 were not the most frequently occurring ones in the experiments. In 9% of the test cases, we observed a variant of coordination pattern 3 (blue).

A metachronal wave coordination pattern (coordination pattern 1, yellow in Fig. 3), a wave-like activity that propagates through all segments in the posterior-anterior direction, also shown in Fig. 4a for ϕ_{14}=0.07 and ϕ_{21}=0.32 arose in 9% of the test cases. Fig. 4b displays a variant of coordination pattern 2 obtained with the model when ϕ_{14} was 0.07 and ϕ_{21}=0.02. In this case, CPG1 (red) and CPG4 (purple) are in the protraction phase simultaneously followed by CPG3 (blue) and CPG2 (green). This pattern occurred in 51% of the test cases (green, Fig. 3). The panels on the left of Fig. 4 show the electrical activity of the four protractor CPG neurons for each of the three coordination patterns. The panels on the right are the footfall patterns of all four ipsilateral legs. 4 denotes the hind leg, 3 and 2 the middle legs, and 1 the front leg. The coloured bars represent the protraction (swing) phases of the CPGs.

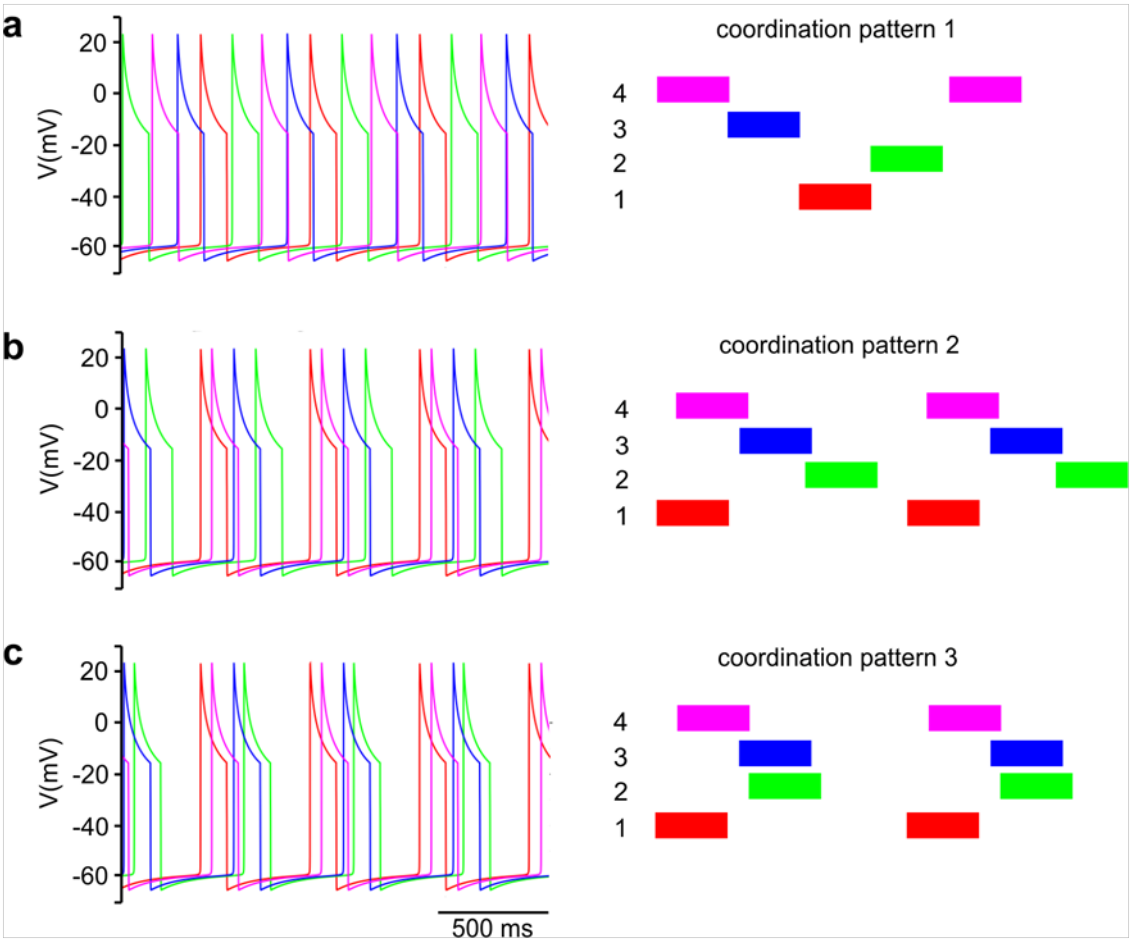

Fig. 4 Examples of coordination patterns 1, 2 and 3. a: coordination pattern 1. The time courses of the electrical activity of all four protractor neurons are shown on the left hand side. On the right hand side, the successive protractor phases (colour bars) of the 4 legs are displayed in the different coordination patterns (4-1 are 4 right legs, 4 being the hind leg etc.) b: coordination pattern 2. In the simulations, the overlap between the activities of CPG4 and CPG1 is not perfect. c: coordination pattern 3. As in b, the simulated activities of CPG4 and CPG1 as well as CPG3 and CPG2 show a slightly imperfect overlap as in the animal.

It was surprising that although it was possible to obtain all different coordination patterns 1, 2, and 3 by varying a single ϕ, only (e.g. first row in the (ϕ_{14}, ϕ_{21})-matrix of Fig. 3), a high proportion of value combinations of ϕ_{ij} resulted in failure (30% of the test cases, grey areas in Fig. 3). This high proportion of failures was also representative when other combinations of ϕ were varied. A failure was defined as the state when one of the two CPG neurons remained in steady state. In other words, the activity of the protractor or retractor neuron, or both of any of the four CPGs became or remained tonically active or was at rest. The other CPGs could still continue exhibiting rhythmic

(periodic) activity. Another form of failure could be that at least two CPGs oscillated independently of each other. This can happen due to an increase of the synaptic drive to both CPG cells and therefore lead to different oscillation periods of the four CPGs.

We also encountered activities that satisfied the aforementioned criterion for stable coordination patterns but had not been observed in experiments. We called such coordination patterns undefined. Fig. 3 shows that such coordination patterns could be observed in about 1% of the test cases (red area in Fig. 3).
With the value combinations of ϕ_{ij} that are shown in Fig. 3, it was not possible to reproduce the variant of coordination pattern 3 that had been most frequently observed in walking crayfish and crabs. The light blue areas (9% of the test cases) represent a rather rare variant of coordination pattern 3. To obtain the former (most frequent) variant of coordination pattern 3, all four ϕ values had to be changed when starting from coordination pattern 1. An example of such a coordination pattern is displayed in Fig. 4c. Here, two pairs of CPGs, CPG4 (purple) and CPG1 (red), and CPG2 (green) and CPG3 (blue) are alternately in protraction phase, i.e. each pair of CPGs oscillates synchronously. This happened at the following values of ϕ: $\phi_{14} = 0.05$, $\phi_{21} = 0.64$, $\phi_{32} = 0.04$ and $\phi_{43} = 0.25$. The gap between protraction activities of the CPG pairs (blue and green and purple and red) is due to the longer duration of the corresponding retractor activities of these CPGs. In all cases shown, the ratio of the lengths of the protractor and retractor activity was 1:3, i.e. the retractor being active in ¾ of the oscillatory period and the protractor in the remaining ¼.

Transitions between the different coordination patterns

As insects, crustaceans can also exhibit several coordination patterns within one walking sequence by switching between them (Ross and Belanger 2013; Barnes 1974). Also short perturbations of a leg in the swing or stance phase can change the coordination pattern with a transition time of only a few periods until the new coordination pattern sets in (Cruse and Müller 1986). While this always works in (intact) animals, there is no guarantee that the transition would also be successful in the simulations. We therefore called a transition 'stable' (successful) if, as a result, a stable coordination pattern (of any kind) emerged after a transition time of at most four periods of CPG oscillation prior to the transition. Otherwise, it was called 'unstable' or a 'failed transition'. The choice of four oscillatory periods is in accordance with experimental observations (Cruse and Müller 1986).
Indeed, we found in the simulations that the success of a transition from one coordination pattern to another crucially depended on when the transition was triggered within the actual oscillatory period of the CPGs. Thus we sought to find the phase values (the instants of time within one oscillatory period) at which the transition remained stable. The simulation results showed that if the transition was triggered in the last third of the retraction phase of the CPG oscillation then the transition proved to be stable for all coordination patterns. Starting the transition in phases different from the above, for example in the protractor phase of the oscillatory period, led to unstable transitions (data not shown). This was a general result of testing the individual coordination patterns. We now present the related simulation results. For triggering of the transition between the coordination patterns 1 and 2, we increased ϕ_{14} =0.17 by 0.7. The transition started with a slight increase of the protractor phase of CPG1, followed by a strong extension of the protractor phase of the activity of CPG2. At the end of transition, synchrony between the activities of CPG2 and CPG4 ensued. Fig. 5a shows this process. Fig. 5b displays the transition in the opposite direction, from coordination pattern 2 to coordination pattern 1. Here, the transition was also triggered in

the last third of the retraction phase of the activity of CPG1. The transition could be effected by simply switching back ϕ_{14} to its former value of 0.17. Thus an increase or decrease of the original value of ϕ_{14} sufficed to bring about a stable transition between the coordination patterns 1 and 2 in both directions. The transition from coordination pattern 2 to 1 lasted four periods, two periods longer than the transition from coordination pattern 1 to 2. In both cases, a prolongation of the protraction phase of the activity of CPG1 and CPG2 could be observed. In Fig. 5b, the protraction phase of the activity of CPG1 did not coincide with the protraction phase of that of CPG2, but ended together with it.

With the extended network model introduced above, transition from coordination pattern 2 to a frequent variant of coordination pattern 3, or from coordination pattern 1 to a frequently occurring variant of coordination pattern 3 was not possible by just changing the value of a single ϕ parameter.

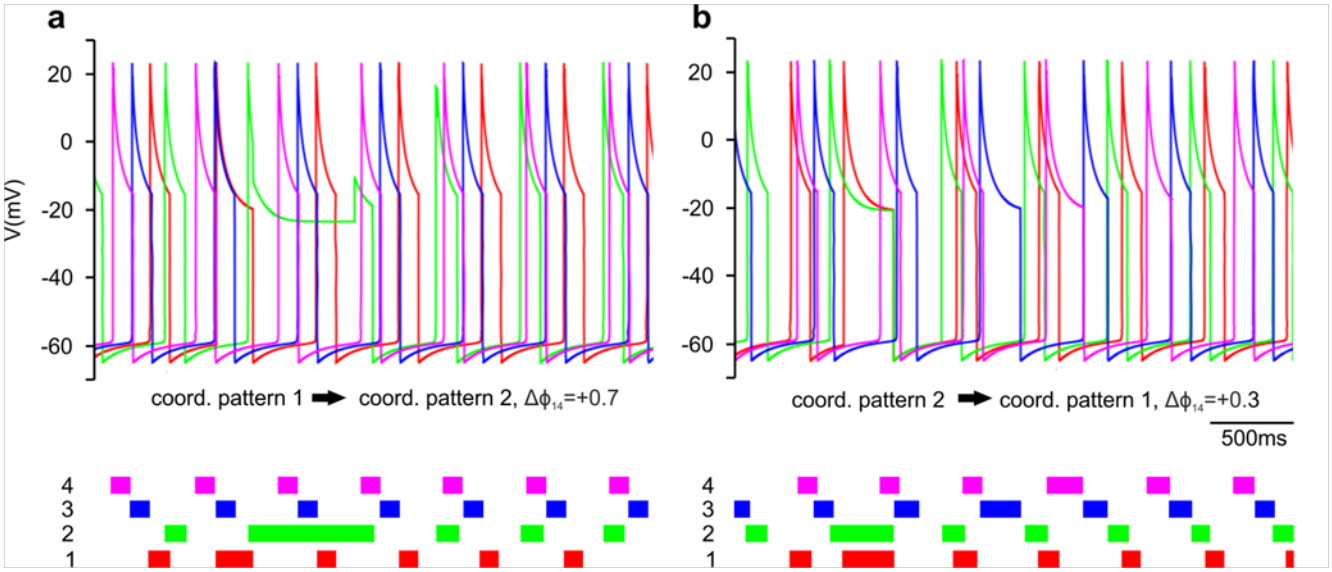

Fig. 5 Transitions between coordination pattern 1 and 2. a: Transition from coordination pattern 1 to coordination pattern 2. The transition with a prolonged protraction phase of the activity of CPG1 (red), followed by an even longer depolarized phase of CPG2 (green). The protraction phase of the activity of CPG2 and CPG4 (purple) then ends almost at the same time, and coordination pattern 2 ensues in the next cycle. b: transition from coordination pattern 2 to coordination pattern 1. In this case, the transition also begins with a prolonged activity of the protractor neurons of CPG1 (red) and CPG2 (green). The transition lasts four periods until coordination pattern 1 is attained.

Using the central drive to the CPGs for changing the oscillation dynamics

Crayfish and crabs can increase their walking speed during locomotion (Ross and Belanger 2013). A change in walking speed is often associated with a change in the coordination pattern (Ross and Belanger 2013). In the present network model, an increase in oscillation frequency, and a change in the ratio between the protractor and retractor phases of the CPG activity can be achieved by changing the value of the conductance g_{app} of the central driving synaptic current. We systematically varied the value of g_{app} using step sizes from 0.001nS to 0.1nS. To find a range in which the coordination patterns were stable, we first varied g_{app1} and g_{app2} by increasing or decreasing one of them, only (see Fig. 1). Then we varied both gapp1 and g_{app2} at the same time and amount.

An increase in g_{app1} led to an increase in relative length of the retractor phase, and an increase in g_{app2} in that of the protractor phase within the oscillatory regime of the CPG. To attain a 1:3 ratio of the protractor-to-retractor phase, we had to choose different values for g_{app1} and g_{app2}: g_{app1}=0.2500 nS, g_{app2}=0.1855 nS. However, increasing g_{app1} further beyond this value abolished the oscillation in the CPGs. Similarly, when g_{app2} exceeded the value 0.1870 nS, the oscillation stopped again.

We also obtained tonically active CPG neurons when setting $g_{app1}=g_{app2}$ in the interval [0.1855,0.1870] nS. The range of oscillations of the CPGs turned out to be rather small: $g_{app1} \in [0.23, 0.25]$ nS and $g_{app2} \in [0.1855,0.1870]$ nS. Furthermore, stable periodic oscillations occurred only if $g_{app1} > g_{app2}$.

In summary, we could simulate the commonly observed coordination patterns 1 and 2 when changing the value of the phase shift ϕ_{14}. However, the model could not reproduce the most typical variant of coordination pattern 3. Furthermore, we could only make minor changes of the oscillation dynamics, which is, in turn, important for determining the walking speed, by increasing or decreasing the values of g_{app1} and g_{app2}.

Modifying the network topology in order to improve the model

The basic idea of this study is to show that a 3-CPG-MN network model, mimicking the stick insect's walking behaviour, can be extended to simulate 8-legged locomotion. We modified the original network topology by first including an additional CPG, and by making connection to this CPG in the same manner as it was done in the 3-CPG-MN network. That is, the first CPG received sensory input from the last CPG. This connection was crucial in the 3-CPG-network model for the reproduction of stable coordination patterns and the transitions between them. We performed simulations with this model as reported in the preceding subsections but found serious limitations using it as outlined above. As one possible way of remedy, we modified its properties by changing its topology. In this modified network model, CPG1 receives a feedback signal from CPG3 and CPG2 one from CPG4 (green pathways in Fig. 6). We called this new topology of the modified network model 'topology 2' as opposed to 'topology 1' of the former version of the model. In functional terms, this means that CPG2 now does not only receive sensory information about the ground contact of the front leg, but also from the hind leg, whereas CPG1 now receives sensory information from CPG3. Accordingly, this is another specific extension of the 3-CPG-MN network model, an embodiment of the basis for more complex network models used in the present work.

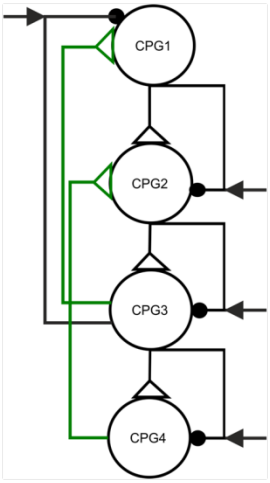

Fig. 6 Schematic illustration of network topology 2. CPG2 receives two excitatory inputs, one from CPG1, the other from CPG4. This topology makes use of the idea of an excitatory feedback from a CPG to the second preceding one, i.e. here from CPG4 to CPG2 and from CPG3 to CPG1. This is clearly an extension of the topology of the 3-CPG-MN model by Daun-Gruhn and Tóth (2011).

Simulating coordination patterns 1, 2, and 3 with the modified model (topology 2) by varying ϕ

The modified model having topology 2 could reproduce all coordination patterns that had been described for crabs and crayfish (Table 1). Fig. 7 shows one example each of the coordination patterns 1, 2 and 3 that were produced by this model. In the left panels, the activities of the protractor neurons of the four segmental CPGs are displayed. In Fig. 7a, coordination pattern 1 starts with the activity in CPG4 followed by activities in CPG3, CPG2 and4 CPG1. In Fig. 7b, during coordination pattern 2, both CPG1 and CPG4 are in protraction phase almost at the same time, followed by CPG 3 and CPG2. Fig. 7c shows coordination pattern 3, where CPG4 and CPG2 are simultaneously in the protraction phase followed by corresponding simultaneous activities of CPG 1 and CPG3. We started testing the network model with topology 2 by varying the system parameter ϕ for each CPG separately, and then by changing the values of ϕ of two CPGs and fixing the other values.

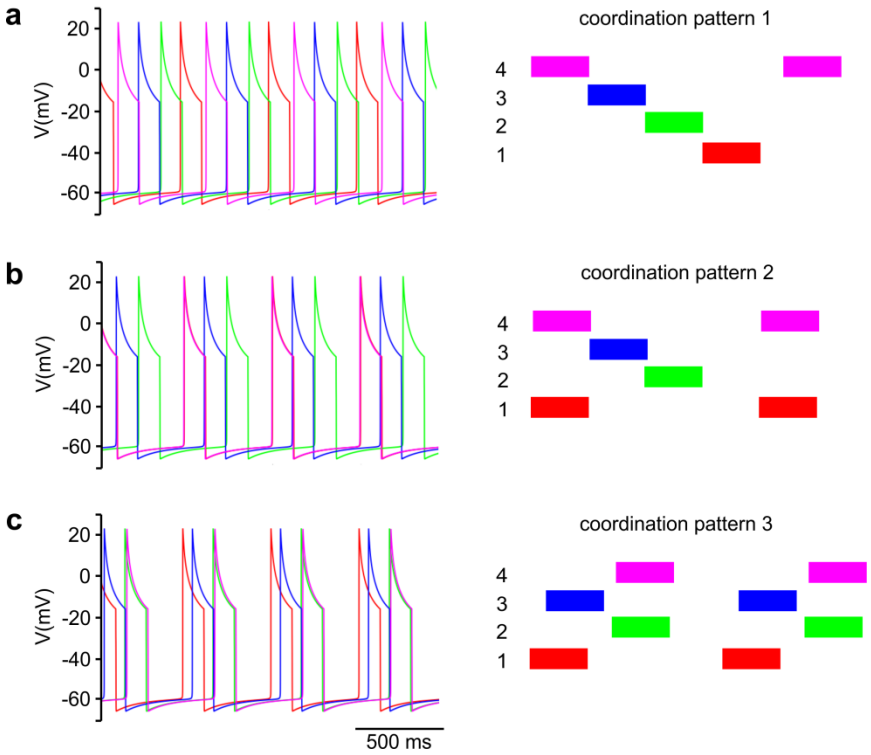

Fig. 7 Examples of coordination patterns 1, 2 and 3 produced by the 4-CPG-MN model with topology 2. a: Coordination pattern 1: wave-like activity spreading from CPG4 (purple) to CPG1 (red) via CPG3 (blue) and CPG2 (green). b: Coordination pattern 2: CPG1 (red) and CPG4 (purple) are simultaneously active, followed by the activity of CPG3 (blue) and then of CPG2 (green). c: Coordination pattern 3: CPG4 (purple) and CPG2 (green) are active at the same time, followed by simultaneous activity of CPG1 (red) and CPG3 (blue).

The three diagrams in Fig. 8 show examples of simulation results that were obtained by varying pairs of ϕ to produce different coordination patterns (The colour codes in Fig. 8 match those in Table 1.). Thus in Fig. 8a: ϕ_{13} and ϕ_{43}; in Fig. 8b: ϕ_{13} and ϕ_{21} at ϕ_{32} =0.12, and in Fig. 8c: ϕ_{13} and ϕ_{21} at ϕ_{32} =0.82 were varied. The simulation results obviously depend on the chosen pairs of ϕ. This is well illustrated in Fig. 8, where each panel shows a different distribution of coordination patterns. Among the simulation results, as these panels witness, there are fewer failures than among the results obtained with the previous version of the model having topology 1. Similarly, the proportion of failures (grey areas in Fig. 8) is considerably smaller (10%) here than with the previous version (33%) (cf. Fig. 5). The darker the colour of the coordination pattern, the more likely it is to appear in crabs and crayfish. Fig. 8a and b show the difference a small change in ϕ can make to the whole system. Although the system

was very sensitive to small changes of ϕ, it remained stable. We did not observe more than 10% failed attempts to produce coordination patterns. We could also show that the relative frequency of occurrence of a specific coordination pattern in our simulations is highly dependent on the combination of the values of ϕ. The diagrams in Fig. 8b and c differ only in the (fixed) value of ϕ_{32} (0.12 in Fig. 8b, and 0.82 in Fig. 8c). As with topology 1, the aim of the new simulations using the model with topology 2 was to find a set of values of ϕ_{ij} with which all three coordination patterns could be reproduced. This is illustrated in Fig. 8c. We can thus fix the value of one of the ϕs and vary the other one in Fig. 8c to produce the transitions between all different coordination patterns. In summary, we can state that the model version with topology 2 can produce a larger proportion of stable results when varying ϕ than the one with topology 1.

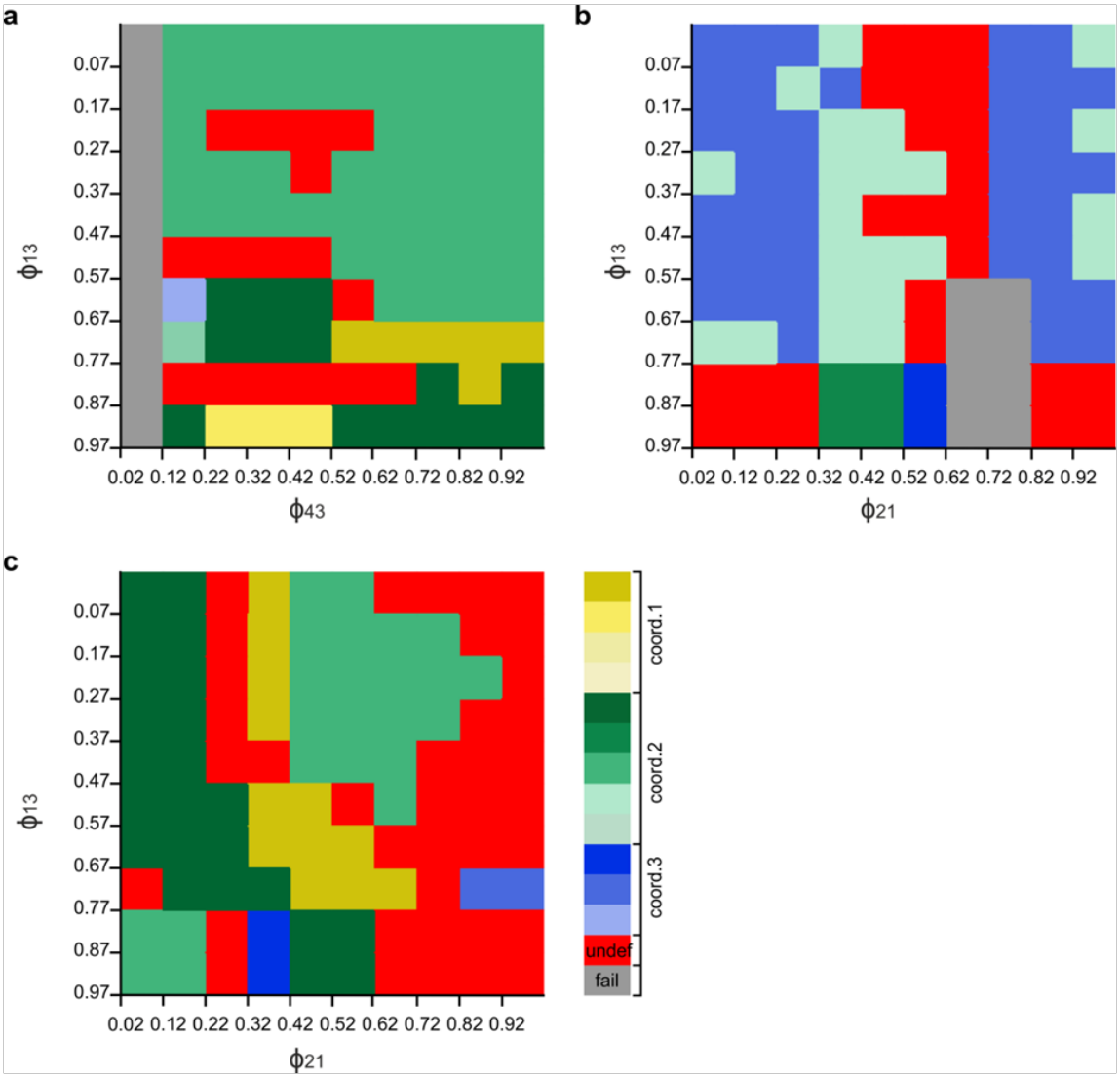

Fig. 8 Dependence of the coordination patterns on different pairs of ϕ. The colour codes for the different coordination patterns agree with the ones shown in Table 1. a: ϕ_{13} (y-axis) versus ϕ_{43} (x-axis). The failures amounted to 10% of all test cases, only. All of them occurred at ϕ_{43} =0.02. Coordination pattern 2 was found in 34% of the test cases compared to 9% for coordination pattern 1 and only 1% for coordination pattern 3. The proportion of undefined coordination patterns was 16%. The remaining ϕ values were: ϕ_{21} = 0.52, ϕ_{24}=0.12 and ϕ_{32}=0.82. b: ϕ_{13} (y-axis) versus ϕ_{21} (x-axis). Here, the proportion of coordination pattern 3 was very high: 41%. Coordination pattern 2 was present in 26% of the test cases. 25% of the coordination patterns were undefined and only 8% were failures. The fixed values of the remaining ϕ were ϕ_{24}=0.12, ϕ_{32}=0.12 and ϕ_{43}=0.62. c: ϕ_{13} (y-axis) versus ϕ_{21}(x-axis), as in b, but now at a changed ϕ_{32}=0.82, the same value as in a. With these settings, no failures were observed. In 46 % of the test cases, coordination pattern 2 appeared, in 12% of the test cases, coordination pattern 1, and in 4%, coordination pattern 3. 38% of the test cases yielded undefined but stable coordination patterns.

Transitions between coordination patterns 1, 2, and 3 produced by the model with topology 2 when changing the value of ϕ_{21}

To produce transitions between the coordination patterns, we proceeded the same way as with the previous version of the network model (of topology 1). Using the new topology (topology 2, Fig. 6), we found that, for the transitions between the coordination patterns, it now sufficed to change only a single ϕ, namely ϕ_{21}. The values of the other ϕ parameters were kept constant: ϕ_{13} =0.77, ϕ_{24} =0.12, ϕ_{32} =0.82, and ϕ_{43} =0.62. The results are summarized in Fig. 8c. We started with coordination pattern 1 (Fig. 7a) at which ϕ_{21}=0.42. In order to trigger the transition to coordination pattern 2, ϕ_{21} was changed to 0.12 (Fig. 9a).

A further change of this parameter to 0.82 resulted in the transition to coordination pattern 3 (Fig. 9b). The transition from coordination pattern 1 to coordination pattern 3 could be achieved by setting ϕ_{21}= 0.82 (Fig. 9c). The transitions in the opposite directions took place when the changes of ϕ_{21} were simply reversed (all panels on the right hand side in Fig. 9a-c). As with the model having topology 1, all of these changes of ϕ_{21} had to be carried out during the last third of the retractor phase to produce a stable transition. It is to be noted that, in these cases, it sufficed to change one system parameter, only, on a single CPG. The simulations showed that there were different ways of producing transitions between the coordination patterns just by changing the value of a single ϕ parameter.

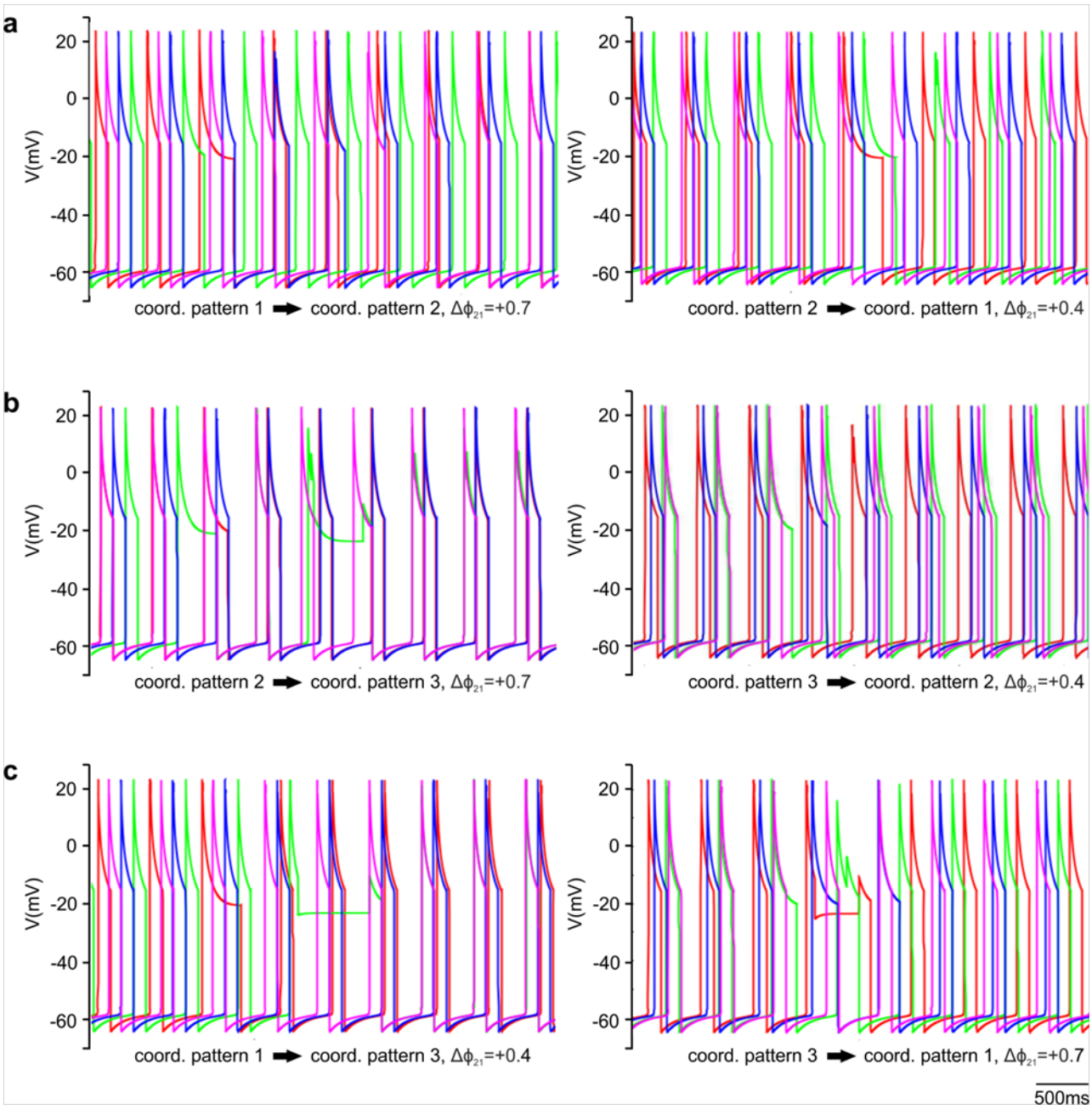

Fig. 9 Transitions between coordination patterns 1, 2 and 3. a: left: Transition from coordination pattern 1 to coordination pattern 2. The transition starts with a prolonged protraction phase of CPG1 (red) and lasts for 3 periods. Right: transition from coordination pattern 2 to coordination pattern 1. The transition starts with a longer protraction phase of CPG2 (green), and CPG1 (red) and lasts for 1 period. b: left: transition from coordination pattern 2 to coordination pattern 3. The protraction phase of CPG2 (green) is prolonged. The system needs 3 periods to attain coordination pattern 3. Right: transition from coordination pattern 3 to coordination pattern 2. An elongated protraction phase of CPG2 (green) can be observed at the start of the transition, which lasts for 2 periods. c: left: transition from coordination pattern 1 to coordination pattern 3. As in the transition in a, it starts with a prolonged protractor phase of CPG1 (red), and lasts for 2 periods. Right: transition from coordination pattern 3 to coordination pattern 1. This transition, too, similarly to the cases in a and b, starts with a longer protraction phase of CPG2 (green), and lasts for 2 periods.

Network topology 2 ensures stability when changing the central drive to the CPGs

In the preceding section, we have showed that the transitions between coordination patterns remained stable when using the modified network topology (topology 2).

We then varied the parameters g_{app1} and g_{app2} of the central drive to the CPGs in order to see their effect on the oscillatory period and the protractor (swing) and retractor (stance) phase. In contrast to the results obtained with the network model of topology 1, we could vary both g_{app}s by the same values and still produce stable coordination patterns that were observed in crayfish and crabs during walking. Another advantage was the wider range of admissible g_{app} values: $g_{app1} \in [0.19, 0.3]$ nS and $g_{app2} \in [0.1852, 0.1905]$ nS.

During these variations, the relative lengths of the protractor and retractor phase within one CPG period remained unaltered. However, the absolute length of the CPG period decreased with increasing drive intensities (values of g_{app}s). Change of the g_{app} values in the opposite direction resulted in an increase of the CPG period. When increasing g_{app2} alone, we observed a prolonged protraction phase of the CPGs and therefore a shorter retraction phase. When increasing g_{app1} only, the retraction (stance) phase became longer and the protraction (swing) phase shorter. In all of these cases, coordination pattern 3 remained stable. Fig. 10a shows coordination pattern 3 with g_{app1}=0.25 nS and g_{app2}= 0.1855nS. The ratio of the protractor and retractor phases was, in this case, 1:3. However, that could be changed to 1:1 when the conductances of central driving currents were set to g_{app1}=0.2510 nS and g_{app2}= 0.1900 nS, producing another variant of coordination pattern 3 (Fig. 10b). The relative length of the retractor phase within one CPG oscillatory period could even be varied by increasing g_{app2}, while keeping g_{app1} constant (Fig. 10c). This figure also shows that the oscillatory period also decreased with decreasing retractor phase. Nevertheless, the protractor phase remained constant. This is in good agreement with experimental findings.

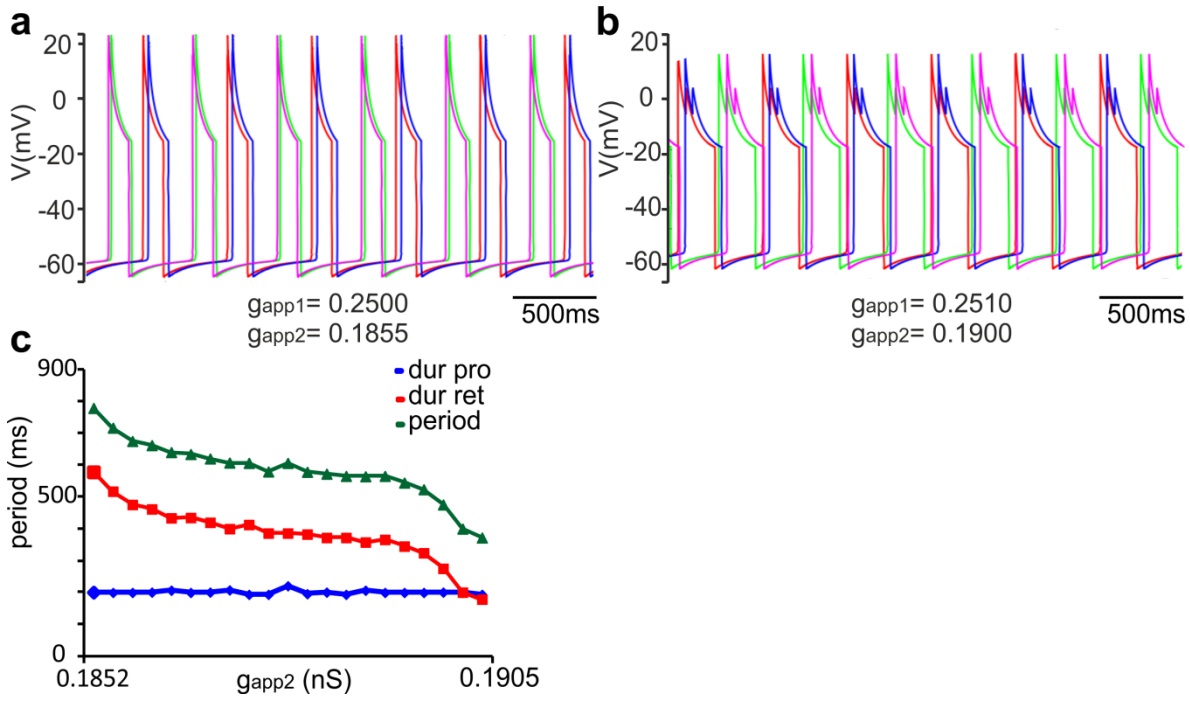

Fig. 10 Changing the values of g_{app1} and g_{app2} resulted in a change in the oscillatory period of the CPG units. a: coordination pattern 3 with a protraction phase of 125ms and a ratio of protractor-retractor phase of 1:3. b: coordination pattern 3 with a protraction duration of 250ms and a ratio of protractor-retractor phase of 1:1. Here, g_{app2} was increased by 0.0045nS and g_{app1} by 0.001nS. c: dependence of the CPG period on g_{app2} when g_{app1}=0.25nS was fixed. As it can be seen, the retractor phase of the CPG (red) shortened, and the oscillatory period (green) decreased. At the same time, the duration of the protractor phase remained constant (blue).

DISCUSSION

In this work, we set out to model the coordination patterns that are exhibited by animals walking on eight legs, in particular by crayfish and forward walking crabs. The work was inspired by the results on modelling coordination patterns of 6-legged animals, in particular of the stick insect (Daun-Gruhn and Tóth 2011). In this model, the coordination of the three ipsilateral legs during (normal) walking was simulated. More precisely, the electrical activity of the protractor neurons of segmental protractor-retractor CPGs was reproduced in the model, and their temporal coordination yielded the coordination patterns tetrapod and tripod. This model was also capable of reproducing transitions between the two coordination patterns.

We used this model for 6-legged locomotion, denoted as the 3-CPG-MN model, and extended it by one CPG-MN local network controlling a "second middle leg" but preserved the basic construction principles of the original model, first and foremost the cyclic connection of the segmental CPGs in it. With the resulting model, which we called the extended model with topology 1, we could reproduce coordination patterns of the ipsilateral legs in animals walking on eight legs. As in the original (3-CPG-MN) model, in the extended model, too, the different coordination patterns could be generated by varying the phase shifts ϕ between the oscillatory activities of the segmental CPGs and the sensory signals from the cyclically preceding segment that modulate the (cyclically) descending excitatory connections between the protractor-retractor CPGs. While we could reproduce all three coordination patterns listed in Table 1, the failure rate, i.e. the combinations of ϕ values at which no coordination pattern was produced, was high (about 30% of the test cases, cf. Fig. 3). In addition, some transitions between the coordination patterns could only be reproduced by changing the values of ϕ at all four segments. Furthermore, a considerable proportion of the transitions proved to be unstable.

Trying to remedy these shortcomings of the extended model, we changed its topology. We abolished the connection from CPG4 to CPG1 and introduced the connections from CPG4 to CPG2 and from CPG3 to CPG1 (cf. Fig. 6). Here, we used another property of the topology of the 3-CPG-MN network model, namely the feedback (ascending) connection to the second anterior segment (i.e. from CPG3 to CPG1). We called this version of the extended model the model with topology 2. With this version of the extended model, we could reduce the failure rate significantly (to 10% of all test cases, cf. Fig. 8). Furthermore, the transition between the coordination patterns in either direction now only required the change of one ϕ value (cf. Fig. 8). Thus, this version of the model (i.e. the version with topology 2) has proven to be satisfactory for the simulation of the coordination patterns of legs on the ipsilateral side of animals walking on eight legs during (normal) walking.

As with all models of physiological systems, the following question arises here, too: how and to what extent is the extended model (with topology 2) supported by physiological findings? To answer it, we first point out that the 3-CPG-MN network model by Daun-Gruhn and Tóth (2011) was already based on physiological results concerning the existence and structure of the local segmental protractor-retractor control network. In addition, physiologically reasonable assumptions helped complete their model (For details see Daun-Gruhn and Tóth (2011)). As mentioned in the introduction, there are close similarities in the structure and organization of the nervous systems of stick insects and crustaceans. It was therefore quite natural to transfer those similarities and analogies between the models, too. For example, Clarac (1982) found that proprioceptive feedback seemed to stabilize the centrally generated rhythm in intact crayfish (Clarac 1982; Libersat et al. 1987). This underpins the importance of peripheral

influences in these biological systems, hence in their models (Cruse 1990; Sillar et al. 1986; Clarac 1982; Libersat 1987; Cruse and Müller 1991; Jamon and Clarac 1995). In both the original 3-CPG-MN network model and the extended 4-CPG-MN models, the peripheral sensory signals that represent ground contact and load play an important role in the inter-leg coordination. In these models, they gate (modulate) the excitatory connections between the segmental CPGs. In the stick insect, the load signals most likely originate in the campaniform sensilla, signals indicating position in proprioceptors, while those encoding for (angular) velocity in chordotonal organs (Akay et al. 2001; Bässler and Büschges 1998; Bucher et al. 2003; Borgmann et al. 2007; Borgman et al. 2009). Comparable sensory inputs in crayfish and crabs are the thoracic–coxal muscle receptor organ (TCMRO) (Sillar et al. 1986), and the cuticular stress detectors (CSDs) (Clarac, Wales and Laverack 1971; Klärner and Barth, 1986, Klärner and Barnes 1986). Both sensory organs are responsible for the timing and intensity of rhythmic output of two or more ipsilateral ganglia (Sillar et al. 1986; Klärner and Barnes 1986). These are clear physiological analogies between the structure and function of the nervous systems of the stick insect and crustaceans. They amply justify our approach to the modelling task as outlined above.

The models with both network topologies revealed that a small change in the timing of the sensory input (ϕ at the different segments) had a strong influence on the output of the system. The change of timing resulted in different coordination patterns although the synaptic strength of the connections remained the same during the simulations (Fig. 8). This is in close agreement with the results of experiments in which the TMCRO was stimulated. There, it was found that the timing and intensity of the rhythmic output of the promotor and remotor MN activity in the same segment and adjacent segments was strongly affected by the stimulation (Sillar, Clarac and Busch 1987).

Our extended model could also be tested in the following way. It was shown in experiments that, without sensory feedback, the MNs of the ipsilateral ganglia of crustaceans exhibited a strong tendency to burst in phase (Clarac 1982). Our 4-CPG-MN network model also has this property: by blocking the inter-segmental sensory pathways in the model, we observed synchronous activity of all four CPGs (data not shown).

In constructing the 3-CPG-MN model, Daun-Gruhn and Tóth (2011) could restrict their considerations to an ipsilateral side, since experimental evidence showed a negligibly small contralateral influence of leg movements (Borgmann et al. 2007; Borgmann et al. 2009; Westmark et al. 2009). In crustaceans, too, the contralateral influences that were found also proved to be weak (Cruse 1990; Cruse and Müller 1991; MacMillan 1975).

The simulation results showed that the model behaviour, the period and the relative lengths of the protractor and retractor phases are quite sensitive even to small changes in the intensity of the central drive (the conductance g_{app}) to them. This affects the robustness of the model behaviour. To tackle this point, we should like to point out that the two-neuron CPG is most likely a strong reduction (simplification) of the CPG in the animals (stick insect and crayfish, crabs). In an ensemble of several neurons, the sensitivity of the (oscillatory) behaviour diminishes, because the driving current can be assumed to be distributed between the neurons of the real CPG. We therefore do not feel that this type of parameter sensitivity found in the simulations is serious shortcoming of our model.

Another important point to be tackled is the physiological viability of producing variable phase shifts (values of ϕ) between the segmental sensory signals and the periodic oscillations of the segmental CPGs. Here, we can only speculate that the sensory signals might pass through polysynaptic pathways of different length within the segmental ganglion. By doing so, their delay with regard to a fixed phase of the CPG oscillation is changed. Selectively blocking these polysynaptic pathways by central nervous mechanisms, delays of various lengths of the sensory signals, corresponding to changing the value of ϕ, might be brought about in the segmental ganglia of the nervous system.

In summary, our study shows that the 4-CPG-MN network model with topology 2 can successfully be applied to simulation of coordinated locomotion in arthropods with more than six legs. The basis for this model, as already mentioned, was the model by Daun-Gruhn and Tóth (2011), which was constructed using experimental data from the stick insect. The extended 4-CPG-MN model could be obtained without changing the main properties of the original model by Daun-Gruhn and Tóth (2011). The results in the present work suggest that coordinated walking in arthropods could have a common origin based on the similar architecture of the respective nervous systems. The differences arise due to the different number of legs in the individual species but the main principles of inter-segmental organization do remain the same. One of the most important common properties is the crucial role of sensory influences on the coordination of rhythmic activity of the different segments. The simulations proved that experimentally observed coordination patterns and the transitions between them could be simulated by changing the phase shift between the segmental sensory signals and the oscillatory activity of the affected segmental CPG, that is the value of ϕ. Moreover, our model displays a wide variety of coordination patterns by changing the value of just a single system parameter ϕ. Even though our model, in its present form, is partly hypothetical, it is logically consistent by being able to synthesize experimental evidence and physiologically reasonable assumptions. Moreover its assumptions and its predictions based on these assumptions can be tested in suitable experiments.

ACKNOWLEDGEMENTS

We would like to thank Dr. A. Büschges for useful discussions in the course of the work. The work was supported by DFG Grants to SDG: DA1182/1-1, GR3690/2-1 and GR3690/4-1.

REFERENCES

Akay, T., Bässler, U., Gerharz, P., Büschges, A. (2001). The Role of Sensory Signals From the Insect Coxa-Trochanteral Joint in Controlling Motor Activity of the Femur-Tibia Joint. *The American Physiological Society,* doi: 0022-3077/01.

Akay, T., Haehn, S., Schmitz, J., Büschges, A. (2004). Signals from load sensors underlie interjoint coordination during stepping. *Journal of Neurophysiology*, 96, 3532-3537.

Akay, T., Ludwar, B., Goritz, M.L., Schmitz, J., Büschges, A. (2007). Segment specificity of load signal processing depends on walking direction in the stick insect leg muscle control system. *Journal of Neuroscience*, 27, 3285-3294.

Barnes, W.J.P. (1975). Leg coordination during walking in the crab, *Uca pugnax*. *Journal of comparative Physiology*, 96, 237-256.

Bässler, U. and Büschges, A. (1998). Pattern generation for stick insect walking movements. Multisensory control of a locomotor program. *Brain Res. Rev*, 27, 65–68

Borgmann, A., Hooper, S. L., and Büschges, A. (2009). Sensory feedback induced by front-leg stepping entrains the activity of central pattern generators in caudal segments of the stick insect walking system. *Journal of Neuroscience*, 29, 2972–2983.

Borgmann, A., Scharstein, H., and Büschges, A. (2007). Intersegmental coordination: Influence of a single walking leg on the neighboring segments in the stick insect walking system. *Journal of Neurophysiology*, 98, 1685–1696.

Bowerman, R. F. (1977). The control of arthropod walking. *Comp. Biochemical Phvsiology*, 56A, 231-247.

Bucher, D., Akay, T., DiCaprio, R.A., Büschges, A. (2003). Interjoint Coordination in the Stick Insect Leg-Control System: The Role of Positional Signaling. *Journal of Neurophysiology* , 89, 1245-1255

Burrows, M., Hedwig, B. (1996). Presynaptic inhibition of sensory neurons during kicking movements in the locust . *Journal of Neurophysiology*, 75, 1221-1232.

Büschges, A. (1995). Role of local nonspiking interneurons in the generation of rhythmic motor activity in the stick insect. *Journal of Neurobiology*, 27, 488–512.

Büschges, A. (1998). Inhibitory synaptic drive patterns motoneuronal activity in rhythmic preparations of isolated thoracic ganglia in the stick insect. *Brain Research*, 783, 262–271.

Büschges, A. (2005). Sensory control and organization of neural networks mediating coordination of multi segmental organs for locomotion. *Journal of Neurophysiology*, 93, 1127–1135.

Büschges, A., Kudwar, B. Ch., Bucher, D., Schmidt, J., DiCaprio, R. A. (2004). Synaptic drive contributing to the rhythmic activation of motoneurons in the deafferented stick insect walking system. *European Journal of Neuroscience*, 19, 1856-1862.

Cattaert, D., El Manira, A., Marchand, A., Clarac, F. (1990). Central control of the sensory afferent terminals from a leg chordotonal organ in crayfish in vitro preparation. *Neurosci. Lett.*, 108, 81-87.

Cattaert, D., Le Ray, D. (2001). Adaptive motor control in crayfish. *Progress in Neurobiology,* 63, 199 –240.

Chasserat, C. and Clarac, F. (1983). Quantitative analysis of walking in a decapod crustacean, the rock lobster *Jasus lalandii*. II. Spatial and temporal regulation of stepping in driven walking. *Journal of experimental Biology*, 107, 219-243.

Chrachri, A. and Clarac, F. (1989) Synaptic connections between motor neurons and interneurons in the fourth thoracic ganglion of the crayfish, *Procambarus clarkii. Journal of Neurophysiology*, 62, 1237-1250

Chrachri, A., and Clarac, F. (1990). Fictive locomotion in the fourth thoracic ganglion of the crayfish, *Prorambarus darkii. Journal of Neuroscience*, 10(3), 707-719.

Clarac, F. (1982). Decapod crustacean leg coordination during walking. In C. F. Herreid and C. R. Fourtner (Ed.), *Locomotion and Energetics in Arthropods* (pp. 31-71). New York: Plenum Press.

Clarac, F., and Barnes, W. J. P. (1985). Peripheral influences on the coordination of the legs during walking in decapod crustaceans. In Coordination of Motor Behaviour . In B. M. H. Bush and F. Clarac (Ed.), *Soc. exp. Biol. Seminar Series 24* (pp. 249-269). Cambridge: Cambridge University Press.

Clarac, F., Cattaert, D., Le Ray, D., (2000). Central control components of a 'simple' stretch reflex. *Trends in Neuroscience*, 23, 199-208.

Clarac, F., Wales, W., Laverack, M. S. (1971). Stress Detection at the Autotomy Plane in the Decapod Crustacea II. The Function of Receptors Associated with the Cuticle of the Basi-ischiopodite. *Journal of comparative Physiology*, 73, 383-407.

Cruse, H. (1985). Which parameters control the leg movement of a walking insect? I. Velocity control during the stance phase. *Journal of Experimental Biology*, 116, 343–355.

Cruse, H. (1990). What mechanisms coordinate leg movement in walking arthropods. *TINS,* 1(13), 15-21.

Cruse, H. and Müller, U. (1986). Two coupling mechanisms which determine the coordination of ipsilateral legs in the walking crayfish. *Journal of experimental Biology*, 121, 349-369.

Cruse, H., Dürr, V., Schilling, M. and Schmitz, J. (2009). Principles of insect locomotion. In P Arena and L. Patanè (Ed.) *Spatial Temporal Patterns for Action-Oriented Perception in Roving Robots* (pp. 1-57). Berlin: Springer.

Cruse, H., Dürr, V., Schmitz, J. (2007). Insect walking is based on a decentralized architecture revealing a simple and robust controller. *Philos Trans R Soc A*, 365(1850), 221–250

Daun, S., Rybak, I. A., and Rubin, J. (2009). The response of a halfcenter oscillator to external drive depends on the intrinsic dynamics of its components: A mechanistic analysis. *Journal of Computational Neuroscience*, 27, 3–36.

Daun–Gruhn, S. (2011). A mathematical modeling study of inter-segmental coordination during stick insect walking. *Journal of Computational Neuroscience*, doi:10.1007/s10827-010-0254-3.

Daun-Gruhn, S., Toth, T. I. (2011). An inter-segmental network model and its use in elucidating gait-switches in the stick insect. *Journal of Computational Neuroscience*, doi:10.1007/s10827-010-0300-1.

Delcomyn, F. (1981). Insect locomotion on land. In C. F. Herreid and C. R. Fourtner (Ed.), *Locomotion and Energetics in Arthropods* (pp. 103-125). New York: Plenum Press.

Dürr, V., Schmitz, J., Cruse, H. (2004). Behavior-based modelling of hexapod locomotion: linking biology and technical application. *Arthropod Structure and Development,* 33, 237–250.

Ekeberg, Ö., Blümel, M., & Büschges, A. (2004). Dynamic simulation of insect walking. *Arthropod Structure and Development*, 33, 287–300.

Elson, R. (1996). Neuroanatomy of a Crayfish Thoracic Ganglion: Sensory and Motor Roots of the Walking-Leg Nerves and Possible Homologies With Insects. *Journal of comparative Neurology*, 365, 1-17.

Elson, R.C., Sillar, K.T., and Bush, B.M.H. (1992). Identified proprioceptive afferents and motor rhythm entrainment in the crayfish walking system. *Journal of Neurophysiology*, 67, 530-546.

Grabowska, M. J, Godlewska, E., Schmidt, J., Daun-Gruhn, S. (2012). Quadrupedal gaits in hexapod animals – inter-leg coordination in free-walking adult stick insects. *The Journal of Experimental Biology*, 215, 4255-4266.

Graham, D. (1985). Pattern and control of walking in insects. *Adv. Ins. Physiol*, 18, 31-140.

Grillner, S. (2006). Biological pattern generation: The cellular and computational logic of networks in motion. *Neuron*, 52, 751–766.

Grillner, S., Markram, H., De Schutter, E., Silberberg, G., and LeBeau, F. E. N. (2005). Microcircuits in action—from CPGs to neocortex. *Trends in Neurosciences*, 28, 525–533.

Grillner, S., Wallen P. (2002). Cellular bases of a vertebrate locomotor system – steering, intersegmental and segmental co-ordination and sensory control. *Brain Research Reviews,* 40, 92–106.

Hess, D. and Büschges A. (1999). Role of proprioceptive signals from an insect femur-tibia joint in patterning motoneuronal activity of an adjacent leg joint. *Journal of Neurophysiologly*, 81, 1856–1865.

Hodgkin, A. L., and Huxley, A. F. (1952). A quantitative description of membrane current and its application to conduction and excitation in nerve. *Journal of Physiology*, 117, 500–544.

Izhikevich, E. (2006). *Dynamical systems in neuroscience: The geometry of excitability and bursting*. Cambridge: MIT.

Jamom, M., Clarac, F. (1995). Locomotor patterns in freely moving crayfish (*Procambarus clarkii*). *The Journal of Experimental Biology*, 198, 683–700.

Klärner, D., and Barnes, W. J. P. (1986). The cuticular stress detector (CSD2) of the crayfish. II. Activity during walking and influences on the leg coordination. *The Journal of Experimental Biology*, 122,161–175.

Klärner, D., Barth, F. G. (1986). The cuticular stress detector (CSD2) of the crayfish I physiological properties. *The Journal of Experimental Biology*, 122, 149-159.

Leise, E. M., Hall, W. M., and Mulloney, B. (1987). Functional organization of crayfish abdominal ganglia: II. Sensory afferents and extensor motor neurons. *Journal of Comparative Neurology*, 266, 495-518.

Libersat, F., Zill, S., and Clarac, F. (1987). Single-unit responses and reflex effects of force sensitive mechanoreceptors of the dactyl of the crab. *Journal of Neurophysiology*, 57, 1601–1617.

Ludwar, B. C., Göritz, M. L., and Schmidt, J. (2005). Intersegmental coordination of walking movements in stick insects. *Journal of Neurophysiology*, 93, 1255-1265.

MacMillan, D. L. (1975). A physiological analysis of walking in the American Lobster (*Homarus americanus*). *Phi. Trans. R. Soc. Ser. B*, 270, 1-59.

Müller, U., and Cruse, H. (1991). The contralateral coordination of walking legs in the crayfish *Astacus leptodactylus*. I. Experimental results. *Biologicval Cybernetics*, 64, 429–436.

Parrack, D.W. (1964). Stepping sequences in the crayfish. *PhD. Thesis, University of Illinois*.

Pearson, K. G. (2000). Neural Adaptation In The Generation Of Rhythmic Behavior. *Annual Reviews in Physiology*, 62, 723–53.

Ritzmann, R. E., and Büschges, A. (2007). Adaptive motor behavior in insects. *Current Opinion in Neurobiology*, 17, 629-636.

Ross, R. B., and Belanger, J. H. (2013). Passive Mechanical Properties of Crustacean Walking Legs. *Poster, Sfn, Annual meeting, San Diego*

Sillar, I. K., Clarac, F., Busch, B. M. H. (1987). Intersegmental coordination of central neural oscillators for rhythmic movements of the walking legs in crayfish, *Pacifastacus leniusculus*. *Journal of Experimental Biology*, 131, 245-264.

Sillar, K. T., Skorupski, P., Elson, R. C., and Bush, B. M. H. (1986). Two identified afferent neurones entrain a central locomotor rhythm generator. *Nature*, 323, 440-443.

Sillar, K.T., and Skorupski, P. (1986). Central input to primary afferent neurons in the crayfish, *Pacifastacus leniusculus*, is correlated with rhythmic motor output of thoracic ganglia. *Journal of Neurophysiology*, 55(4), 678-688.

Skinner, F., Kopell, N., and Marder, E. (1994). Mechanisms for oscillation and frequency control in reciprocally inhibitory model neural networks. *Journal of Computational Neuroscience*, 1, 69–87.

Skinner, K. (1985). The structure of the fourth abdominal ganglion of the crayfish*, Procarnbnrus clarhzi* (Girard). I. Tracts in the ganglionic core. *Journal of Comparative Neurology*, 234,168-181.

Skorupski, P., and Sillar, K.T. (1988). Central synaptic coupling of walking leg motor neurones in the crayfish: Implications for sensorimotor integration. *Journal of Experimental Biology*, 140, 355-379.

Toth, T.I., Schmidt, J., Büschges, A., Daun-Gruhn, S. (2013). A neuro-mechanical model of a single leg joint highlighting the fundamental physiological role of fast and slow muscle fibres of an insect muscle system. *PLOS ONE*, doi:10.1371/journal.pone.0078247.

Von Twickel, A., Büschges, A., Parsemann, F. (2011). Deriving neural network controllers from neuro-biological data: implementation of a single-leg stick insect controller. *Biological Cybernetics*, 104, 95–119.

Westmark, S., Oliveira, E. E., and Schmidt, J. (2009). Pharmacological analysis of tonic activity in motoneurons during stick insect walking. *Journal of Neurophysiology*, 102, 1049–1061.

Wilson, D. M. (1966). Insect walking. *Ann. Rev. Entomol,* 11, 103-122.

Zill, S. N., Keller, B. R., Duke, E.R. (2009). Sensory Signals of Unloading in One Leg Follow Stance Onset in Another Leg: Transfer of Load and Emergent Coordination in Cockroach Walking. *Journal of Neurophysiology*, 101, 2297-2304.

Zill, S., Schmitz, J., Büschges, A. (2004). Load sensing and control of posture and locomotion. *Arthropod Structure Development*, 33, 273-28

5. Unpublished Study

5.1 Investigation of an inter-segmental pathway arising at the metathoracic segment and modulating a pilocarpine-induced rhythm in the prothoracic protractor-retractor CPG

Martyna Grabowska, Tibor Istvan Toth, Anke Borgmann, Ansgar Büschges, Silvia Daun-Gruhn

Author contributions

Conceived and designed the experiments
Martyna Grabowska, Tibor Istvan Toth, Anke Borgmann Ansgar Büschges, Silvia Daun-Gruhn

Performed the experiments
Martyna Grabowska

Analyzed the data
Martyna Grabowska, Tibor Istvan Toth, Anke Borgmann Ansgar Büschges, Silvia Daun-Gruhn

Figure preparation:
Martyna Grabowska

First version of manuscript
Martyna Grabowska

Wrote the paper
Martyna Grabowska

Contributed reagents/materials/analysis tools
Ansgar Büschges, Silvia Daun-Gruhn

MATERIALS AND METHODS

All experiments were performed on adult female stick insects *Carausius morosus* (Brunner 1907), at room temperature (18°C-23°C) under reduced light conditions. Animals were obtained from a breeding colony maintained at the University of Cologne. For the experiments, all legs of the stick insect, except both hind legs, were removed by amputating them at mid coxa. The animals were fixed dorsal side up by thin minutien pins to a foam platform. In the preparation, the abdomen did not touch the foam platform at any time and was able to move freely. The thorax of the stick insect was opened with a sagittal cut along the midline of the cuticle from the most rostral point of the prothorax to the most caudal side of the mesothoracic ganglion. The gut, as well as the connective tissue, was removed in order to expose the prothoracic and mesothoracic ganglia, their connectives, and their lateral leg nerves. The mesothoracic ganglion was completely deafferented by cutting all lateral leg nerves on both sides, and the body cavity was filled with saline (according to Weidler & Diecke, 1969). On the left side of the prothorax, the lateral leg nerves nl2, containing the axons of the *protractor coxae* motoneurons (MNs), and nl5, containing the axons of the *retractor coxae* MNs (Marquardt, 1940; Graham, 1985), were recorded by means of extracellular hook electrodes (modified after Schmitz et al., 1991), and crushed distally to the recording site. All other lateral nerves of the prothoracic ganglion were transected. The connectives to the suboesophageal ganglion (SOG), and the ones to the mesothoracic ganglion, as well as the connectives between the meso- and metathoracic ganglia were left intact.

For the split bath preparation, the cuticle of the thorax was cut transversally between the prothoracic and the mesothoracic ganglia, and a small u-shaped portion was removed. The connectives were left intact. The gap was filled by highly viscous silicone grease in order to create a leak-free barrier between the prothoracic and mesothoracic segments. The activation of the prothoracic central pattern generating networks was achieved by perfusing the prothoracic ganglion with saline containing the muscarinic acetylcholine agonist pilocarpine ($5x10^{-3}$ M) (Büschges, 1995). As a result, rhythmic activity of the recorded protractor and retractor MNs was elicited. Due to the split bath preparation, exclusive perfusion of the prothoracic ganglion with the pilocarpine-saline solution was ensured. The cavity posterior to the silicone barrier, exposing the deafferented mesothoracic ganglion, was filled with saline (Weidler and Diecke, 1969). The left hind leg, ipsilateral to the nl2 and nl5 recording site, performed steps on a passive, lightweight, low friction treadmill (modified after Gabriel et al., 2003) positioned parallel to the body axis. This stepping movement resembles closely kinematics during forward and backward straight walking in stick insects (Cruse and Bartling, 1995). Stepping of the hind leg was monitored by electromyograms (EMGs) of the flexor activity in the moving leg. The recordings were performed by two thin copper wires (40µm) inserted into the flexor. A stance phase of the hind leg led to an acceleration of the treadmill. This movement was monitored by a tachometer. A positive amplitude in the tachometer trace represents the start of the stance phase of a forward hind leg step. A negative amplitude represents the start of a stance phase of a backward hind leg step. The maximum of an amplitude represents the end of a stance phase. Stepping sequences were induced by gently touching the abdomen of the animal with a paintbrush until it

started to walk. These walking sequences were referred to as “active walking”, and the steps within these sequences were named “active” steps. “Passive movements” were sequences in which the hind leg was standing on the treadmill and the treadmill was passively moved forward and/or backward. In cases in which the treadmill was moved passively forward **or** backward, providing a stance phase, the leg continued with an active swing phase to reposition the leg. In cases of forward **and** backward movements of the treadmill, the leg remained on the treadmill during the whole time, which means that no swing phase was present. The experimental results for the inter-segmental influence of the two different kinds of passive movements of the treadmill showed no significant difference (weighted and pooled data, Wilcoxon rank sum test: $p=0.67$). Therefore the term “passive movements of the legs” results from both kinds of the aforementioned experimental conditions.

In order to identify the sensory signals that contribute to the modulation of the prothoracic rhythm generating networks, an additional experimental setup was introduced in which the *femoral* and *trochanteral campaniform sensilla* were stimulated. In this preparation, the left hind leg was amputated at the *femur-tibia* joint, and the *coxa-trochanter* joint was fixed by dental cement (PROTEMP II, ESPE). The stump was then moved in a posterior or anterior direction to the stick insect’s body resulting in load signals, detected by the *femoral* and *trochanteral campaniform sensilla* (Schmitz, 1993). The further preparation was performed the same way as the single hind leg/ split bath preparation.

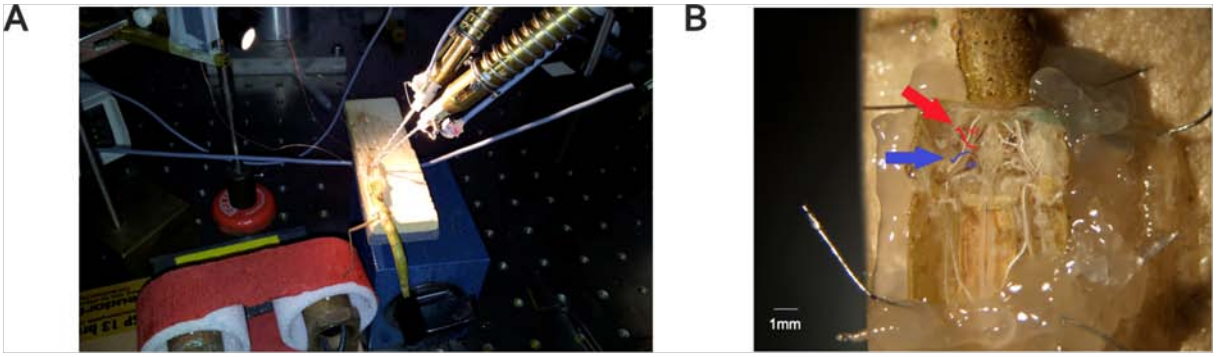

Fig. 1 Experimental setup and close up of the isolated prothoracic ganglion. A) Photography of the experimental setup. The intact hind leg was stepping on the treadmill. Two extracellular monopolar hook electrodes recorded the activity of the lateral nerves nl2 (axons of protractor MNs) and nl5 (axons of retractor MNs). B) Photography of the isolated prothoracic ganglion. The lateral nerves nl2 (red) and nl5 (blue) are marked by the red and blue arrow, respectively.

Extracellular recordings and EMGs were amplified (500x-5000x, depending on the recording quality) and filtered (250Hz- 5kHz for extracellular recordings, 50Hz-1kHz for EMGs). Finally, the recordings were digitalized by a MICRO 1401 A/D converter (sampling rate: 12.5 kHz). For recordings, SPIKE2 data analysis software (version 5.21, Cambridge Electronic Design) was used. For a better analysis of noisy data samples, the extracellular recordings were rectified and smoothed ($\tau \in [0.008, 0.08]$) with the smoothing function of SPIKE2. To analyze the transitions between the protractor and retractor MN burst activities depending on the stepping of the hind leg, the experimental conditions were divided into active and passive forward stepping, and active and passive backward stepping. The results were counted and weighted for all animals. The occurrences of different transitions during stepping were compared, and tested for significance (significance levels: $p<0.05$(*); $p<0.01$(**); $p<0.001$(***)) using the Wilcoxon rank sum test in MATLAB® (Version: R2011b (7.13.0.564) The MathWorks, Inc.). Phase histograms were made using the SPIKE2 analysis software to compare the relative spike distribution of the protractor and retractor bursts within a step cycle. Circular statistics for the spike distributions of a step cycle in a unit circle were performed using the circular statistics toolbox for MATLAB® (Version: R2011b (7.13.0.564) The MathWorks, Inc.) (Berens, 2009). The Rayleigh test (Batschelet, 1981) was used to test whether spikes of the protractor and retractor MN activity were randomly distributed or whether a predominant directionality is present (same significance levels as for the Wilcoxon rank sum test). For the investigation of the influence of the SOG, perfused with pilocarpine, on the prothoracic ganglion, experiments were performed with intact and cut connectives between the prothoracic ganglion and the SOG. For the supplementary figure, cross correlations of the rectified and smoothed protractor and retractor MN activities in the prothoracic and mesothoracic ganglion were calculated (using SPIKE2 analysis software for cross correlations). To analyze the influence of the stepping hind leg on the pilocarpine induced protractor and retractor MN rhythm in the prothoracic ganglion, phase response curves were calculated. In the text and in the figures, N represents the number of animals and n the number of step cycles.

RESULTS

In former studies an inter-segmental influence between the ipsilateral segmental CPGs of the stick insect's leg has been shown for the anterior to the posterior segments or for to the adjacent segments of the middle leg. For the inter-segmental influence from the posterior to the anterior segments, Borgmann et al. (2009) showed that a forward stepping hind leg induced a general increase in activity in the prothoracic and mesothoracic protractor and retractor MNs, but no rhythmicity. In 2/3 of the experiments, a backward stepping hind leg induced a general increase in activity in the mesothoracic protractor and retractor MNs and in 1/3, alternating activity was observed. The influence on the prothoracic joint-CPGs was not studied so far.

In this study, I investigated the influence of a stepping ipsilateral hind leg on a pilocarpine-induced rhythm in the prothoracic protractor and retractor MN pools. The animals were stepping on a treadmill in a forward or backward direction as well as passive movements of the hind leg.
In both experimental setups, I observed an entrainment of the pilocarpine-induced rhythm in the prothoracic ganglion to the stepping hind leg. In order to get a first insight in the origin of the sensory signals providing the inter-segmental influence, I cut the hind leg at the middle of the femur in order to exclude signals from the hind leg, encoding position and ground contact.

In the first set of experiments, I investigated the influence of active forward and backward ipsilateral hind leg steps on the prothoracic protractor/retractor CPGs.
Therefore, I recorded the alternating, rhythmic protractor and retractor MN activity extracellularly, using monopolar hook electrodes. The rhythmic activity of the prothoracic rhythm generating networks was induced by application of a pilocarpine solution (5x10-3 M) on the prothoracic ganglion (Fig. 1, Fig. 2). By gently tickling the abdomen of the stick insect, I induced stepping of the hind leg on the treadmill. The stepping of the hind leg was monitored by EMGs of the flexor muscle in the femur and by the tachometer trace of the treadmill (Fig. 1, Fig. 2).
A negative amplitude in the tachometer trace resembles stance phases during backward steps of the hind leg, a positive amplitude resembles stance phases during forward steps.

Active backward steps

Fig. 2 shows the influence of the backward stepping hind leg on the ipsilateral protractor and retractor MNs of the prothoracic ganglion. The backward steps, that had a higher frequency than the pilocarpine rhythm, entrained the alternating activity in the prothoracic protractor and retractor MNs. In addition, the beginning of the stance phase of the backward stepping hind leg (red lines in Fig. 2) was in phase with the activity of the retractor MNs in the prothoracic ganglion.

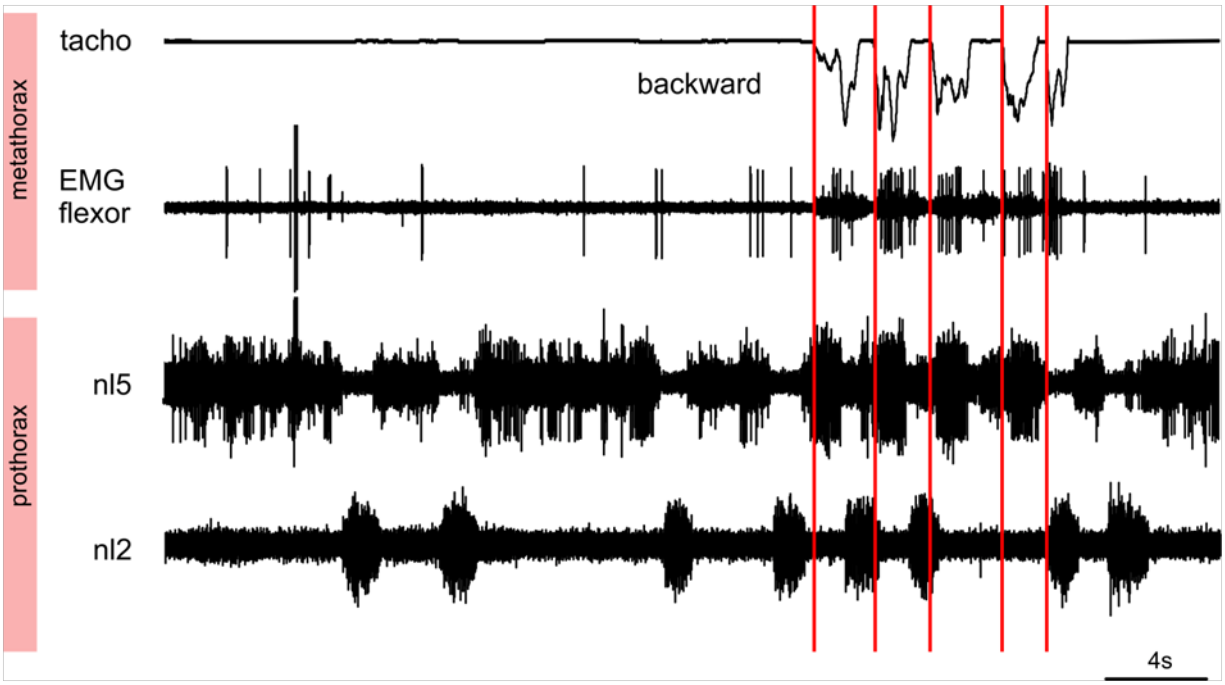

Fig 2. Active backward stepping entrained the pilocarpine-induced rhythm in the prothoracic protractor and retractor MN pools. The amplitudes of the tachometer trace (smoothed: τ= 0.1s) resemble backward steps of the hind leg. The beginning of the stance is marked by red lines. The end of the retraction is indicated by the most negative peak in the trace. Additionally, hind leg stepping is monitored by flexor muscle activity in the hind leg. This activity increased during stance phase. The irregular pilocarpine-induced rhythm in the retractor and protractor MNs in the prothoracic ganglion was entrained by the stepping of the hind leg. Between the third and fourth step, no protractor MN burst was observed.

Active forward steps

As for the experiments with the active backward stepping ipsilateral hind leg, active forward steps of the hind leg entrained the pilocarpine-induced rhythm in the prothoracic protractor/retractor system (Fig. 3). The red lines in Fig. 3 mark the beginning of the stance phases during forward steps of the hind leg (positive amplitude). Forward hind leg stepping led to in-phase activity of the burst of the prothoracic protractor MNs and the beginning of the stance phase of the hind leg. Note that the tachometer trace is very noisy. This might have been the result of a very sensitive adjustment of the treadmill. With this tachometer trace, I could not distinguish between the single forward steps. The activity of the flexor provided the information about a proper forward step though.

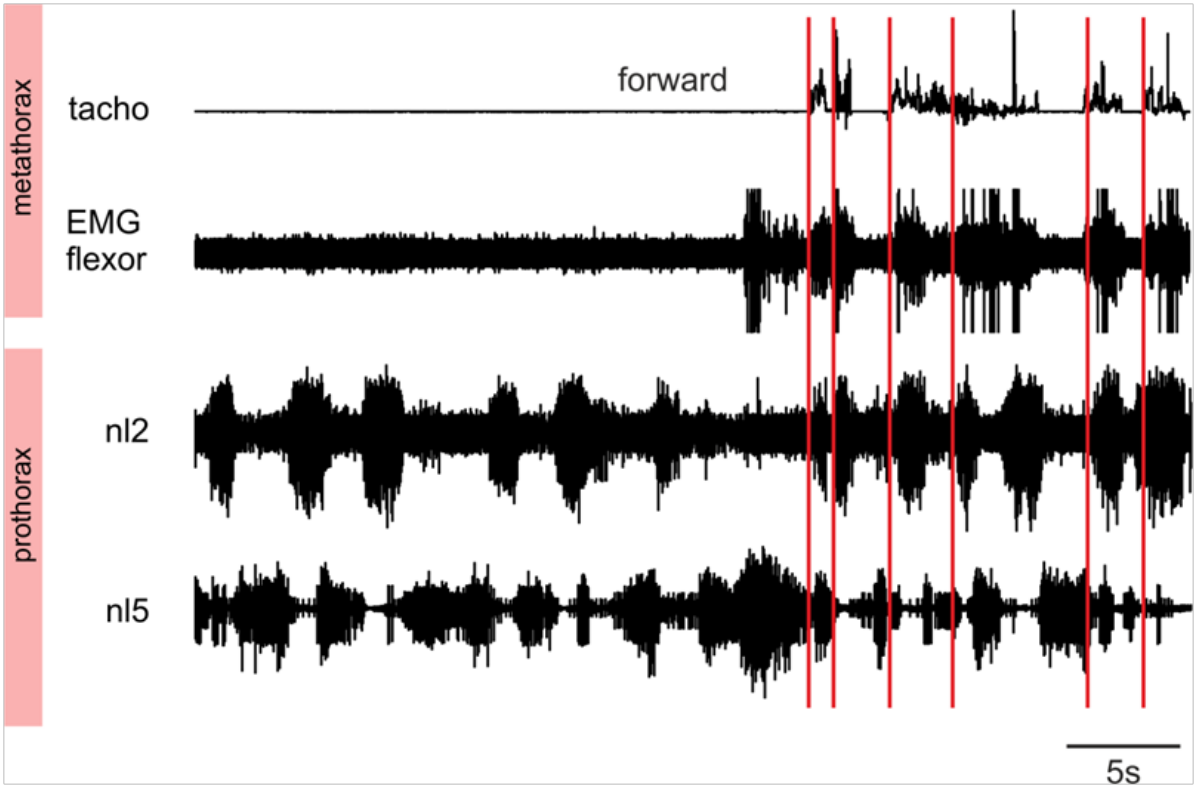

Fig 3. Active forward stepping of the ipsilateral hind leg entrained the pilocarpine-induced rhythm in the prothoracic protractor and retractor MN pools. The positive amplitudes of the tachometer trace indicate forward steps. The beginning of the stance phase is marked by red lines. During stepping, an increase in flexor activity was observed. The irregular pilocarpine-induced rhythm in the prothoracic retractor and protractor MNs was entrained by stepping of the hind leg. Between the fourth and fifth step no stepping activity was observed. Before stepping, the protractor burst activity had a frequency of 0.4Hz. During stepping the frequency increased to 0.54Hz.

A stick insect that lacks both front and middle legs prefers to walk backward than forward (Bässler and Breutel, 1985). In order to increase the number of walking sequences with a forward stepping ipsilateral hind leg, I introduced a second set of experiments, in which the treadmill was moved passively in order to mimic forward and backward directed stance phases of the ipsilateral hind leg.

Passive forward and backward movements

The passive movements of the treadmill did not only increase the number of forward directed stance phases of the hind leg, they were also beneficial in order to regulate the stepping frequency of the hind leg. In some cases the frequency of the pilocarpine-induced rhythm in the prothoracic protractor/retractor MN bursts was close to the stepping frequency of the hind leg (Fig. 3). Fig. 4 A) shows the influence of a moved hind leg, on the pilocarpine-induced rhythm of protractor and retractor MN bursts in the prothoracic ganglion. In this experimental situation, the treadmill was moved back and forth, inducing forward and backward directed stance phases in the hind leg (hind leg was standing on the treadmill, no protraction was performed) The higher frequency of the hind leg movements entrained the slower and irregular pilocarpine-induced rhythm of the prothoracic protractor and retractor MNs (grey area). During the hind leg movements, an increase of flexor muscle activity was observed.

I analyzed the influence of the start of a forward directed stance phase of the ipsilateral hind leg on the pilocarpine-induced rhythm by calculating a phase response curve. For this purpose, I calculated the mean duration Tp (green in Fig. 4 B)) of three prothoracic protractor burst cycles. One cycle was defined by the beginning of a protractor MN burst to the next beginning of a protractor MN burst. The time between the beginning of the influenced burst cycle and the start of the stimulus (red line, start stance phase) was defined as d (red in Fig. 4 B)). After the stimulation, the beginning of the next protractor burst occurred after a certain time T (blue in Fig. 4 B)). Fig. 4 C) shows the resulting phase response curve. There the relative changes in pilocarpine-induced prothoracic protractor cycle periods [(T/Tp)/Tp] were plotted against the phase of the first, passively induced forward hind leg movement of a stepping sequence in the prothoracic protractor burst cycle (d/T) for nine animals and 35 steps (black dots). Except of seven data points, where the beginning of the next burst after the stimulation was delayed, the linear curve indicates a reset of the pilocarpine-induced rhythm in the prothoracic MN pools. These results are in accordance with the calculations of the latencies between the beginning of a forward step (passive) and the beginning of a prothoracic protractor burst. These results show that all protractor bursts occurred after a mean of 0.55s±0.33s (no significant difference between different animals and different stepping sequences ($p<0.001$, Wilcoxon rank sum test).

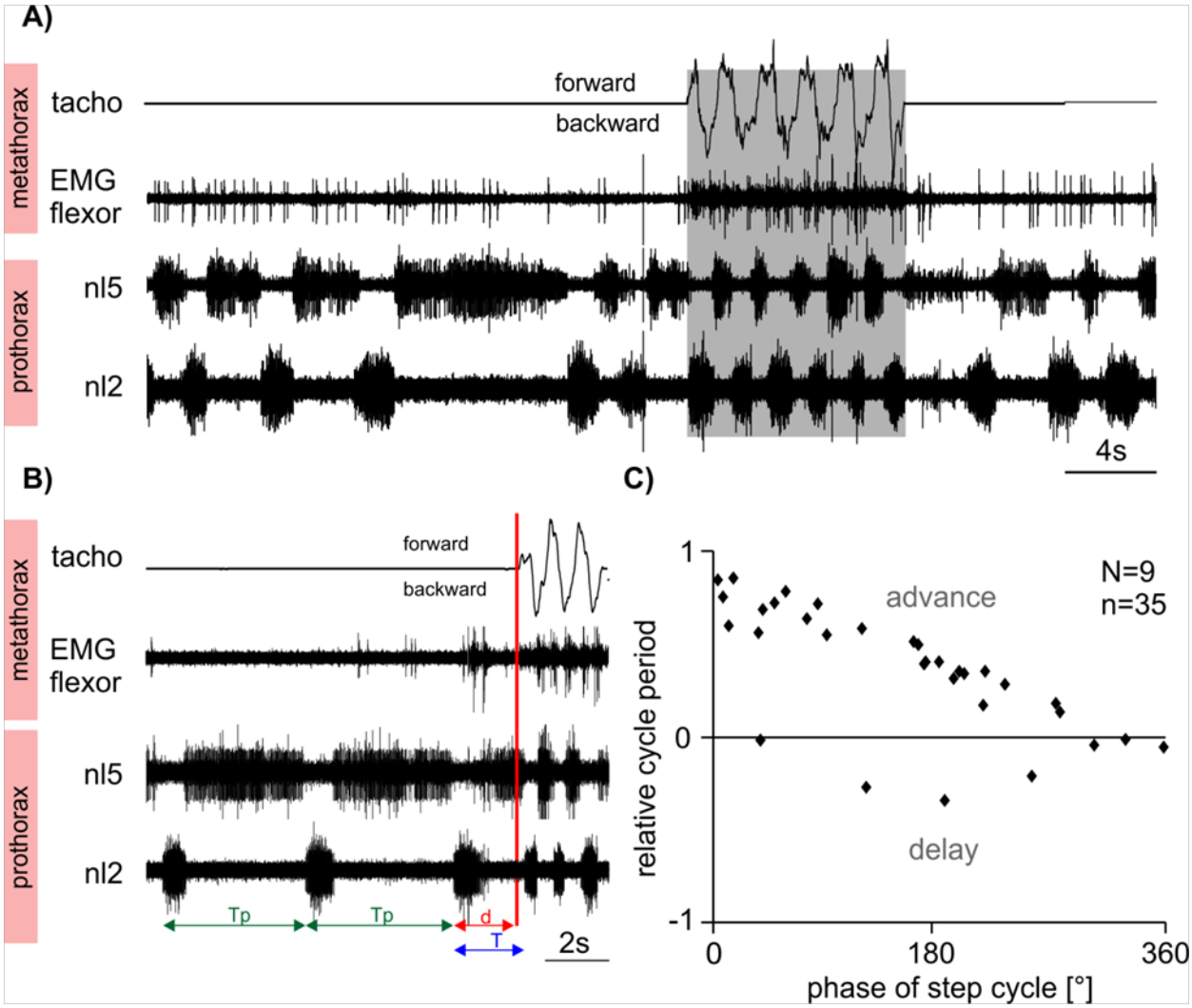

Fig. 4 Passive forward and backward movements of the ipsilateral hind leg entrained the pilocarpine-induced rhythm in the prothoracic protractor and retractor MNs. A) The hind leg was standing on the treadmill which was moved forward and backward. In this case, the ipsilateral hind leg did not perform a swing phase. The passive forward and backward directed stance phases entrained the rhythmic activity of the pilocarpine induced rhythm of the protractor and retractor MN bursts (grey area). B) Example for the calculation of a phase response curve (PRC) for the hind leg's movements occurring during pilocarpine-induced rhythm in prothoracic protractor and retractor MN bursts. C) PRC. Relative change in pilocarpine-induced prothoracic protractor cycle period [(T /Tp)/Tp] plotted versus phase of first, passively induced forward hind leg movement of a stepping sequence in the prothoracic protractor burst cycle (d/T) for nine animals and 35 steps (black dots). The linear curve indicates a resetting of the pilocarpine-induced rhythm in the prothoracic MN pools by the hind leg steps.

The protractor MN burst activity was entrained by a forward directed stance phase of a hind leg step. The retractor MN burst activity was entrained by a backward directed stance phase of the hind leg.

For a better comparison of the influence of passive and active leg activity in the ipsilateral hind leg on the prothoracic rhythm generators of the protractor/retractor system, I investigated the transitions of the alternating protractor and retractor MN bursts and the in-phase activities with the stance phases of the hind leg in the particular experimental setup. In order to distinguish between the different influences a forward and backward step of a hind leg can have on the ipsilateral ThrC-joint CPG, I investigated the different protractor and retractor MN reactions of the prothoracic ganglion in the active (N=9) and passive (N=11) walking situations for all steps. p+r- stands for a simultaneous occurrence of activity of the protractor MNs and the stance phase of the hind leg (Fig. 5 A)), p-r+ for an entrainment of the activity of the retractor MNs to the stance phase of a hind leg step. (Fig. 5 B)), p+r+ for a simultaneous activity of both antagonistic MN pools during a stance phase of a hind leg (Fig. 5 C)), and p-r- for the absence of MN bursts during the stance phase of a hind leg step. This was evaluated for the forward and backward steps.

In the prothoracic ganglion, active forward steps of a hind leg (Fig. 5 D) black bars) (N=3, n=23), resulted in a p+r- situation in 65.2%, a p-r+ transition in 17.4%, p+r+ in 13%, and no reaction to the stepping (p-r-) in 4.4% of all steps investigated. Passive forward movements (Fig. 5 D) grey bars) of hind legs on the treadmill (N=11, n=225) showed a p+r- reaction in 83.6%, a p-r+ transition in 2.7%, simultaneous activity in 9.8% in the prothoracic ganglion. In 3.9%, reaction to the stimulus was observed. There was no significant difference between the occurrences of transitions between active and passive stepping. For forward steps, p+r- transition occurred significantly more often than p-r+, p+r+, and p-r- transitions ($p<0.001$, Wilcoxon-rank-sum Test).

Active backward steps (Fig. 5 E), black bars) resulted in 6.5% in a p+r- reaction, in 56.5% in an r-p+ transition. In 34.8% hind leg stepping entrained the alternating prothoracic protractor-retractor MNs rhythm to the retractor MNs (p+r+), and in 2.2% no reaction (p-r-) to the stimulus (hind leg step) was observed (N=9, n=92).

Passive backward movements (Fig. 5 E), grey bars), led in 3.5% to a p+r- transition, in 69.8% to a p-r+ transition, in 24.3% retractor and protractor MNs bursts were active at the same time (p+r+). In 2.4% no reaction was observed (p-r-). The proportion of p-r+ transitions was higher than p+r+ at a significant level $p<0.001$. The occurrence of p-r+ transitions was higher than the occurrence of p-r, and p-r- transitions ($p<0.001$). The last two situations showed no significant difference. Also, there was no significant difference between active and passive forward stepping.

In both experimental situations (active and passive stepping), the prothoracic protractor MNs were active when the ipsilateral hind leg performed a forward step, whereas during a backward step of the ipsilateral hind leg, the prothoracic retractor MNs were active. These results are presented in the phase histograms in Fig. 5 for forward stepping of the hind leg, and in Fig. 6 for backward stepping of the hind leg.

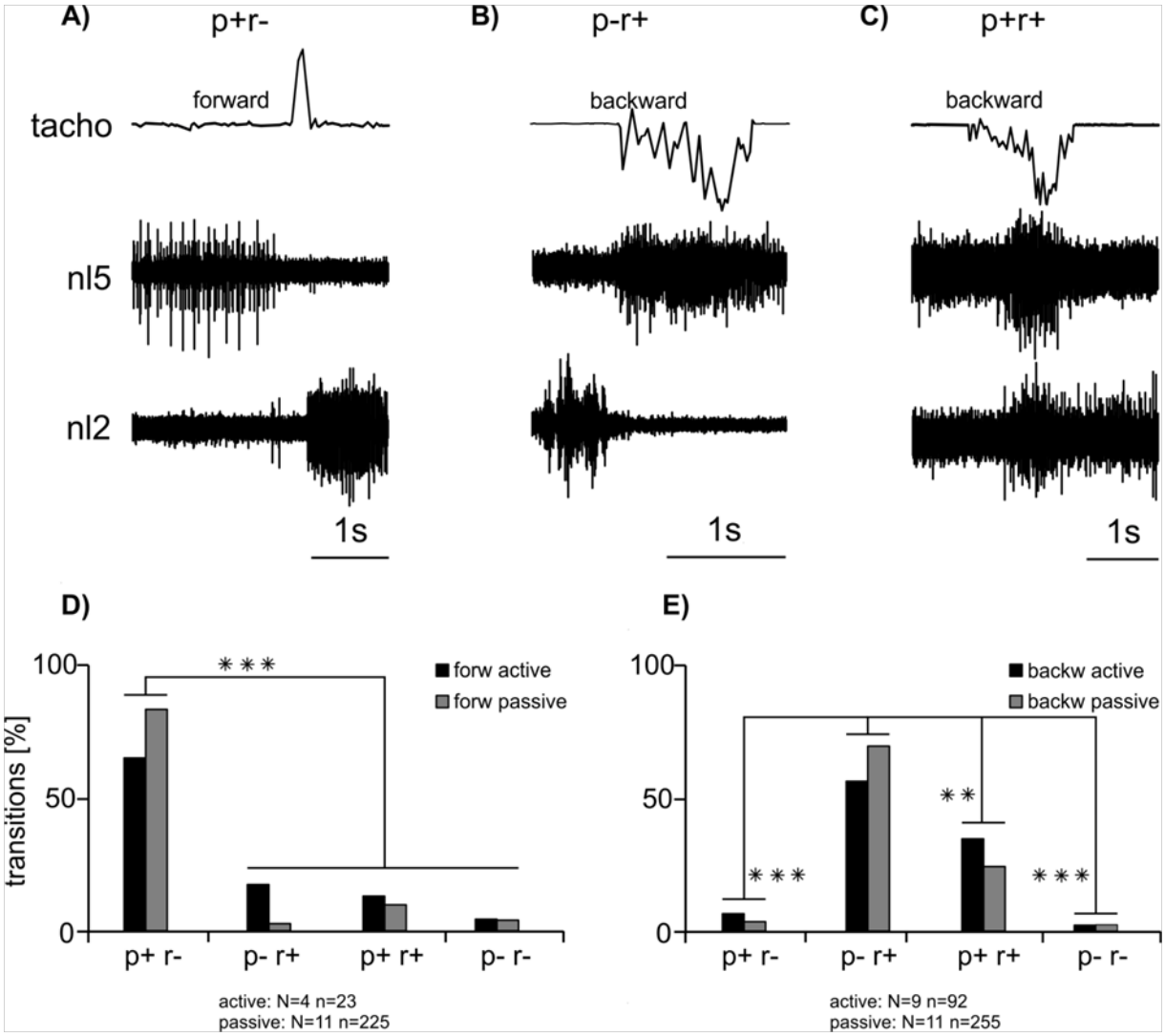

Fig. 5 Protractor MNs are entrained by the beginning of a stance phase of a forward stepping ipsilateral hind leg and retractor MNs to the stance phase of backward steps. The tachometer monitors the hind leg movements A) p+r-: The stance phase of a forward stepping hind leg activates protractor (nl2) MN burst activity B) p-r+: A backward stepping hind leg entrains the retractor MNs (nl5) of the prothoracic rhythm generating networks C) p+r+: During backward stepping of a hind leg both MN pools are active D) Distributions of transitions in % between protractor and retractor MNs during active (black, N=4, n=23 steps) and passive (grey, N=11, n=225 steps) forward stepping of an ipsilateral hind leg. Active and passive forward steps entrained protractor activity (active 65.2%, passive 83.6%). In 17.4% of active hind leg steps, no activity of protractor MNs could be observed, but the retractor MNs were active. For passive stepping, this was the case in 2.7%. In 13% of the active forward steps, the protractor MNs were active at the same time as the retractor MNs. In 9.8%, this was observed during passive forward stepping. In 4.3% (active) and 4% (passive), no activity in the protractor and retractor MNs was observed during a forward step (p-r-). The percentage of p+r- transitions was significant ($p<0.001$, Wilcoxon-rank-sum- Test) different to the percentage of p-r+, p+r+ and p-r-. The last three situations showed no significant difference. There was also no significant difference between active and passive forward stepping. E) Transitions (%) between protractor and retractor MNs during active (black, N=9, n=92 steps) and passive (grey, N=11, n=255 steps) backward steps of an ipsilateral hind leg. Active and passive backward steps entrained the protractor MN burst activity (active 6.5%, passive 3.5%) in the prothoracic ganglion. In 56.5%, retractor MN activity was entrained to active hind leg steps. For passive stepping, this was the case in 69.8%.In 24.3% of the active backward steps, the protractor MNs were active at the same time as the retractor MNs. In 9.8%, this was observed during passive forward stepping. The portion of p-r+ was significantly different to p+r+ ($p<0.01$). In 2.1% (active) and 2.4% (passive), no activity in the protractor and retractor MNs was observed during a backward step. The difference of p-r+ transitions to p-r, and p-r- was significant ($p<0.001$, Wilcoxon-rank-sum- Test). The last two situations showed no significant difference. Again, there was no significant difference between active and passive forward stepping.

Prothoracic protractor MN bursts were in phase with the stance phase of a forward step of the ipsilateral hind leg.

During the stance phase of an active forward step of the ipsilateral hind leg, prothoracic MN activity was observed (Fig. 6 A)). The phase histogram in Fig. 6 A shows the alternating activity of both neuron pools (protractor MNs, retractor MNs) for one walking sequence with nine cycles for one animal. The circular mean of the spike counts of protractor MN bursts (nl2 ,red) was at 112.4° within a hind leg step cycle. The circular mean for the relative spike count of the retractor MNs (nl5, blue) was at 335.7° within a hind leg step cycle. The unit circle contains the circular means and mean vector lengths of three animals for each stepping sequence (nl2: red; nl5: blue). The Rayleigh test, for the significance of the mean direction in a cycle (period) showed a significant directionality ($p<0.01$ and $p<0.001$) for all data sets (occurrence of the MN spikes within a step cycle), except for one dataset for the retractor MN spike distribution within a step cycle (circular mean: 173.9°, vector length: 0.311, $p=0.063$). The remaining circular means were between 47.2° and 343.8° for protractor MN spike distribution and between 170.8 and 335.8° for retractor MN spike distribution. Note, that although the statistical tests for the distribution of the protractor and retractor MN spikes within an active hind leg step cycle showed a significant directionality, still more experiments for active walking have to be performed. Nevertheless, the phase histogram in Fig 6 A) shows alternating activity of the MN pools, which is a clue for the kind of influence an active stepping forward leg has on the prothoracic protractor-retractor CPGs.

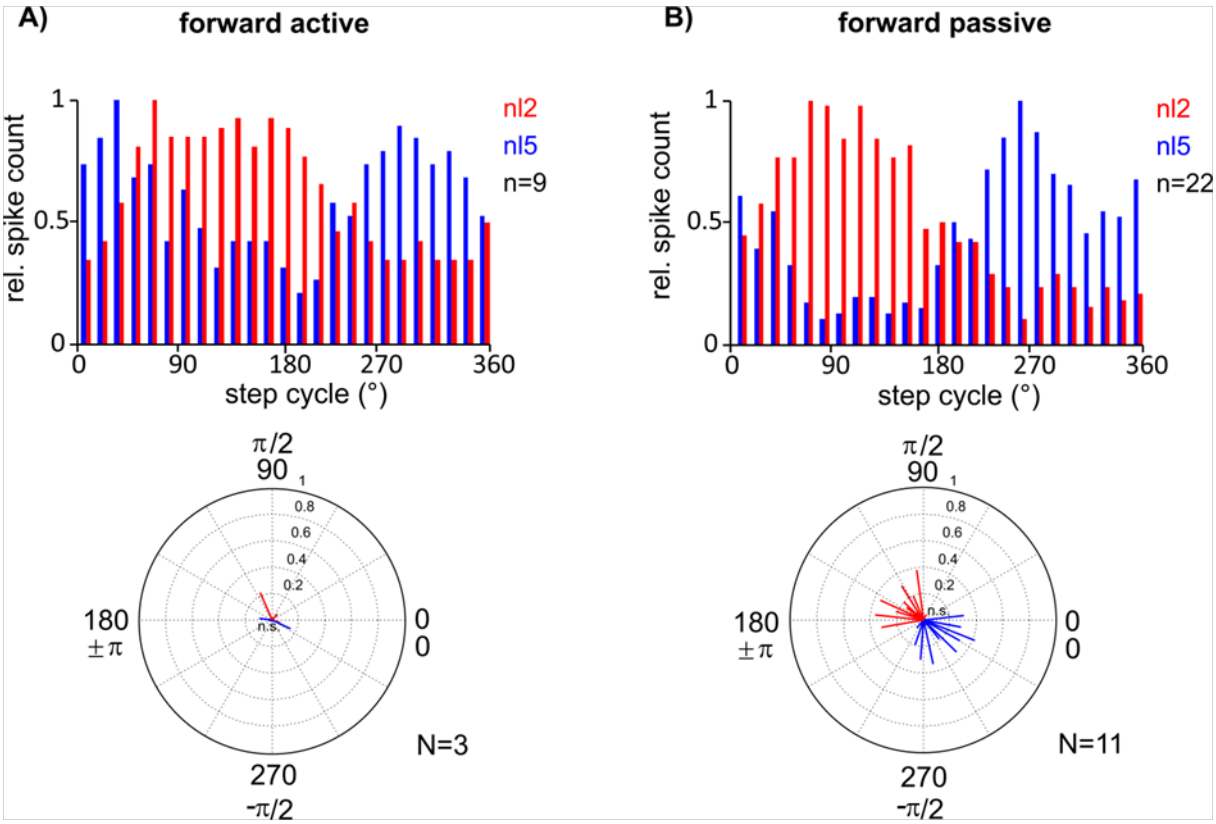

Fig. 6 Protractor MN burst activity was observed during active and passive forward stepping of an ipsilateral hind leg. A) Upper panel: Phase histogram, showing the relative spike distribution of prothoracic protractor MNs (nl2, red) and retractor MNs (nl5, blue) within an step cycle of an active forward step of the ipsilateral hind leg (N=1; n=9 step cycles). The protractor and retractor MNs showed alternating activity. Lower panel: Distribution of the circular means of three animals (N=3) of protractor MN (red) and retractor MN (blue) activity. All mean vectors showed a significant directionality of the protractor MN spike distribution at a significance level of $p<0.01$ (Rayleigh test), except for one mean vector for prothoracic protractor MN spike distribution. The mean values for the distribution of protractor and retractor MN activity within a hind leg step cycle were between 47.2° and 343.8° for protractor MNs and between 170.8° and 335.7° for retractor MNs B) Upper panel: Relative spike distribution of prothoracic protractor (nl2, red) and retractor (nl5, blue) MNs during a step cycle of a passive forward step of the ipsilateral hind leg (N=1, n=22 step cycles). As in A), the protractor MNs were active during the first 180° of a step cycle and the retractor motoneurons during the last 180°. Both MN pools showed alternating activity. Lower panel: The distribution of the circular means of protractor MN and retractor MN spike distribution within a step cycle of the hind leg of eleven animals (N=11) shows an opposite directionality. All mean vectors of the distribution of protractor and retractor MN spikes, except of one mean vector for the retractor MN spikes, showed a significant directionality ($p<0.001$, Rayleigh test). The mean values for the distributions of protractor and retractor MN activity during a hind leg step cycle were between 94° and 196° for protractor MNs and between 246° and 8° for retractor MNs.

Prothoracic retractor MN bursts were in phase with the stance phase of a backward step of the ipsilateral hind leg.

During the stance phase of backward movements of the ipsilateral hind leg (passive) prothoracic retractor MNs were active (Fig 7 B). Here the relative spike distributions of protractor and retractor MNs within a step cycle were narrower that the ones resulting from

the active backward stepping. The phase histogram in Fig. 7 B) shows the relative spike count distribution within one step cycle for 22 cycles in one animal. The protractor and retractor MN activities were alternating. The circular mean for the protractor MN spike distribution was 82.2° and for protractor MN spike distribution 210.7°. Both mean directions were significant at a level of $p<0.001$ (Rayleigh Test). The unit circle shows the mean vectors of prothoracic protractor and retractor MN activity within a step cycle for all walking sequences of eleven animals. The mean values for the distribution of protractor and retractor MN spike activity during a hind leg step cycle range from 82.2° to 196° for protractor MN spikes and between 210° and 8° for retractor MN spikes.

Active backward walking of the stick insects hind leg was easier to induce than forward walking. The start of a stance phase of a backward step entrained the rhythmic activity of the retractor MNs. In some cases, both MN pools were simultaneously active during a backward step (Fig. 7 A). The phase histogram in Fig. 7 shows the distribution of the relative spike count within a step cycle of twelve cycles in one animal. The mean values for the distributions were 300.9° for protractor MNs spikes (red) and 115.9° for retractor MN spikes (blue). In the lower panel, the unit circle contains all mean values, and the corresponding vectors for the protractor and retractor MN spike distributions within a hind leg step cycle of all walking sequences for nine animals. All mean vectors showed a directed distribution at a significance level of $p<0.001$ (Rayleigh test), except for one mean vector for the distribution of protractor MN spikes (circular mean 301.2°, vector length: $r=0.0332$ $p=0.39$). The mean values for the distributions were between 294° and 10° for protractor MN spikes and between 58° and 188° for retractor MN spikes.

As in the experiments with passive forward movements of the legs, the distribution of relative spike count of protractor and retractor MNs, resulting from passive backward movements of the hind leg were narrower compared to the active steps. Fig. 7 B) shows the distribution of the relative spike count within a step cycle of 20 stepping cycles in one animal. The circular mean for the retractor MN values in this histogram was 71.8° and 278.3°

for the protractor MN spike distribution. The lower plot shows the circular means and vector lengths of protractor and retractor MN spike distributions within a hind leg step cycle for all walking sequences for eleven animals. All mean vectors showed a significant directionality at a value of $p<0.001$ (Rayleigh test). The mean values for the prothoracic protractor MN spikes were between 278.3° and 89.2° and for retractor MN spikes between 71.8° and 210.9°.

In summary, a caudo-rostral inter-segmental influence was shown, arising at the metathoracic ganglion, induced by hind leg stepping in forward and backward direction that influences the CPG rhythm of the prothoracic protractor-retractor system.

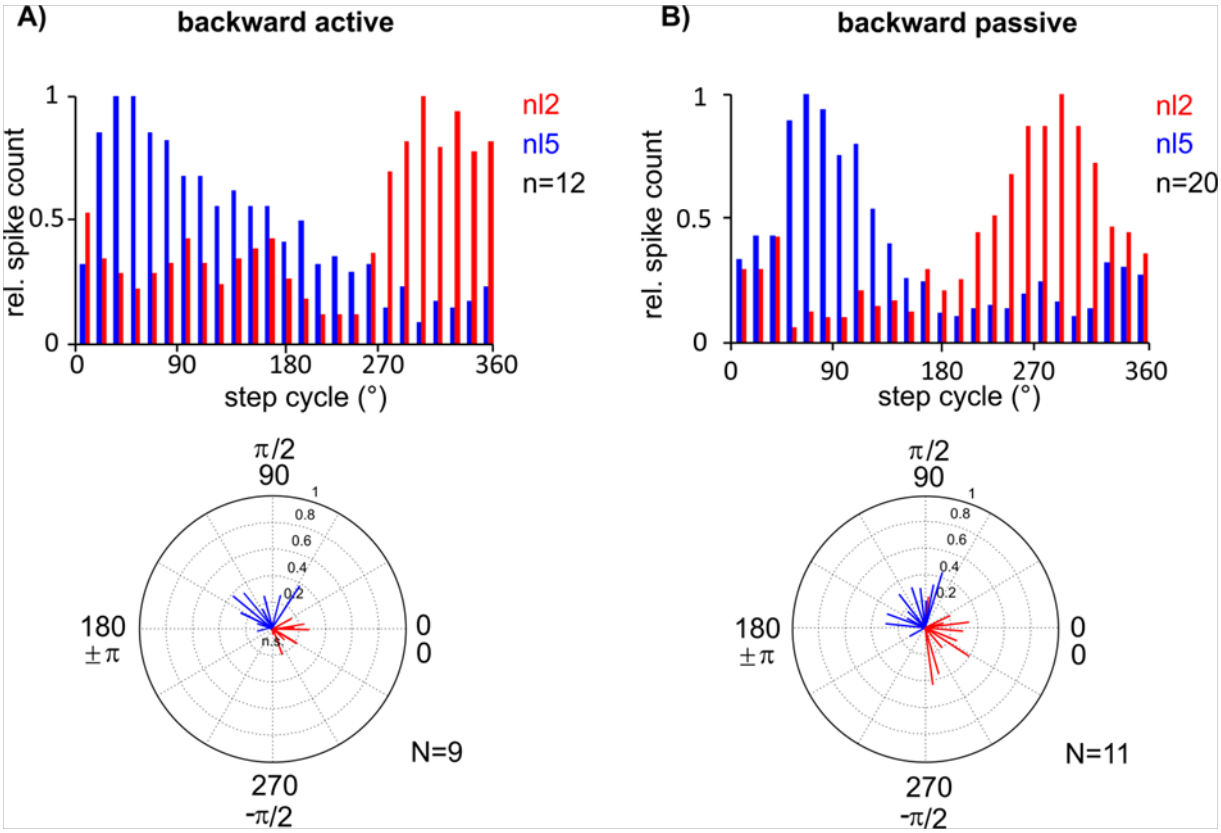

Fig. 7 Retractor MN burst activity was observed during active and passive backward stepping of an ipsilateral hind leg s. A) Upper panel: Phase histogram, showing the relative spike distribution of prothoracic protractor MNs (nl2, red) and retractor MNs (nl5, blue) within a step cycle of an active forward step of the ipsilateral hind leg (N=1; n=12 step cycles). The protractor and retractor MNs showed alternating activity. Lower panel: Distribution of the circular means of nine animals (N=9) of protractor MN (red) and retractor MN (blue) activity. All mean vectors showed a significant directionality of the protractor and retractor MN spike distribution at a significance level of $p<0.01$ (Rayleigh test), except for one mean vector for prothoracic protractor MN spike distribution. The mean values for the distribution of protractor and retractor MN activity within a hind leg step cycle were between 294° and 10° for protractor MNs and between 58° and 188° for retractor MNs B) Upper panel: Relative spike distribution of prothoracic protractor (nl2, red) and retractor (nl5, blue) MNs during a step cycle of a passive forward stepof the ipsilateral hind leg (N=1, n=20 step cycles). Both MN pools were showed alternating activity. Lower panel: The distribution of the circular means of protractor MN and retractor MN spike distribution within a step cycle of the hind leg of eleven animals (N=11) shows an opposite directionality. All mean vectors of the distribution of protractor and retractor MN spikes showed a significant directionality ($p<0.001$, Rayleigh test). The mean values for the distributions of protractor and retractor MN activity during a hind leg step cycle were between 279° and 89° for protractor MNs and between 71° and 210° for retractor MNs.

Unspecific stimulation of femoral and trochanteral campaniform sensilla (backward) entrains the pilocarpine-induced rhythm in the prothoracic protractor-retractor system.

In order to locate the source of the sensory information that arises at the stepping hind leg and modulates the pilocarpine-induced rhythm in the prothoracic protractor-retractor system CPG, preliminary stimulation experiments were performed.

For these experiments, the hind leg was fixed at the coxa-trochanter level. In this way the leg could not move in any direction at this joint. The leg was cut in the middle of the femur in order to exclude ground contact, and information arising from the femoral chordotonal organ. The stump was then bend in forward and backward direction, which provided a loading signal of the hind leg, encoded by campaniform sensilla of the stick insect.

Fig. 8 shows the results of these experiments in 3 animals. Bending the leg in a caudal direction resulted in flexor activity in the hind leg and prothoracic protractor MN activity in the pilocarpine-induced rhythm. The protractor MN burst occurred directly after the stimulus, which resulted in an advancement of the pilocarpine-induced rhythm in response to the stimulus (Fig. 8 B).

The presented results in this very preliminary data indicate that the sensory signals, modulating the prothoracic protractor-retractor CPG could derive from load signals detected by the campaniform sensilla.

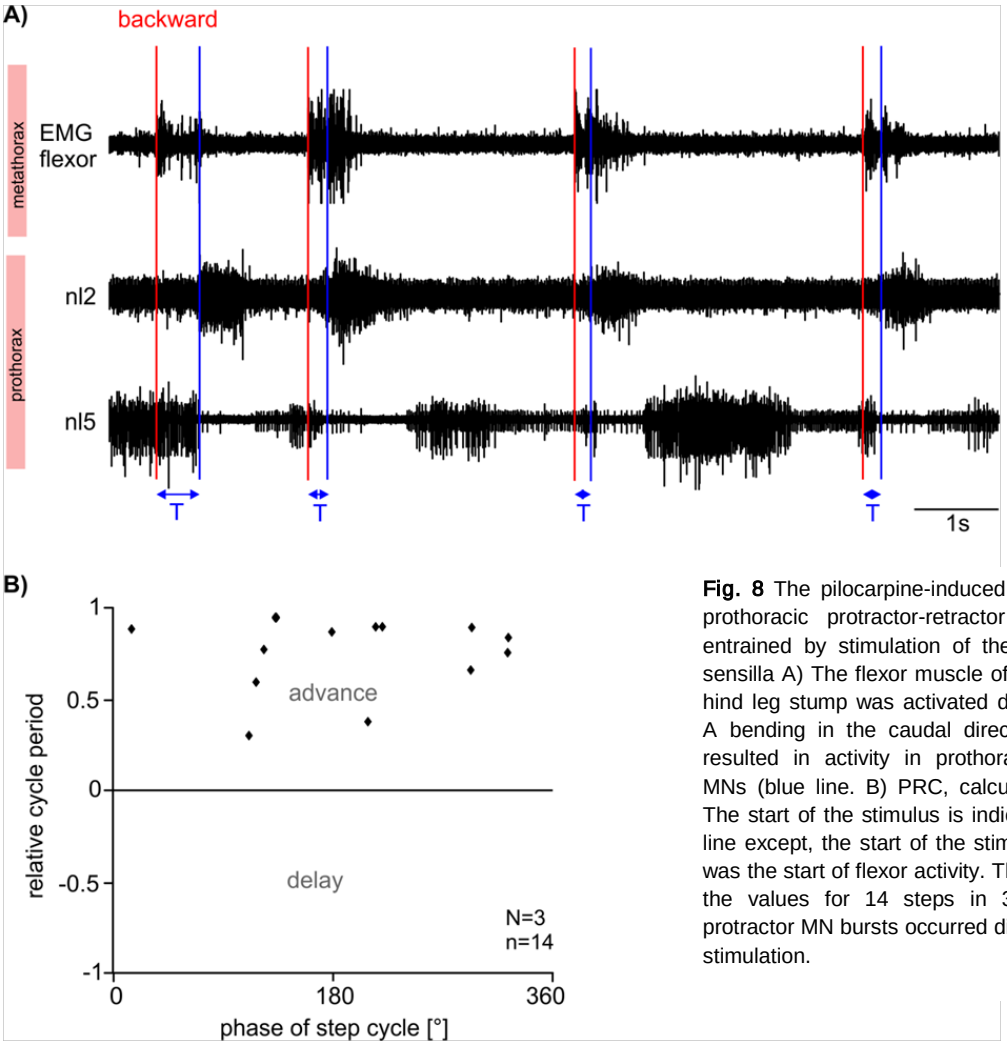

Fig. 8 The pilocarpine-induced rhythm in the prothoracic protractor-retractor system was entrained by stimulation of the campaniform sensilla A) The flexor muscle of the remaining hind leg stump was activated during bending. A bending in the caudal direction (red line) resulted in activity in prothoracic protractor MNs (blue line. B) PRC, calculated as Fig3. The start of the stimulus is indicated by a red line except, the start of the stimulus (red line) was the start of flexor activity. The PRC shows the values for 14 steps in 3 animals. All protractor MN bursts occurred directly after the stimulation.

6. Discussion

The present work introduces different approaches to the investigation of inter- and intra-segmental coordination. I start with the analysis of walking behavior of stick insects in different walking conditions (see Grabowska et al., 2012). Next, I will present a neuromechanical model that comprises all three main antagonistic muscle pairs of a stick insect leg. This model was applied to describe the neuronal and muscular activities of the musculo-skeletal system at start and stop during stick insect locomotion. The model emphasizes the differential roles of the slow and fast muscle fibers during these events. Then, I will show how the aforementioned 3-CPG-MN network model by Daun-Gruhn and Tóth (2011) was extended in order to describe eight-legged locomotion. The purpose of this work was to modify the 3-CPG-MN network model, based on anatomical and physiological analogies between the stick insect and arthropods, in order to model locomotion in crustaceans and other eight-legged animals. Finally, I will treat the experiments concerning the caudo-rostral inter-segmental influence between the three segmental protractor-retractor CPGs, which are situated in the segmental hemi-ganglia of the stick insect. The experiments were performed to test a hypothesis arising from an existing network model for locomotion, and possibly validate it. This model describes the activity of the protractor-retractor CPG systems of the three segments (pro-, meso-, metathorax) of the stick insect (3-CPG-MN network model) during walking.

In the first study (see Grabowska et al., 2012), the influence of different walking situations on the coordination in walking stick insects was analyzed. First, the results show that depending on the slope the animals walked on, the resulting coordination patterns of the walking legs change during locomotion. These results indicate, that a different distribution of load on the walking legs, and therefore different sensory information that is encoded by the sensory organs detecting load, leads to different phase relations between the single legs during walking. Second, the amputation experiments show that the different leg pairs, meaning front, middle and hind legs, may contribute differently to inter-segmental coordination. While the front and hind leg amputations result in more regular coordination patterns during walking, the amputation of the middle legs lead to an impairment of the coordination. Additionally, the front legs can serve as sense organs during walking, and their movements therefore lead to irregular coordination patterns (Dürr, 2001; Cruse, 1976). Nevertheless, they can also become part of the regular pattern generating mechanism during walking.

In the second study (see Tóth et al., 2013), an explanation was provided of how walking in the stick insect is stopped and started using a neuromechanical model. This neuromechanical model was complemented by making physiologically plausible assumptions with regard to the stopping and starting of stepping. In particular, three fundamental assumptions are of importance: the first one postulates the differential role of the slow and fast muscle fibers at start and stop. The second assumption is about the coordinating roles of sensory signals reflecting position and velocity of the leg's main joints. This assumption relates to the crucial role of sensory feedback in coordinating the activities of the leg's neuromuscular systems during locomotion, standing, and during the transition processes between these states. The third important assumption claims that none of the processes at starting and stopping interfere with the activities of the three CPGs, which produce the rhythmic activities of the single leg joints during locomotion. This study thus formulates physiological relevant hypotheses about the role of the slow and fast muscle fibers, and their differential neuronal control at starting and stopping of a stick insect leg.

In the third study (Grabowska et al., 2014, under review.) I show that the 3-CPG-MN network model (Daun-Gruhn and Tóth, 2011) can serve as a basis for modeling arthropod walking. To demonstrate this, the 3-CPG-MN network model was extended by an additional segmental unit in two different ways, resulting in two different network topologies. The first topology (topology 1) constituted a clockwise, cyclical connection from the last segment to the first segment, as in the case of the 3-CPG-MN network model. This topology showed its limits when in the simulations the parameter values of the excitatory tonic drive, and the timing of the arriving excitatory signals from neighboring segments were changed. In the second topology (topology 2) every second segment was connected by a caudo-rostral inter-segmental pathway. In this way, segment 1 received excitatory signals from segment 3, as in the 3-CPG-MN network, and segment 2 received excitatory signals from segment 4. Topology 2 proved to produce stable output for a larger range of parameters for the excitatory tonic drive than topology 1, and the model became more sensitive to the timing of the excitatory signals arriving from neighboring segments. Using this topology, a large variety of walking behavior of crustaceans could be simulated. Additionally, this network model emphasizes the importance of excitatory sensory signals for the generation of various walking behaviors. Taking the similarities in the neuroanatomy of the thoracic ganglia and in the function of the leg muscles of arthropods into account, the 4-CPG-MN network model also proposes possible inter-segmental connections that can be tested in experiments.

In the fourth study (Grabowska et al., in prep), I investigated the caudo-rostral inter-segmental influence from the metathoracic ganglion to the prothoracic ganglion in the stick insect. The existence of such an inter-segmental pathway was hypothesized by Daun-Gruhn and Tóth (2011), and implemented in their 3-CPG-MN network model of stick insect locomotion. The results of this study provide evidence for this connection. Pilocarpine, a muscarinic agonist of acetylcholine, induced rhythmic activity in the

protractor/retractor system of the prothoracic ganglion. This rhythmic activity was entrained by active and passive forward and backward steps of the ipsilateral hind leg. In addition, the stance phase during hind leg steps could reset the pilocarpine-induced rhythm in the prothoracic ganglion. Preliminary findings show the entrainment of pilocarpine-induced rhythm in the prothoracic ganglion by stimulations of femoral campaniform sensilla in the ipsilateral hind leg. These results indicate that the modulating sensory influence could derive from load signals, as it is proposed in the 3-CPG-MN network model.

The common result of all four presented studies is the evidence for the strong influence of sensory feedback on segmental rhythm generators of locomotion during walking in the stick insect *Carausius morosus* and in crustaceans, such as crayfish and forward walking crabs. The sensory feedback is provided by sensory organs encoding the position of the legs, the velocity of angular movements between the leg joints, and the loading of the legs.

Suggestion for a possible gaiting mechanism for the different functions of the front legs during locomotion

The behavioral experiments on stick insects that walked on different slopes provided fundamental information on how changes in the walking environment affect the walking behavior of stick insects. Also, the amputation of leg pairs, and therefore the absence of sensory input arising at the sensory organs in the different walking legs, contributes to changes in the motor output of stick insects.

The neuronal control of leg movements during walking and standing is found within the prothoracic, mesothoracic and metathoracic ganglia that control the front, middle and hind legs, respectively (Bässler and Büschges, 1998; Pearson and Fourtner, 1975). It is known that the motor pattern in every leg emerges from interactions of afferent signals from the leg with the corresponding CPGs that govern the action of the three individual leg joints of the stick insect's leg (Büschges and El Manira, 1998). To control the movements of the adjacent leg joints in a leg, sensory signals, as well as central commands, are necessary for a proper coordination of the leg (Bässler and Büschges, 1998; El Manira et al., 1991; Hess and Büschges, 1999). The rhythm generating networks of the individual legs are also coupled by sensory information that come from different sensory receptors, situated within each leg (Akay et al, 2001; Borgmann et al. 2009; Borgmann et al. 2011). In chapter 5, I could show that the inter-segmental sensory information flow is not only rostro-caudally directed, but also caudo-rostrally, and that the information flow may emerge from load sensitive signals in the campaniform sensilla (Fig 7). Behavioral rules by

which all six leg movements of a stick insect are controlled, are described by Cruse et al. (1998). Nevertheless, a path, or rule, that describes the relation between hind and front leg movements was lacking. The experiments in chapter 5 provide a new coordination rule that connects the hind and front legs in the caudo-rostrally direction.

On the one hand, stick insects can use their front legs as searching organs in order to explore their environment (Dürr, 2001; Cruse, 1976). In the experimental study presented in this work (see results, Chapter 4.1, Grabowska et al., 2012), ignoring the front legs in the analysis of the coordination patterns led to a regular quadruped coordination pattern of the middle and hind legs. This means that during walking, the animal is able to uncouple the front legs from the locomotor system, and use them as searching organs, while the middle and hind legs make regular movements. The touching frequency of the front legs did not correlate with the stepping frequency of the walking middle and hind legs (Grabowska et al. 2012). However, it was shown for stick insects that the antennal abduction and adduction cycle leads to a coupling of the protraction and retraction cycle of the front legs with a stable phase shift (Dürr et al., 2001). Therefore, simultaneous antennal activity can be observed during searching movements (Dürr, 2011). The sensory information that influences the rhythmic activity of the antennal joint and therefore their movements emerges in mechanoreceptors in the antenna (Cappe de Baillon, 1936; Weide, 1960; Slifer, 1966). The sensory neurons project in the antennal lobe and to the corresponding motor centers. The central complex (CC) of insect brains is a group of midline neuropils in the protocerebrum (Williams, 1975; Straußfeld, 1999). It is known to supervise different forms of locomotion, like regular walking, turning, and searching movements of the front legs (Ritzmann et al., 2007). In this area neurons were found that respond to mechanical antennal stimulation. In cockroaches, a lesion of the CC affects controlled climbing over blocs due to the lack of processing of sensory information from the antennal mechanoreceptors (Ridgel et al., 2007, Ritzmann et al., 2005). Additionally, large populations of multisensory neurons in the CC were found that contribute to the control of regular locomotion, since electrical stimulations in this brain area evokes changes in locomotion (Huber, 1960; genetic studies for Drosophila: Strauß et al., 1992; Martin et al., 1999; Strauß, 2002). For the cockroach, Ritzmann and colleagues (2007) suggested that antennae provide important information in order to supervise climbing behaviors. This information is used by the CC to supervise the decisions to climb or use normal locomotion which would lead to the subsequent movements. This assumption is supported by lesion experiments with cut connectives from the CC to the suboesophageal ganglion (SOG) in the cockroach (Ritzmann, 2005). The experimental results in my thesis show that pilocarpine-induced rhythms in the prothoracic ganglion are more irregular than the ones in the mesothoracic ganglion (Chapter 5, supplementary Fig. 1). Isolation of the prothoracic ganglion from the SOG resulted in more regular pilocarpine-induced rhythms in the prothoracic ganglion. Applying pilocarpine on the non isolated prothoracic ganglion resulted in a simultaneous application on the SOG. In this case rhythmic antennae movements were also observed. On the one hand, pilocarpine-induced rhythmicity of the prothoracic protractor and retractor system in the thoracic ganglion itself. On the

other hand, the rhythmic activity of the antennal rhythm-generating networks, also induced by pilocarpine, seems to influence the pattern generating networks in the prothoracic ganglion via the SOG, which induced irregularities in the prothoracic protractor/retractor system. In the experiments described in chapter 5, the prothoracic ganglion was not isolated from the SOG (see irregular pilocarpine rhythm in the prothoracic protractor/retractor MN recordings in Fig. 3). Therefore rhythmic movements could be observed the whole time during my experiments (personal observation). Nevertheless, this irregular rhythm became more regular when entrained by the walking hind leg. In this case, the neural control within the thoracic segments seemed to have a larger influence on the locomotion system.

It becomes obvious that also in my experiments, there is a subdivision into local circuits that are responsible for the organization of the leg movements, and into higher processing centers in the stick insects brain that generate descending connections in order to alter walking behavior (Ritzmann and Büschges, 2007).

In the following paragraph, I will propose a gating mechanism that is supported by feedback from the front legs' sensory organs. This mechanism determines the motor output of the front legs. The motor output could produce searching movements of the front legs, phase locked to the antennal movements or regular walking behavior of the middle and hind legs.

The first influence could be, for instance, an increase in load on the front legs, due to changes in the slope as it is the case in downward walking. In Grabowska et al. (2012), stick insects used different coordination patterns depending on the slope of the walking surface. Walking on plane surfaces or surfaces with a slope of 15° resulted in a higher proportion of the tetrapod coordination pattern and irregular walking pattern than the tripod coordination pattern. Compared to these walking situations, climbing (90°) resulted in an even lower proportion of the tripod coordination pattern. In contrast to this, walking on a surface with a 15° downward slope led to a higher rate of observed tripod coordination pattern than walking upwards or on a plane surface. One reason for the use of different coordination patterns could be the different distribution of load for the single legs during walking. This was also reported for locust: there, different walking conditions, such as horizontal walking, climbing and upside down walking led to alternations in motor patterns due to changes in posture of the leg and different loading of the leg joints (Duch and Pflüger, 1995). Standing or walking on declining surfaces results in an enlargement of the component of the gravitational force parallel to the walking direction of the stick insect. This explains the increased use of tripod coordination patterns and the decreased amount of probing behavior during walking. In this situation, the front legs have to be included in the locomotor system to provide stability during walking. The increase in load induces stronger sensory load signals that modulate the front legs CPGs. This influence may override central commands arriving from the

insect's brain that normally would induce searching movements. Therefore, the excitatory sensory input on the adjacent mesothoracic segment could be stronger.

This sensory input originates in the sensory organs of the hind legs during stepping. The stronger sensory signals in the front legs may have a higher impact compared to other influencing factors. The electrophysiological results presented in this thesis (Chapter 5) prove thus a modulation of the pilocarpine-induced rhythmic activity in the prothoracic protractor-retractor CPG.

The second modulating influence is present during searching or probing and is the sensory feedback from the sensory organs of the antenna coupling the front leg rhythm to the antenna movements. For the front legs, load differs from feedback during ground contact in the stance phase during regular locomotion from the load signals during searching (Zill et al., 2012). The second modulating input derives from the central complex of the insect's brain via the SOG (Ritzmann et al., 2007). It is known that during searching movements of the front leg, simultaneous antennal activity can be observed (Dürr, 2001). These rhythmic antennal movements can alter the normal movement pattern of the front legs during locomotion (Dürr, 1999; Dürr et al., 2001). The prothoracic leg CPGs, that normally provide the rhythmic activity of the front legs of an animal during walking, could now obtain a stronger influence via the SOG than from the sensory input from the metathoracic ganglion and could thereby modulate the stepping activity of the front legs. The influence from the SOG could transfer the rhythmic activity of the antennal searching movements on the prothoracic CPGs and be stronger than the sensory influence.

During upward walking of the stick insect, there is a component of the gravitational force, antiparallel to the direction of the movement. Now the muscles of the hind legs have to exert larger force than the front ones in order to continue upward walking. At the same time, reduction of load in the front legs allows the animals to perform more active searching movements with the front legs. This behavior is important in the natural habitat of the stick insect during climbing in bushes or on trees where the searching movements occur mainly due loss of ground contact.

I propose that the descending influence of the CC via the SOG is present at any time during locomotion of the animals. However, if the load of the front legs exceeds a certain as yet unknown threshold, the central descending information will be overwritten by local segmental sensory signals.

Comparison of my studies to different mathematical models

Coordination patterns exhibited by walking insects show great variability, due to the different temporal and spatial relations between the activities of the single legs. Stick insects, in particular, show several coordination patterns, starting with a metachronal wave coordination pattern, an intermediate tetrapod

coordination pattern, up to a very fast tripod coordination pattern (Grabowska et al. 2012). These coordination patterns are not rigidly wired in neural structures but can be regarded as emergent properties. This behavior was described for crayfish (Cruse and Müller, 1986), but is also legitimate for stick insects (Büschges and Gruhn 2008, Fischer et al. 2000). These emergent properties are controlled by the specific timing of the leg movements in the different segments. The timing is influenced by sensory cues that report on the state of neighboring legs (Cruse, 1990).

Theoretical models are useful to investigate functions of biological systems, such as the locomotion of arthropods. When designing mathematical models, or robots that are able to replicate insect walking behavior, results from behavioral experiments on walking and results concerning the neuronal control of walking are combined and implemented in the model or robot. In each model or robot, specific properties have to be selected that are critical for reproducing walking. In this study, I presented experimental data that validate a hypothesized structure in the 3-CPG-MN network model proposed by Daun-Gruhn and Tóth (2011). This network model describes rhythmic activity of the ipsilateral protractor-retractor rhythm generating systems of the stick insect. In this specific case, an inter-segmental influence was necessary to generate tetrapod (ipsilateral wave) and tripod coordination patterns, and continuous transitions between them. The inter-segmental connections are modulated (gated) by segmental sensory signals. These artificial sensory signals act via excitatory sensory interneurons (SIN), and represent load signals of the leg, whose source is the depressor activity of the adjacent segment. My experimental results (Chapter 5) indicate that the modulation of the pilocarpine-induced rhythm in the prothoracic protractor-retractor system may derive from load signals of the hind legs. These load signals are generated by campaniform sensilla. Comparing the phase response curves (PRC) expressing the influence of the stimulations on the mesothoracic protractor-retractor rhythm of a forward stepping front leg (Borgmann et al. 2009, Tóth et al., submitted) with my PRCs expressing of the influence of the stimulations on the prothoracic protractor-retractor rhythm of a forward stepping hind leg (Chapter 4, Fig 4), one finds good agreement between them.

In chapter 4.1, I showed that the amputation of the middle leg leads to maladapted walking patterns. These results are in accordance with electrophysiological experiments of Borgmann et al. (2009) where the metathoracic ganglion only produced rhythmic activity in the presence of a stepping middle leg. Furthermore, the presence of a stepping middle leg led to a tonic increase of motoneuronal activity in the prothoracic and metathoracic ganglion, which may be a sign of the middle leg's stabilizing function. The inter-segmental influence from the stepping hind leg to the stepping front leg provides stable coordination patterns in 72% of the test cases (Grabowska et al. 2012, Figure 9). These results are also in agreement with the electrophysiological experiments in chapter 5.

The failure of coordination described above, as a result of lacking middle legs was also observed in "walknet" simulations (Kindermann, 2002; Schilling et al. 2012; Schilling et al. 2014). "Walknet" is an artificial neuronal network for modeling stick insect locomotion, which is also implemented in several

robot platforms (Espenschied et al., 1993; Pfeiffer et al., 1995; Schmitz et al., 2008, Paskarbeit et al. 2010, Schneider et al. 2011, Schilling et al. 2012). In this model, the coordination rules for locomotion by Cruse (1990) (Cruse 1990, Dürr et al. 2004, Schilling et al., 2012) were implemented, in order to control the stepping movements of adjacent legs of the stick insect. Using these coordination rules, the model could overcome the loss of up to two legs, namely the front and hind legs (Schilling et al., 2012). This behavior was also observed in the amputation experiments (cf. Chapter 4.1), where the loss of the front legs, even increased the regularity of the stepping pattern of stick insects walking on a horizontal surface (Chapter 4.1, Grabowska et al. 2012, Fig. 7). The same was observed for hind legs (Chapter 4.1, Grabowska et al. 2012, Fig. 8). In order to simulate the loss of middle legs in "walknet", the introduction of a new coordination rule connecting hind and front leg is necessary. The findings of the electrophysiological experiments reported in chapter 5 provide a basis for this new coordination rule. The beginning of the stance phase in a forward stepping hind leg positioned at the anterior extreme position (AEP) of the hind leg leads to an entrainment of activity in the prothoracic protractor activity, which is the beginning of a swing phase in a forward walking front leg.

The extension of the 3-CPG-MN network of Daun-Gruhn and Tóth (2011) by an additional segmental module was successful in reproducing coordination patterns and walking behavior of arthropods walking on eight legs (Chapter 4.3, Grabowska et al., under review). There, a caudo-rostral inter-segmental connection, connecting every second CPG was necessary in order to provide stability of the network topology. When considering a truly cyclic inter-segmental connection of the four segmental modules of the 4-CPG-MN network only, the model could not reproduce an increase in oscillation activity of the coupled protractor-retractor systems in a large enough range. Also, stable transitions between the three kinds of coordination patterns observed in forward walking crayfish and crabs could not be obtained (Barnes 1974, Parrack 1964, Ross and Belanger 2013). This makes sense though, because it is hard to imagine, that movements of a hind leg of the last segment of a millipede, for instance, could provide an inter-segmental connection through sensory input on the first segment. The latency until the signal would arrive at the first segment would be too long, and this connection therefore is physiologically unplausible. In chapter 4.3, I focused mainly on the influence of ϕ_{ij}. This is the parameter that describes the phase shift between the (periodic) sensory signal that gates the excitatory inter-segmental pathway, and the (periodic) activity of the affected protractor-retractor CPG module. Varying this parameter using topology 1 as well as topology 2 led to the reproduction of a large variety of coordination patterns observed, since both networks proved to be sensitive to changes in ϕ_{ij}. Of course, I also tested the influence of the phase shift between the (periodic) sensory signal gating the local inhibitory pathway and the (periodic) activity of the affected protractor-retractor CPG module of the same segment (unpublished data). Varying this parameter led to hardly any changes in the coordination patterns. One reason might be that the synaptic strength for the gated inhibitory signal is much weaker

than the one for the excitatory pathway. Indeed, the results of a theoretical study in which inter-segmental connections of the 3-CPG-MN model were investigated suggest that excitatory connections must be strong while inhibitory ones can be neglected (Tóth et al., submitted). This underpins my finding that the strength of the excitatory connections was crucial for the replication of the coordination patterns with the 4-CPG-MN network model (Chapter 4.3, Grabowska et al. under review).

The design of insect robots has gained a lot from the study of animal locomotion. Insects can namely successfully adapt to their complex continuously changing walking environment. However, the construction of hexapods robots makes mostly use of specific aspects of insect locomotion. These are, for instance, the relation between the adjacent walking segments based on walking experiments of insects and the dynamics and kinematics of single legs during walking. In chapter 4.2 (Tóth et al. 2013), I presented a neuromechanical model that heavily relies on the control of the activity of slow and fast muscle fibers of the three main leg muscle pairs within the stick insect's leg. The model describes their activity at start and stop, which are basic phenomena of stick insect locomotion. The coordination of the activities of slow and fast muscle fibers in the antagonistic muscle pairs contributes to the high efficiency of locomotion in stick insects. If beside the biomechanical properties of the different muscle pairs during insect walking (Guschlbauer et al., 2007), the neuronal control of these muscle groups, especially the timing of those activities by specific sensory signals, are also taken into account this can considerably improve the locomotion properties of hexapod robots.

The influence of hind leg stepping on the pilocarpine-induced rhythm in the prothoracic protractor-retractor system of the stick insect

The experiments in chapter 5 show that sensory information, which is provided by a stepping hind leg of a stick insect, is able to entrain a pilocarpine-induced rhythm in the prothoracic protractor-retractor system. As mentioned earlier, this connection was assumed by Daun-Gruhn and Tóth (2011) in their 3-CPG-MN network model of stick insect locomotion.

The experimental results emphasize three important points concerning this inter-segmental pathway that provides a caudo-rostral influence on the stick insect locomotor system.

First, the results show that this influence is most likely a modulating one: without the rhythmic activity of the rhythm generating networks of the prothoracic protractor-retractor system, induced by

pilocarpine, no rhythmic activity could be induced by a stepping hind leg (personal observation). These results are in contrast to the results, showing the rostro-caudal influence of a stepping front leg on the activity in the mesothoracic ganglion (Borgmann et al., 2007). There, a stepping front leg was able to induce rhythmic activity in the mesothoracic protractor-retractor system of the stick insect and a tonic increase of metathoracic protractor and retractor MNs. Additionally, this rhythmic activity was in phase with the protractor/retractor activity of the stepping front leg (stance phase of front leg in phase with retractor MN burst activity in the mesothoracic ganglion). However, front leg stepping had a modulating influence on the pilocarpine-induced rhythm in the protractor-retractor CPGs in the metathoracic ganglion. There, a stance phase of a front leg entrained the retractor MN burst activity of the metathoracic ganglion (Borgmann et al., 2009). In my experiments, however, the stance phase of the forward stepping ipsilateral hind leg was in phase with the activity of the protractor MNs of the pilocarpine-induced rhythm in the prothoracic ganglion.

Second, there appears to be no or negotiable inter-segmental influence of the mesothoracic ganglion on the modulation of the pilocarpine-induced rhythm in the prothoracic protractor-retractor system by the stepping hind leg. In my experiments, the mesothoracic ganglion was completely deafferented. For the mesothoracic ganglion, it was shown that a backward stepping hind leg was able to induce rhythmic activity in one third of the experiments, and in two thirds an increase in tonic MN activity (Borgmann et al., 2009). As mentioned in the preceding paragraph, this finding does not concern the activity of the rhythm generating networks of the prothoracic ganglion. For the inter-segmental connection in the rostro-caudally direction, the presence of the middle leg, and ,therefore, the afferent signals deriving from the middle leg, are important in order to produce rhythmic activity in the metathoracic rhythm generating networks (Borgmann et al., 2009). In my experiments this is not the case. In order to entrain the pilocarpine-induced rhythm in the prothoracic protractor-retractor system, afferent signals from the mesothoracic ganglion were not necessary. I therefore, can conclude that this influencing pathway may be a direct one.

Third, the afferent signals, modulating the activity of the rhythm generating networks of the prothoracic protractor-retractor system, may have their origin in the detection of load by the femoral and trochanteral campaniform sensilla. My preliminary results, concerning the stimulation of the hind leg's campaniform sensilla by moving the hind leg stump in the posterior direction parallel to the body, also show an entrainment of the pilocarpine-induced rhythm. These results are in agreement with previous experiments on the inter-segmental coordination of rhythm generating networks in the stick insect (Akay et al., 2001; Borgmann et al., 2009). Nevertheless, it has to be kept in mind that this stimulation was very unspecific, and more specific experiments will have to be set up for a thorough investigation of the effects, the campaniform sensilla may have.

Also, more aspects of this inter-segmental connection have to be analyzed. First of all, Daun-Gruhn and Tóth (2011) hypothesized in their model a gated inter-segmental connection that is excitatory.

Therefore, experiments will have to be designed, which can effectively contribute to answering this question. Second, additional experiments will have to be performed in order to verify, if the modulation of the pilocarpine-induced rhythm in the prothoracic ganglion is only present in the protractor-retractor system, or perhaps in the levator-depressor system, too. Accordingly, I will record, additionally, levator and depressor MN activity by means of extracellular electrodes in the prothoracic ganglion. Furthermore, the prothoracic ganglion will also be perfused with pilocarpine solution to produce rhythmic activity in the prothoracic protractor-retractor system and levator-depressor system. The effect of the stepping hind leg on this rhythm will then be analyzed. It was demonstrated that the rhythm generating networks of the three main leg joints of a stick insect leg show no constant phase relations when getting activated by pilocarpine (Büschges et al., 1995). It will, therefore, be interesting to see, whether the pilocarpine-induced rhythms in the prothoracic protractor-retractor and levator-depressor systems can be coupled in the presence of sensory input deriving from stepping activity of the ipsilateral hind leg.

7. Conclusion

All the different works in my thesis have in common that they reveal new results on the inter-leg control of walking stick insects. In particular, the studies stress the effects of intra-segmental modulating influences, between the rhythm generating networks in the three main leg joints, and inter-segmental modulating influences, between the three thoracic rhythm generating networks. Moreover, my thesis combines the results of mathematical models, based on experimental data on stick insect locomotion, and experiments, validating these models. Both, the mathematical models, presented here, and my experiments indicate an important sensory intra- and inter-segmental influence, modulating the rhythmic output of the CPGs, and connecting those.

Expanding the results of previous experimental studies (Cruse, 1990; Ludwar et al., 2005; Borgmann et al., 2007, 2009), my experiments in chapter 5, contribute to the knowledge of modulating caudo-rostrally directed inter-segmental influences, between the metathoracic and prothoracic rhythm generating networks. These results validate the hypothesized inter-segmental sensory pathway between the ipsilateral metathoracic and prothoracic protractor-retractor CPG modules (3-CPG-MN model network (Daun-Gruhn and Toth, 2011)). The next attempt for the validation of this mathematical network would be to investigate, if the modulating inter-segmental influences, observed in experiments, are of excitatory or inhibitory nature.

Furthermore, I want to emphasize, the fact that an existing model network (3-CPG-MN network model (Daun-Gruhn and Tóth, 2011)) for the reproduction of motor pattern of the ipsilateral protractor-retractor system of a stick insect, can serve as a basis for the rendition of walking behavior of animals with eight-walking legs. This study does not only prove the mathematical model, to be flexible enough to be expanded by additional segmental modules and still produce stable simulations of the coordination patterns of forward walking crayfish and crabs, but also hypothesizes possible neuronal structures for the model animals. Additionally, this model points out that excitatory signals, gated by inter-segmental pathways, may be crucial for the generation of specific phase relations between the activities of the rhythm generating networks, hence, the generation of different coordination patterns in walking arthropods.

8. Bibliography

Akay, T., Bässler, U., Gerharz, P., Büschges, A. (2001). The Role of Sensory Signals from the Insect Coxa-Trochanteral Joint in Controlling Motor Activity of the Femur-Tibia Joint. *The American Physiological Society,* DOI: 0022-3077/01.

Akay, T., Haehn, S., Schmitz, J., Büschges, A. (2004). Signals from load sensors underlie interjoint coordination during stepping. *Journal of Neurophysiology*, 96, 3532-3537.

Akay, T., Ludwar, B., Goritz, M. L., Schmitz, J., Büschges, A. (2007). Segment specificity of load signal processing depends on walking direction in the stick insect leg muscle control system. *Journal of Neuroscience*, 27, 3285-3294.

Alexander, R. M. (1989). Optimization and gaits in the locomotion of vertebrates. *Physiological Reviews*, 69, 1199-1227.

Barnes, W. J. P. (1975). Leg Co-Ordination during Walking in the Crab, *Uca pugnax*. *Journal of Comparative Physiology*, 96, 237-256.

Bässler D., Büschges A., Meditz S., Bässler U. (1996). Correlation between muscle structure and filter characteristics of the muscle-joint system in three orthopteran insect species. *Journal Experimental Biology*, 199, 2169–2183.

Bässler U., Stein W. (1996). Contributions of structure and innervation pattern of the stick insect *extensor tibiae* muscle to the filter characteristics of the musclejoint system. *Journal Experimental Biology,* 199: 2185–2198.

Bässler, U. (1977). Sense organs in the femur of the stick insect and their relevance to the control of position of the femur-tibia-joint. *Journal of Comparative Physiology A*, 121, 99–113.

Bässler, U. and Büschges, A. (1998). Pattern generation for stick insect walking movements. Multisensory control of a locomotor program. *Brain Research Reviews*, 27, 65–68.

Bässler, U. (1967). On the regulation of the position of the femur-tibial joint of the walking-stick insect *Carausius morosus* at rest and in motion. *Kybernetik*, 4, 18–26.

Bender, J. A., Simpson, E. M., Tietz, B. R., Daltorio, K. A., Quinn, R. D. and Ritzmann, R. E. (2011). Kinematic and behavioral evidence for a distinction between trotting and ambling gaits in the cockroach *Blaberus discoidalis*. *Journal of Exprimental Biology*, 214, 2057-2064.

Borgmann, A., Hooper, S. L., and Büschges, A. (2009). Sensory feedback induced by front-leg stepping entrains the activity of central pattern generators in caudal segments of the stick insect walking system. *Journal of Neuroscience*, 29, 2972–2983.

Borgmann, A., Scharstein, H., Büschges, A. (2007). Intersegmental coordination: Influence of a single walking leg on the neighboring segments in the stick insect walking system. *Journal of Neurophysiology*, 98, 1685–1696.

Borgmann, A., Toth, T. I., Gruhn, M., Daun-Gruhn, S., Büschges, A. (2012). Dominance of local sensory signals over inter-segmental effects in a motor system: experiments. *Biological Cybernetics,* DOI: 10.1007/s00422-012-0473-y.

Bowerman, R. F. (1977). The control of arthropod walking. *Comparative Biochemistry and Physiology Part A: Physiology*, DOI: 10.1016/0300-9629(77)90190-6.

Bucher, D., Akay, T., DiCaprio, R. A., Büschges, A. (2003). Interjoint Coordination in the Stick Insect Leg-Control System: The Role of Positional Signaling. *Journal of Neurophysiology*, 89, 1245-1255.

Burns M. D. (1973). The control of walking in Orthoptera. I. Leg movements in normal walking. *Journal of Experimental Biology*, 58, 45-58.

Burrows, M., Hedwig, B. (1996). Presynaptic inhibition of sensory neurons during kicking movements in the locust. *Journal of Neurophysiology*, 75, 1221-1232.

Büschges, A. (1995). Role of local nonspiking interneurons in the generation of rhythmic motor activity in the stick insect. *Journal of Neurobiology*, 27, 488–512.

Büschges, A. (1998). Inhibitory synaptic drive patterns motoneuronal activity in rhythmic preparations of isolated thoracic ganglia in the stick insect. *Brain Research*, 783, 262–271.

Büschges, A. (2005). Sensory control and organization of neural networks mediating coordination of multisegmental organs for locomotion. *Journal of Neurophysiology*, 93, 1127–1135.

Büschges, A., Akay, T., Gabriel, J. P., Schmidt, J. (2008). Organizing network action for locomotion: insights from studying insect walking. *Brain Research Reviews*, 57, 162–71.

Büschges, A., Gruhn, M. (2008). Mechanosensory feedback in walking: from joint control to locomotor patterns. *Advances in Insect Physiology*, DOI: 10.1016/S0065-2806(07)34004-6.

Büschges, A., Ludwar, B. Ch., Bucher, D., Schmidt, J., DiCaprio, R. A. (2004). Synaptic drive contributing to the rhythmic activation of motoneurons in the deafferented stick insect walking system. *European Journal of Neuroscience*, 19, 1856-1862.

Büschges, A., Manira, A. E. (1998). Sensory pathways and their modulation in the control of locomotion. *Current Opinion in Neurobiology*, DOI: 10.1016/S0959-4388(98)80115-3.

Calabrese, R. L. (1995). Half-center oscillators underlying rhythmic movements. In Arbib, M. (Ed.), *The Handbook of Brain Theory and Neural Networks,* pp. 444–447. Cambridge, MA: MIT press.

Cappe de Baillon, P. (1936). L'organe antennaire des Phasmes. *Bulletin biologique de la France et de la Belgique*, 70, 1-35.

Cattaert, D., El Manira, A., Marchand, A., Clarac, F. (1990). Central control of the sensory afferent terminals from a leg chordotonal organ in crayfish in vitro preparation. *Neuroscience Letters*, 108, 81-87.

Cattaert, D., Le Ray, D. (2001). Adaptive motor control in crayfish. *Progress in Neurobiology,* 63, 199 – 240.

Chasserat, C. and Clarac, F. (1983). Quantitative analysis of walking in a decapod crustacean, the rock lobster *Jasus lalandii*. II. Spatial and temporal regulation of stepping in driven walking. *Journal of Experimental Biology*, 107, 219-243.

Chrachri, A. and Clarac, F. (1989). Synaptic connections between motor neurons and interneurons in the fourth thoracic ganglion of the crayfish, *Procambarus clarkii. Journal of Neurophysiology*, 62, 1237-1250.

Chrachri, A., and Clarac, F. (1990). Fictive locomotion in the fourth thoracic ganglion of the crayfish, *Prorambarus darkii. Journal of Neuroscience*, 10, 707-719.

Clarac, F. (1982). Decapod crustacean leg coordination during walking. In Herreid, C. F. and Fourtner, C. R. (Ed.), *Locomotion and Energetics in Arthropods*, pp. 31-71. New York: Plenum Press.

Clarac, F., and Barnes, W. J. P. (1985). Peripheral influences on the coordination of the legs during walking in decapod crustaceans. In B. M. H. Bush and F. Clarac (Ed.), *Coordination of Motor Behaviour*, pp. 249-269, Cambridge: Cambridge University Press.

Clarac, F., Cattaert, D., Le Ray, D., (2000). Central control components of a 'simple' stretch reflex. *Trends in Neuroscience*, 23, 199-208.

Clarac, F., Wales, W., Laverack, M. S. (1971). Stress Detection at the Autotomy Plane in the Decapod Crustacea II. The Function of Receptors Associated with the Cuticle of the Basi-ischiopodite. *Journal of Comparative Physiology*, 73, 383-407.

Cruse H., Ehmanns I., Stubner S., Schmitz J. (2009). Tight turns in stick insects. *Journal of Comparative Physiology A*, 195, 299-309.

Cruse, H. (1976). The function of legs in the free walking stick insect, *Carausius morosus. Journal of Comparative Physiology A,* 112, 235-262.

Cruse, H. (1985). Which parameters control the leg movement of a walking insect? I. Velocity control during the stance phase. *Journal of Experimental Biology*, 116, 343–355.

Cruse, H. (1990). What mechanisms coordinate leg movement in walking arthropods. *Trends in Neuroscience,* DOI: 10.1016/0166-2236(90)90057-H.

Cruse, H. and Müller, U. (1986). Two coupling mechanisms which determine the coordination of ipsilateral legs in the walking crayfish. *Journal of Experimental Biology*, 121, 349-369.

Cruse, H., Dürr, V., Schilling, M., Schmitz, J. (2009). Principles of insect locomotion. In Arena, P. and Patanè, L. (Ed.) *Spatial Temporal Patterns for Action-Oriented Perception in Roving Robots*, pp. 1-57. Berlin: Springer.

Cruse, H., Dürr, V., Schmitz, J. (2007). Insect walking is based on a decentralized architecture revealing a simple and robust controller. *Philosophical Transaction of the Royal Society A*, DOI: 10.1098/rsta.2006.1913.

Cruse, H., Kindermann, T., Schumm, M., Dean., J., Schmitz, J. (1998). Walknet- a biologically inspired network to control six-legged walking. *Neuronal Networks*, 11, 1435-1447.

Daun, S., Rybak, I. A., and Rubin, J. (2009). The response of a half-center oscillator to external drive depends on the intrinsic dynamics of its components: A mechanistic analysis. *Journal of Computational Neuroscience*, 27, 3–36.

Daun–Gruhn, S. (2011). A mathematical modeling study of inter-segmental coordination during stick insect walking. *Journal of Computational Neuroscience*, DOI: 10.1007/s10827-010-0254-3.

Daun-Gruhn, S., Toth, T. I. (2011). An inter-segmental network model and its use in elucidating gait-switches in the stick insect. *Journal of Computational Neuroscience*, DOI: 10.1007/s10827-010-0300-1.

Delcomyn, F. (1971). The locomotion of the cockroach *Periplaneta americana*. *Journal of Experimental Biology*. 54, 453-496.

Delcomyn, F. (1981). Insect locomotion on land. In Herreid, C. F. and Fourtner, C. R. (Ed.), *Locomotion and Energetics in Arthropods*, pp. 103-125. New York: Plenum Press.

Delcomyn, F. (1981). Insect locomotion on land. In Locomotion and Energetics in Arthropods. In Herreid, C. F. and Fourtner, C. R. (Ed.), pp. 103-125. New York: Plenum Press.

Duch, C. and Pflüger, H. J. (1995). Motor patterns for horizontal and upside-down walking and vertical climbing in the locust. *Journal of Experimental Biology,* 198, 1963-1976.

Dürr, V. (1999). Spatial searching strategies of the stick insect, using antennae and front legs (abstract). Proc Göttingen Neurobiol. Conf. 27, 212.

Dürr, V. (2001). Stereotypic leg searching movements in the stick insect: kinematic analysis, behavioural context and simulation. *Journal of Experimental Biology,* 204 , 1589-1604.

Dürr, V. (2005). Context-dependent changes in strength and efficacy of leg coordination mechanisms. *Journal of Experimental Biology,* 208, 2253-2267.

Dürr, V., Schmitz, J., Cruse, H. (2004). Behavior-based modelling of hexapod locomotion: linking biology and technical application. *Arthropod Structure and Development,* 33, 237–250.

Ekeberg, Ö., Blümel, M., Büschges, A. (2004). Dynamic simulation of insect walking. *Arthropod Structure and Development*, 33, 287–300.

Elson, R. (1996). Neuroanatomy of a Crayfish Thoracic Ganglion: Sensory and Motor Roots of the Walking-Leg Nerves and Possible Homologies With Insects. *Journal of Comparative Neurology*, 365, 1-17.

Elson, R. C., Sillar, K. T., and Bush, B. M. H. (1992). Identified proprioceptive afferents and motor rhythm entrainment in the crayfish walking system. *Journal of Neurophysiology*, 67, 530-546.

Epstein, S., Graham, D. (1983). Behaviour and motor output of stick insects walking on a slippery surface: I. Forward walking. *Journal of Experimental Biology*, 105, 215–229.

Espenschied, K. S., Quinn, R. D., Chiel, H. J., Beer, R. D. (1993). Leg coordination mechanisms in the stick insect applied to hexapod robot locomotion. *Adaptive Behavior,* 1, 455–468.

Fischer, H., Schmidt, J., Haas, R., Büschges, A. (2001). Pattern generation for walking and searching movements of a stick insect leg. I. Coordination of motor activity. *Journal of Neurophysiology,* 85, 341–53.

Godlewska, E. (2012). The histochemical characterization of muscle fiber types in an insect leg. Master Thesis, University of Cologne, Germany.

Grabowska, M. J, Godlewska, E., Schmidt, J., Daun-Gruhn, S. (2012). Quadrupedal gaits in hexapod animals – inter-leg coordination in free-walking adult stick insects. *The Journal of Experimental Biology*, 215, 4255-4266.

Graham, D. (1972). A behavioural analysis of the temporal organisation of walking movements in the 1st instar and adult stick insect (Carausius morosus). *Journal of Comparative Physiology A,* 81, 23-52.

Graham, D. (1977). The effect of amputation and leg restraint on the free walking coordination of the stick insect Carausius morosus. *Journal of Comparative Physiology A,* 116, 91-116.

Graham, D. (1985). Pattern and control of walking in insects. *Adv. Ins. Physiol*, 18, 31-140.

Graham, D., Epstein, S., 1985. Behaviour and motor output for an insect walking on a slippery surface: II. Backward walking. *Journal of Experimental Biology,* 296, 287–296.

Grillner, S, (2003). The motor infrastructure: from ion channels to neuronal networks. *Nature Review Neuroscience*, 4(7), 573-586

Grillner, S. (2006). Biological pattern generation: The cellular and computational logic of networks in motion. *Neuron*, 52, 751–766.

Grillner, S., Markram, H., De Schutter, E., Silberberg, G., and LeBeau, F. E. N. (2005). Microcircuits in action—from CPGs to neocortex. *Trends in Neurosciences*, 28, 525–533.

Grillner, S., Wallen P. (2002). Cellular bases of a vertebrate locomotor system – steering, intersegmental and segmental co- ordination and sensory control. *Brain Research Reviews,* 40, 92–106.

Guschlbauer, C., Scharstein, H., Büschges, A, (2007). The extensor tibiae muscle of the stick insect: biomechanical properties of an insect walking leg muscle. *Journal of Experimental Biology,* 210, 1092-1108

Hess, D. and Büschges, A. (1999). Role of proprioceptive signals from an insect femur-tibia joint in patterning motoneuronal activity of an adjacent leg joint. *Journal of Neurophysiologly*, 81, 1856–1865.

Hodgkin, A. L., and Huxley, A. F. (1952). A quantitative description of membrane current and its application to conduction and excitation in nerve. *Journal of Physiology*, 117, 500–544.

Hoyt,, D.F., Taylor, C.R. (1981). Gait and the energetics of locomotion in horses. *Nature* 292(5820):239-240.

Huber, F. (1960) Untersuchungen über die Funktion des Zentralnervensystems und insbesondere des Gehirns bei der Fortbewegung und Lauterzeugung der Grillen. *Journal of Comparative Physiology*, 44:60–132

Hughes, G. M. (1952). The co-ordination of insect movements. I. The walking movements of insects. *Journal of Experimental Biology,* 29, 167-285.

Ijspeert, A. J., Crespi, A., Ryczko, D., and Cabelguen, J. M. (2007). From swimming to walking with a salamander robot driven by a spinal cord model. *Science*, 315, 1416–1420

Izhikevich, E. (2006). Dynamical systems in neuroscience: The geometry of excitability and bursting. Cambridge, MA: MIT press.

Jamom, M., Clarac, F. (1995). Locomotor patterns in freely moving crayfish (*Procambarus clarkii*). *The Journal of Experimental Biology*, 198, 683–700.+

Johnston, R. M., & Levine, R. B. (2002). Thoracic leg motoneurons in the isolated CNS of adult Manduca produce patterned activity in response to pilocarpine*. Invertebrate Neuroscience*, 4, 175–192.

Kindermann, T. (2002). Behavior and adaptability of a six-legged walking system with highly distributed control. *Adaptive Behavior,* 9:16–41

Klärner, D., and Barnes, W. J. P. (1986). The cuticular stress detector (CSD2) of the crayfish. II. Activity during walking and influences on the leg coordination. *The Journal of Experimental Biology*, 122,161–175.

Klärner, D., Barth, F. G. (1986). The cuticular stress detector (CSD2) of the crayfish I physiological properties. *The Journal of Experimental Biology*, 122, 149-159.

Knops, S., To´th, T..I, Guschlbauer, C., Gruhn, M., Daun-Gruhn, S. (2013). A neuromechanical model for the neuronal basis of curve walking in the stick insect. *Journal of Neurophysiology,* 109: 679–691.

Leise, E. M., Hall, W. M., and Mulloney B. (1987). Functional organization of crayfish abdominal ganglia: II. Sensory afferents and extensor motor neurons. *Journal of Comparative Neurology*, 266, 495-518.

Libersat, F., Zill, S., and Clarac, F. (1987). Single-unit responses and reflex effects of force sensitive mechanoreceptors of the dactyl of the crab. *Journal of Neurophysiology*, 57, 1601–1617.

Ludwar, B. C., Göritz, M. L., and Schmidt, J. (2005). Intersegmental coordination of walking movements in stick insects. *Journal of Neurophysiology*, 93, 1255-1265.

MacMillan, D. L. (1975). A physiological analysis of walking in the American Lobster (*Homarus americanus*). *Philosophical Transactions of the Royal Society B*, 270, 1-59.

Marder, E., Bucher, D. (2007). Understanding circuit dynamics using the stomatogastric nervous system of lobsters and crabs. *Annual Review of Physiology,* 69, 291–316.

Marder, E., Bucher, D.(2001). Central pattern generators and the control of rhythmic movements. *Current Biology,* 11 (23), R986–96.

Marder, E., Calabrese, R. L. (1996). Principles of rhythmic motor pattern generation. *Physiological Reviews,* 76 (3), 687–717.

Martin, J., Raabe, T., Heisenberg, M. (1999). Central complex substructures are required for the maintenance of locomotor activity in Drosophila melanogaster. *Journal of Comparative Physiology A*, 185:277–288

Müller, U., and Cruse, H. (1991). The contralateral coordination of walking legs in the crayfish *Astacus leptodactylus*. I. Experimental results. *Biological Cybernetics*, 64, 429–436.

Orlovsky, G.N., Deliagina, T.G., Grillner, S.E. (1999). Neuronal Control of Locomotion: From Mollusc to Man. *New York: Oxford University INC*. 322 p.

Parrack, D.W. (1964). Stepping sequences in the crayfish. *PhD. Thesis, University of Illinois*.

Paskarbeit, J., Schmitz, J., Schilling, M., Schneider, A. (2010). Layout and construction of a hexapod robot with increased mobility. *Proceedings of the 3rd IEEE RAS/EMBS international conference on biomedical robotics and biomechatronics (IEEE BIOROB 2010)*, September 26–29, 2010. Tokyo, Japan, pp 621–625

Pearson, K. G. (2000). Neural Adaptation In The Generation Of Rhythmic Behavior. *Annual Reviews in Physiology*, 62, 723–53.

Pearson, K. G., Fourtner, C. R. (1975). Nonspiking interneurons in walking system of the cockroach. *Journal of Neurophysiology,* 38 (1), 33–52.

Pfeiffer F, Eltze J,Weidemann HJ (1995). Six-legged technical walking considering biological principles. Robot Auton Syst 14:223–232

Ridgel, A.L., Alexander, B.E., Ritzmann, R.E. (2007). Descending control of turning behavior in the cockroach, Blaberus discoidalis. *Journal of Comparative Physiology A,* 193:385–402

Ridgel, A.L., Ritzmann, R.E. (2005). Effects of neck and circumoesophageal connective lesions on posture and locomotion in the cockroach. *Journal of Comparative Physiology A,* 191:559–573

Ritzmann, R. E., and Büschges, A. (2007). Adaptive motor behavior in insects. *Current Opinion in Neurobiology*, 17, 629-636.

Ross, R. B., and Belanger, J. H. (2013). Passive Mechanical Properties of Crustacean Walking Legs. *Poster, Sfn, Annual meeting, San Diego*

Schilling, M., Paskarbeit, J., Schmitz, J., Schneider, A., Cruse, H. (2012). Grounding an internal body model of a hexapod walker—control of curve walking in a biological inspired robot. *Proceedings of IEEE/RSJ international conference on intelligent robots and systems,IROS 2012*, pp 2762–2768.

Schilling, M., Hoinville, T., Schmitz, J. Cruse, H. (2012). Walknet, a bio-inspired controller for hexapod walking. *Biological Cybernetics*, DOI 10.1007/s00422-013-0563-5

Schneider, A., Paskarbeit, J., Schäffersmann, M., Schmitz, J. (2011). Biomechatronics for embodied intelligence of an insectoid robot. *Proc ICRA*, (2)'11, pp 1–11

Schütz, C. and Dürr, V. (2011). Active tactile exploration for adaptive locomotion in the stick insect. *Philosophical Transactions of the Royal Society B*, 366, 2996-3005.

Selverston, A. I., & Moulins, M. (1985). Oscillatory neural networks. *Annual Review of Physiology*, 47, 29–48.

Sillar, I. K., Clarac, F., Busch, B. M. H. (1987). Intersegmental coordination of central neural oscillators for rhythmic movements of the walking legs in crayfish, *Pacifastacus leniusculus*. *Journal of Experimental Biology*, 131, 245-264.

Sillar, K. T., Skorupski, P., Elson, R. C., and Bush, B. M. H. (1986). Two identified afferent neurones entrain a central locomotor rhythm generator. *Nature*, 323, 440-443.

Sillar, K.T., and Skorupski, P. (1986). Central input to primary afferent neurons in the crayfish, *Pacifastacus leniusculus*, is correlated with rhythmic motor output of thoracic ganglia. *Journal of Neurophysiology*, 55(4), 678-688.

Skinner, F., Kopell, N., and Marder, E. (1994). Mechanisms for oscillation and frequency control in reciprocally inhibitory model neural networks. *Journal of Computational Neuroscience*, 1, 69–87.

Skinner, F., and Mulloney, B., (1998). Intersegmental coordination in invertebrates. *Current Opinion in Neurobiology*, 8, 725-732.

Skinner, K. (1985). The structure of the fourth abdominal ganglion of the crayfish*, Procarnbnrus clarhzi* (Girard). I. Tracts in the ganglionic core. *Journal of Comparative Neurology*, 234,168-181.

Skorupski, P., and Sillar, K.T. (1988). Central synaptic coupling of walking leg motor neurones in the crayfish: Implications for sensorimotor integration. *Journal of Experimental Biology*, 140, 355-379.

Slifer, E. H. (1966). Sense organs on the antennal flagellum of walking stick Carausius morosus Brünner (Phasmida). *Journal of Morphology*, 120, 189-202.

Spirito, C. P. and Mushrush, D. L. (1979). Interlimb coordination during slow walking in the cockroach*. Journal of Experimental Biology*, 78, 233-243.

Strausfeld N.J. (1999). A brain region in insects that supervises walking. *Progress in Brain Research,* 123:273–284

Strauss R. (2002). The central complex and the genetic dissection of locomotor behaviour. *Current Opinion in Neurobiology*, 12:633–638

Toth, T.I., Schmidt, J., Büschges, A., Daun-Gruhn, S. (2013). A neuro-mechanical model of a single leg joint highlighting the fundamental physiological role of fast and slow muscle fibres of an insect muscle system. *PLOS ONE*, doi:10.1371/journal.pone.0078247.

Von Twickel, A., Büschges, A., Parsemann, F. (2011). Deriving neural network controllers from neuro-biological data: implementation of a single-leg stick insect controller. *Biological Cybernetics*, 104, 95–119.

Wallén, P., and Williams, T. L., (1984). Fictive locomotion in the lamprey spinal cord in vitro compared with swimming in the intact and spinal animal. *Journal of Physiology*, 374, 225-239

Weide, W. (1960) Einige Bemerkungen über die antennalen Sensillen sowie über das Fühlerwachstum der Stabheuschrecke Carausius (Dixippus) morosus. Br (Insecta: Phasmida). *Wiss Z Martin-Luther-Univ Halle-Wittenberg Math-Naturwuss Reihe* IX/2, 247-250

Wendler, G. (1964). Laufen und Stehen der Stabheuschrecke Carausius morosus: Sinnesborstenfelder in den Beingelenken als Glieder von Regelkreisen. *Journal of Comparative Physiology,* 48(2):198-250.

Wendler, G. (1966). The co-ordination of walking movements in arthropods. *Symposia of the Society for Experimental Biology,* 20:229-249.

Westmark, S., Oliveira, E. E., and Schmidt, J. (2009). Pharmacological analysis of tonic activity in motoneurons during stick insect walking. *Journal of Neurophysiology*, 102, 1049–1061.

Williams, J.L.D. (1975) Anatomical studies of the insect nervous system: a ground plan of the midbrain and an introduction to the central complex in the locust Schistocerca gregaria (Orthoptera). *Journal of Zoology,* 176:67–86

Wilson, D. M. (1966). Insect walking. *Annual Review of Entomology,* 11, 103-122.

Zill, S. N., Keller, B. R., Duke, E.R. (2009). Sensory Signals of Unloading in One Leg Follow Stance Onset in Another Leg: Transfer of Load and Emergent Coordination in Cockroach Walking. *Journal of Neurophysiology*, 101, 2297-2304.

Zill, S. N., Schmitz, J., Chaudhry, S. and Büschges, A. (2012). Force encoding in stick insect legs delineates a reference frame for motor control. *Journal of Neurophysiology*, 108, 1453-1472.

Zill, S., Schmitz, J., Büschges, A. (2004). Load sensing and control of posture and locomotion. *Arthropod Structure Development*, 33, 273-286.

9. Teilpublikationen

10.1 List of publications

Grabowska, M., Tóth, T.I., Smarandache-Wellmann, C. , Daun-Gruhn, S., (2014). A network model comprising 4 segmental, interconnected ganglia, and its application to simulate multi-legged locomotion in crustaceans. Journal of Computational Neuroscience (under review)

Tóth, T.I., Grabowska, M., Schmidt, J., Büschges, A., Gruhn, S., (2013). A neuro-mechanical model explaining the physiological role of fast and slow muscle fibers at stop and start of stepping of an insect leg. PLOS ONE, DOI: 10.1371/journal.pone.0078246

Grabowska, M., Godlewska, E., Schmidt, J., Daun-Gruhn, S., (2012). Quadrupedal gaits in hexapod animals-Stepping patterns in free-walking adult stick insects. Journal of Experimental Biology 215, 4255-4266

10.2 Short communications

Martyna J. Grabowska, Tibor T. Toth, Ansgar Büschges, Anke Borgmann, Silvia Daun-Gruhn, 2014. Experimental analysis of an inter-segmental MN-CPG network model and its theoretical analysis with different topologies and their application to multi-legged locomotion (n<6). SfN, Annual meeting, Washington, USA

Martyna J. Grabowska, Tibor T. Toth, Ansgar Büschges, Anke Borgmann, Silvia Daun-Gruhn, 2014. Theoretical and Experimental Investigations of an Inter-segmental Control Network and its Application to Multi-legged Locomotion. Neurovisionen 10, Jülich (Received the Best Poster Award)

Grabowska, M., Tóth, T.I., Gruhn, S. 2013. Analysis of inter-segmental MN-CPG network models with different topology and their application to multi-legged locomotion. Neurovisionen 9, Cologne, Germany (Received the Best Poster Award)

Grabowska, M., Tóth, T.I., Gruhn, S. 2013. Analysis of an inter-segmental MN-CPG network model with n-CPGs and its application to multi-legged locomotion. SfN, Annual meeting, San Diego, USA

Grabowska, M., Tóth, T.I., Gruhn, S., 2013. Analysis of an inter-segmental MN-CPG network model with 4 CPGs. Interdisciplinary College in Günne (Möhnesee), Germany

Grabowska, M., Godlewska, E., Schmidt, J., Daun-Gruhn, S., 2011. Stepping patterns in free walking adult stick insects. Annual meeting of the German Neuroscience Society, Göttingen, Germany

10. Supplementary Figure

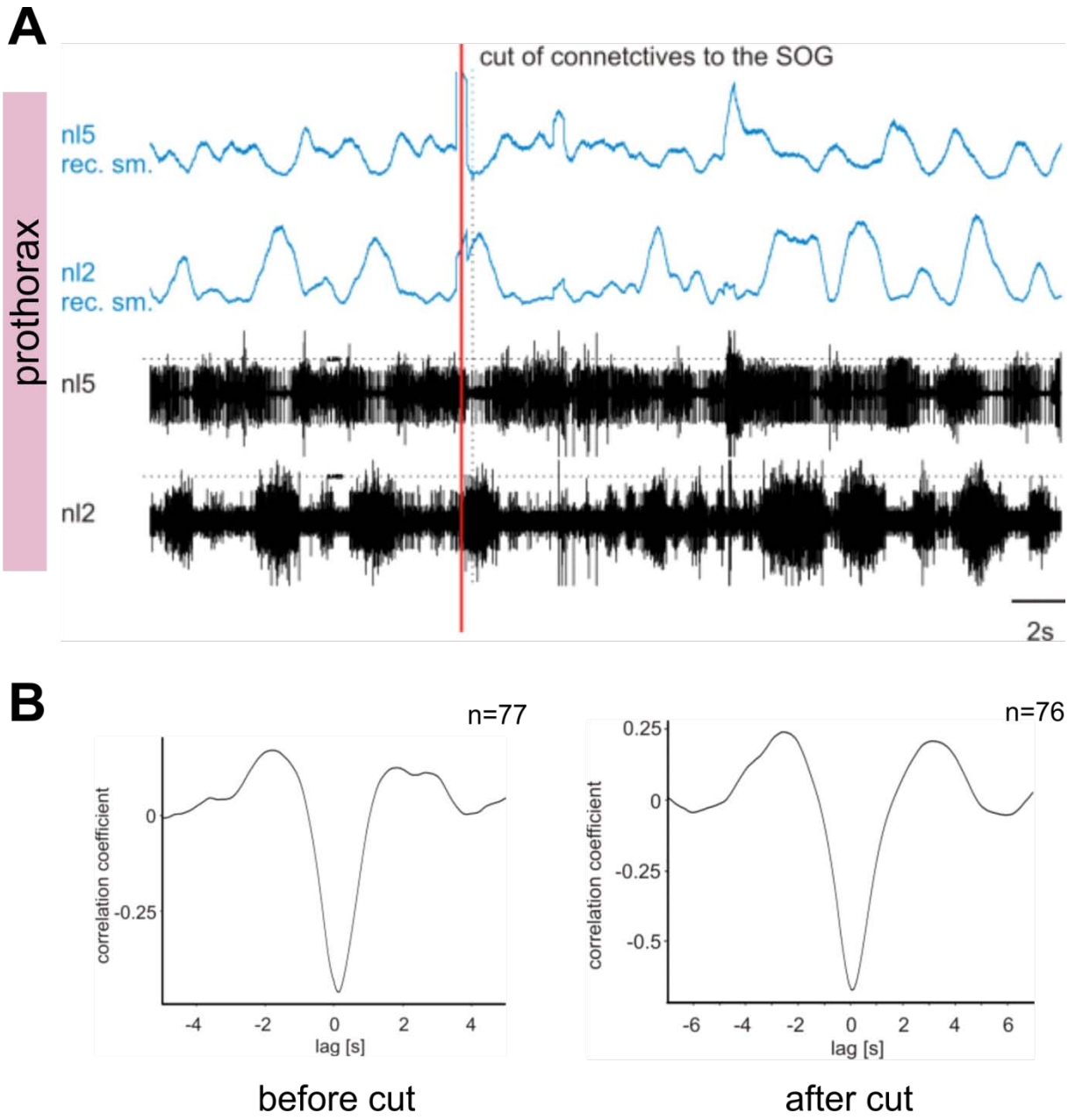

Supplementary Fig 1. *Cutting the connectives to the SOG during an experiment, results in more regular alternating activity of the pilocarpine-induced rhythm in the prothoracic protractor and retractor MN pools A) Example of recordings of prothoracic protractor and retractor MN activity after application of pilocarpine. Before the red line, that indicates the cut of the connectives to the SO, the rhythm is irregular. After the cut, a short disturbance of the pilocarpine-induced rhythm occurs (approx. 6 sec.). Then, alternating activity returns and is more regular than the alternating activity before the cut. B) Cross correlation of rectified and smoothed recordings of protractor and retractor MN burst activity (blue traces in A) τ=0.08s). The correlation coefficient is higher in the cross correlation of the recordings after the cut than the one before the cut. This experiment is representative for four animals in which always a minimum cycle number of 70 before and after the cut were analyzed.*

11. Acknowledgments

Zu allererst möchte ich mich bei meiner Betreuerin PD. Dr. Silvia Gruhn bedanken. Sie hat mich über die letzten Jahre stets gefordert, mir geholfen, mich motiviert, mich für das Thema begeistert und mir Möglichkeiten geboten, für die ich sehr dankbar bin. Es war mir eine Freude dem Nerdarium beizutreten ;)

Natürlich möchte ich mich auch bei Prof. Dr. Ansgar Büschges bedanken, der mir über die Jahre ein Setup zur Verfügung gestellt hat und stets ein offenes Ohr hatte, wenn es Fragen zu meinem Projekt gab. Selbstverständlich möchte ich mich auch für die Übernahme des Zweitgutachtens bedanken.

Prof. Dr. Axel Schneider danke ich ebenfalls für die freundliche Übernahme des Drittgutachtens.

Dr. Carmen Wellmann, Dr. Till Bockemühl, PD. Dr. Jochen Schmidt, Dr. Anke Borgmann und Dr. Tibor Tóth danke ich für das gründliche Korrekturlesen.

Der Arbeitsgruppe Gruhn, danke ich für das tolle Arbeitsklima. Dabei gilt der Dank ganz besonders Dr. Tibor Tóth der mich über die letzten Jahre ebenfalls intensiv betreut hat, mir immer zu Rate stand und sich nie über mein Chaos beschwert hat ☺

Den sagenhaften Editoren Eli, Tommi und Joscha danke ich ganz besonders für den Beistand in den entscheidenden Stunden!!!!

Der gesamten Arbeitsgruppe Büschges und Wellmann danke ich für die Unterstützung im schönen Laboralltag und die großartige Atmosphäre.

Mein Dank gilt auch ganz besonders meinen Mädels: Ute, Ilka, Shideh und Eli, die mir das Leben außerhalb der Uni versüßt haben.

Meinen Eltern, und meiner liebsten Schwester Claudi danke ich für ihren Rückhalt und Verständnis über die ganzen Jahre. CMJM <3

Zum Schluss danke ich noch Martin, meinem Ruhepol, für all seine Unterstützung über die letzten Jahre in jeglicher Hinsicht und auch einfach dafür, dass er immer weiß wie man mich wieder zum Lächeln bringt.

12. Erklärung

Ich versichere, dass ich die von mir vorgelegte Dissertation selbstständig angefertigt, die benutzten Quellen und Hilfsmittel vollständig angegeben und die Stellen der Arbeit einschließlich Tabellen, Karten und Abbildungen, die anderen Werken im Wortlaut oder dem Sinn nach entnommen sind, in jedem Einzelfall als Entlehnung kenntlich gemacht habe; dass diese Dissertation noch keiner anderen Fakultät oder Universität zur Prüfung vorgelegen hat; dass sie abgesehen von oben angegebenen Teilpublikationen noch nicht veröffentlicht worden ist sowie, dass ich eine solche Veröffentlichung vor Abschluss des Promotionsverfahrens nicht vornehmen werde. Die Bestimmungen dieser Promotionsordnung sind mir bekannt. Die von mir vorgelegte Dissertation ist von PD Dr. Silvia Gruhn betreut worden.

Köln, den 06. Oktober 2014 _____

Martyna Grabowska